Transport relationships between bedload traps and a 3-inch Helley-Smith sampler in coarse gravel-bed streams and development of adjustment functions

Report submitted to the

Federal Interagency Sedimentation Project

3909 Halls Ferry Rd.
Vicksburg, MS 39180

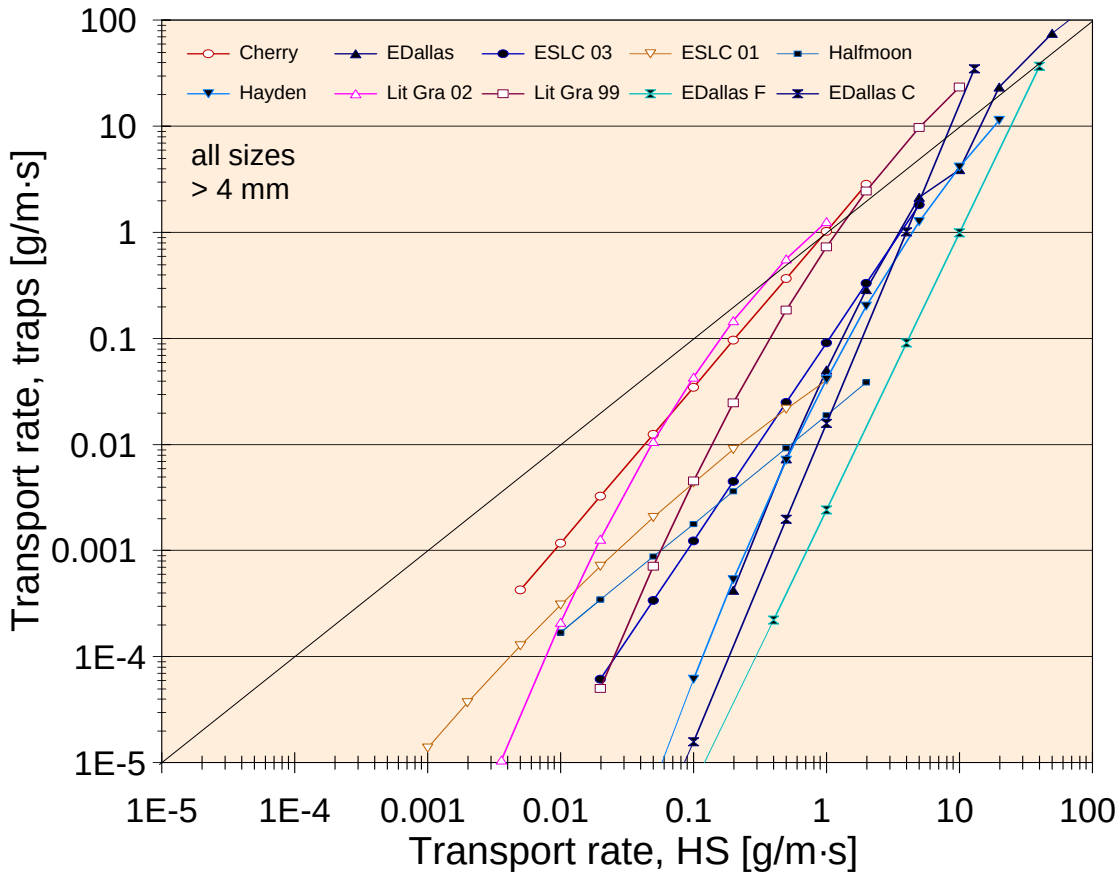

Kristin Bunte and Steven R. Abt

Engineering Research Center
Colorado State University
Fort Collins, CO

December 2009

Executive Summary

Sampling results obtained from a Helley-Smith (HS) sampler have been found to differ from those collected with other samplers, particularly those that are not restricted by a small opening size, a small sampler bag, short sampling times, and direct contact with the bed. The ability to convert HS sampling results to those obtained from a sampler without those restrictions, such as bedload traps, might be beneficial because HS samplers are frequently used in field studies due to their widespread availably and ease of use.

This study compared sampling results from bedload traps with those collected by a 3-inch, thin-walled, wide-flared HS sampler over a wide range of transport rates at nine coarse-bedded mountain stream study sites. Ratios of transport rates collected with both samplers are not constant but change over the range of sampled transport rates. Inter-sampler transport relationships are quantifiable by regression functions that can be used to convert HS transport rates to those that might have been measured with bedload traps.

Inter-sampler transport relationships were established for all gravel size fractions as well as for total gravel transport rates for all study sites. Inter-sampler transport relationships generally follow a similar pattern: they approach or intersect the line of perfect agreement (1:1 line) at high transport rates. At lower transport rates, relationships diverge below the 1:1 line, indicating that transport rates from the HS sampler exceed those from bedload traps by several orders of magnitude. This pattern shifts slightly among particle sizes but is notably variable among streams.

Two approaches were used for the comparison of HS sampling results to those of bedload traps: 1) The rating curve approach fits power functions rating curves to the relationship of bedload transport rates versus discharge that are measured with both samplers and then creates data pairs from transport rates predicted for each sampler at specific discharges. 2) The paired data approach establishes data pairs from transport rates measured almost concurrently with both samplers. Both, the rating curve and the paired data approach clearly suggested a segregation of inter-sampler transport relationships into two groups (termed “red” and “blue”), and both approaches resulted in almost the same classification of streams into the groups. Study streams of the “red” and “blue” group differed significantly with respect to bedload transport conditions. In comparison to “blue” streams, “red” streams have steeper rating and flow competence curves, smaller transport rates and smaller bedload D_{max} particle sizes at 50% Q_{bkf} , and larger bedload D_{max} at Q_b = 1g/m·s. Threshold values for these attributes are provided to differentiate between stream groups.

Inter-sampler transport relationships for all approaches were averaged over the streams within each group. For “blue” streams, the group-average trendlines were quite similar among approaches but less so for “red” streams. Averaging over all approaches yielded an adjustment function for each stream group that serves to convert HS sampling results to those that might have been measured with bedload traps.

While both approaches—rating curve and paired data—have advantages and disadvantages, this study favors the paired data approach. The paired data approach omits the error prone and time-consuming step of fitting rating curves and allows operators to make informed decisions about data trends. Another advantage is that results from the paired data approach offer the possibility to predict stream-specific inter-sampler transport ratios based on a stream's sediment supply and flow competence.

From the various inter-sampler transport relationships identified for the nine study streams using two study approaches, the study distilled two numerical correction functions for HS sampling results. They are meant for gravel transport in coarse-bedded mountain streams depending on threshold values of their characteristics of bedmaterial and bedload transport. Compared to their wide variability among streams, correction functions vary generally much less among size fractions, and this may be ignored for now. More studies are needed to validate conversion functions and to extend the range of stream conditions for which conversion functions are available.

Table of contents

1. Introduction

1.1 Study overview

Several studies have shown that sampling results measured with a 3-inch Helley-Smith sampler (HS) differ from those measured with other samplers. There are known problems of over-sampling and undersampling by the HS sampler in gravel-bed streams depending on the conditions of the channel bed and on bedload transport characteristics. Bedload traps are relatively new sampling devices that were designed to overcome the HS-typical sampling challenges in gravel-bed streams; on these grounds sampling results from bedload traps are assumed to be more encompassing than those from a HS sampler. However, the HS sampler is the most frequently used sampling device due to its widespread availability and ease of use, and a large number of HS data exist. It would be beneficial if HS-measured transport rates could be aligned to those measured with bedload traps. The objective of this study is to provide adjustment functions with which to align transport rates measured by a HS sampler to those measured with bedload traps.

The study will demonstrate that bedload sampling results differ among samplers, particularly those not affected by the design and operational properties of a Helley-Smith sampler. Direct contact with the channel bed appears to be the most influential factor among several HS-typical attributes causing sampling differences. Preliminary analyses of bedload trap and HS sampling results indicate that ratios of HS to bedload trap sampling results vary with bedload transport rates, and the data suggest that these ratios may vary with bedload particle sizes, as well as among streams. These findings suggest that conversion of HS sampling results is not a matter of applying one simple factor. Rather, conversion functions are dependent on transport rates and likely vary among bedload particle sizes, as well as among streams due to differences in bedmaterial conditions and characteristics of bedload transport.

To compute conversion functions, the analyses will utilize an existing body of bedload transport rates that were measured with bedload traps and the HS sampler over snowmelt highflow seasons at nine sites in mountain gravel-bed streams. Two approaches were used to illustrate the relationships between transport rates measured with a HS sampler and bedload traps at the study streams. 1) The rating curve approach employs gravel bedload rating curves established for both samplers and, in a second step, matches transport rates predicted from both rating curves to establish an inter-sampler transport relationship. Inter-sampler transport relationships are quantified via fitted power functions in the general form of $Q_{B\,traps} = a\,Q_{B\,HS}{}^{b}$, and the parameters a and b are used to convert a HS-measured transport rate $Q_{B\,HS}$. 2) The paired data approach uses transport rates measured concurrently with both samplers and fits power functions as well as polynomial functions to the plotted data to characterize inter-sampler transport relationships.

Both comparison approaches indicate that inter-sampler transport relationships vary moderately among particle-size classes, but widely among streams. Inter-sampler relationships for total gravel transport appear to be segmented into two groups that differ mostly for high transport rates in the rating curve approach. In the paired data approach, the two groups differ primarily for low transport rates and appear to converge when transport is high. The study provides a grouping of bedload transport parameters from which a user can estimate into which group a study stream may fall, and subsequently select the appropriate function for adjusting HS sampling results. For

the paired data approach, the study also provides relationships with which a user can determine the adjusted transport rates for selected HS-measured transport rates based on bedmaterial properties and bedload transport characteristics of the study stream.

1.2 Sampling results deviate among various bedload samplers

HS-type samplers are widely used for collecting bedload in gravel-bed streams. HS-type samplers (including the BL-84, the 3-inch and 6-inch HS samplers, the 8 by 4 inch Elwha sampler, and the 12 by 8 inch Toutle River II sampler) differ not only in the size of the sampler opening but also in the shape of the sampler body, as well as the capacity and mesh size of the sampler bag. Several studies show that Helley-Smith-type samplers of different sizes, shapes, and sampler bags collect different transport rates (e.g., Johnson et al. 1977, Beschta 1981, O'Leary and Beschta 1981, Pitlick 1988, Gray et al. 1991; Gaudet et al. 1994, Childers 1991, 1999; Ryan and Troendle 1997; Ryan and Porth 1999, Ryan 2005; Vericat et al. 2006). Sampling results differ not only among HS-type samplers but also from those obtained by bedload samplers that do not have the HS-typical restrictions of small opening sizes, small collection bags, short sampling times, and direct interaction with bedmaterial. For example, when compared to unweighable pit traps excavated into a natural channel bed, the HS sampler (deployed for hours at a time) oversampled sand in near-bed suspension and under-sampled sand and gravel that passed beneath the sampler perched on cobbles (Sterling and Church 2002). The passage of sand under a HS perched on a cobble bed was also observed on flume experiments by O'Brien (1987). Compared to weighable pit traps in a large flume study, the Helley-Smith-type samplers over-sampled sand and gravel bedload (Hubbell et al. 1985, 1987), and the degree of oversampling varied among various HS samplers, albeit that a reanalysis of these data by Thomas and Lewis (1993) suggests less difference. Compared to bedload traps, gravel transport rates (> 4 mm) measured with the 3-inch HS sampler were orders of magnitude higher during low transport at nine study sites. With increasing transport rates, results from both samplers converged, and fitted rating curves intersected on average near 130% Q_{bkf} (or near 125% if the two samplers' transport relationships are multiplied by the Ferguson (1986, 1987) bias correction factor). At higher flows, the HS sampler under-sampled transport rates because coarse gravel and cobbles cannot enter the HS opening (Bunte et al. 2004, 2008) (this is illustrated in Figure A1 in the Appendix). This pattern was exhibited at all study sites where bedload traps and a HS sampler were deployed together. However, details in the relationships between bedload trap and HS transport rates varied among streams: the difference in gravel transport rates between the two samplers measured at flows 50% Q_{bkf} extended over 1 to 4 orders of magnitude, and the intersection points of the rating curves from the two samplers ranged from 93 to 181% Q_{bkf} (illustrated in Figure A2).

1.2.1 Direct bed contact responsible for most differences in sampling results

Several pieces of evidence suggest that much of the difference in sampling results between the HS and other samplers is a result of direct contact between the HS sampler and the channel bed. In two of the nine study streams, the 3-inch, thin-walled HS sampler was deployed not only on the bed but also on the ground plates on which otherwise bedload traps were deployed (see Bunte and Swingle (2008) for study details). Setting the HS sampler onto ground plates greatly reduced transport rates compared to those measured with the HS set directly on the bed, particularly at

low flows. As a result, transport rates measured by the HS on plates approach those measured with bedload traps to within an order of magnitude or less (illustrated in Figure A3) (Bunte and Swingle 2008; Bunte et al. 2007b). The higher transport rates of the HS on the bed are ascribed to the following mechanism. Setting the HS sampler onto the channel bed exerts a slight pressure onto bed particles, dislocating a few particles near the sampler edge from their interlock with neighboring particles. Being slightly more exposed to flow, the hydraulic sampler efficiency of 1.5 from the wide-flared sampler opening can entrain dislocated particles into the sampler and collect gravel particles that are otherwise not in motion on the bed. Ground plates under the HS sampler prevent direct interaction with the gravel bed, and placement of a sampler onto plates avoids inadvertent particle dislocation and entrainment. Avoidance of direct contact with the bed is likely the main reason for collection of similar transport rates with a 3-inch HS placed on a concrete sill and the conveyor belt sampler (Emmett 1980, 1981, 1984).

A comparison of the bedload D_{max} particle sizes sampled by the HS deployed on the bed *vs*. those on grounds plates demonstrates that both sampler deployments collected similar transport rates and similar bedload D_{max} particle sizes during high transport. At low transport, however, the HS on the bed collected not only higher transport rates but also larger bedload D_{max} particle sizes than the HS on the plates (Figure A4). Collection of larger bedload D_{max} particles suggests that inadvertent particle displacement and entrainment is the mechanism that results in oversampling when a HS is placed directly on the bed.

Direct placement of the HS sampler on the bed may add an occasional particle per vertical. Nevertheless, the chance of including an extra particle into the sampler accumulates when the HS is deployed at 15-20 verticals per cross-section (Bunte et al. 2008). Collecting additional gravel particles can overestimate transport rates by orders of magnitude when transport is otherwise very low. When transport is high, an occasionally dislocated and entrained particle in the HS sampler contributes minor amounts in comparison to the large number of particles entering the sampler per time. HS-measured transport rates therefore approach those from bedload traps when transport is high, and the accuracy of the HS measurements likely improves with increasing gravel bedload transport rates. The potential for inadvertent particle dislodgement and entrainment by the HS sampler as well as for active particle "scooping" due to an unfavorable sampler position has been mentioned as a problem for the 3-inch HS sampler by several (Helley and Smith 1971; Beschta 1981; O'Leary and Beschta 1981; Ryan and Troendle 1997), and by Vericat et al. (2006) for the 6-inch HS.

The importance of deploying the HS to ensure good contact with the stream bottom in order to avoid over- or undersampling has been presented (Johnson et al. 1977; Emmett 1980, 1981, 1984; Beschta 1981; O'Brien 1987; Kuhnle 1992; Childers 1999, Sterling and Church 2002; Bunte et al. 2004, 2007b, 2009b). Data shown by Wilcox et al. (1996) indicate that a HS deployed directly on a coarse gravel bed collected more gravel and less sand than a HS deployed on a wooden sill nearby. Collecting less sand can be the result of loosing fine particles beneath the sampler perched on gravel, while collecting more gravel can result from inadvertently dislocating and entraining gravel particles by the sampler on the bed.

1.2.2 Other sampler characteristics contributing to differences in sampling results

Apart from particle dislocation and entrainment (Bunte et al. 2004, 2007b, 2008, Bunte and Swingle 2008), or pedestalling (O'Brien 1987; Childers 1999; Sterling and Church 2002) (Figure 1 a and b) due to direct bed contact, other attributes in the HS sampler design and deployment method contribute to differences in measured transport rates and bedload D_{max} particle sizes as well. For example, gravel transport relationships obtained from two samplers will not be the same if samplers have different sampling times (Bunte and Abt 2005) (Figure 1c), opening sizes (Thomas and Lewis 1993; Gaudet et al. 1994; Childers 1999; Vericat et al. 2006) (Figure 1d), and sampling efficiency (Druffel et al. 1976; Pitlick 1988; Gray et al. 1991; Childers 1991, 1999) (Figure 1 e). The sampler-specific differences in measured transport rates vary with flow and with transport rates. The combined effects caused the HS sampler to measure higher gravel transport rates than bedload traps at low flow and similar or higher transport rates at high flows.

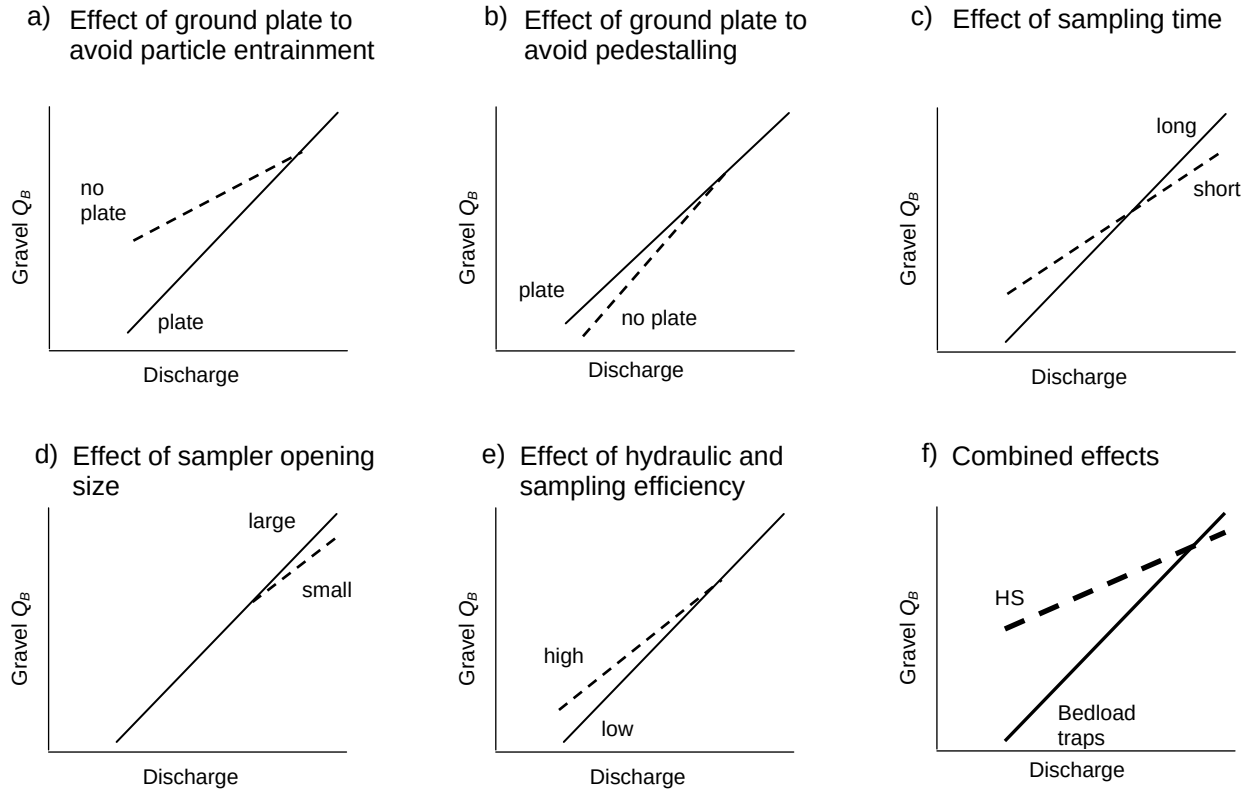

Figure 1: Effects of short sampling time, small opening size, high hydraulic and sampling efficiency, scooping, and pedestalling on sampled gravel transport rates in a coarse-bedded mountain gravel-bed stream over flows ranging from about 15 to 140% of bankfull (i.e., within the range of infrequent motion of pea gravel to frequent motion of coarse gravels including occasional cobbles).

The difference in sampling results among the 3-inch HS sampler and non-HS samplers makes determining adjustment functions to convert transport rates between samplers an important task. Without those functions, sampling results obtained by different samplers cannot be compared.

Once conversion functions are available to account for inter-sampler differences, the choice of bedload sampler for future studies can be guided by convenience or availability. The ability to account for inter-sampler differences may also allow the reanalyzing of old data or compiling them for meta studies.

1.3 Objectives of the study

The objective of the study is to develop conversion functions that can be applied to data collected with a wide-flared, thin-walled, 3-inch Helley-Smith sampler. The conversion functions are directly derived from relationships of transport rates measured with bedload traps to those measured at the same flow with the 3-inch, wide-flared, thin-walled Helley-Smith sampler placed directly on the bed. The study uses a large body of field-measured gravel transport rates that were collected with bedload traps and a 3-inch HS sampler deployed side by side in nine mountain gravel-bed streams during snowmelt runoff over a wide range of flow and transport rates (Bunte et al. 2008).

2. Transport relationships between bedload traps and the HS

2.1 Affecting parameters

Analyses prior to this study had indicated that the variability of bedload trap to HS transport ratios among streams may be influenced by factors such as bedload transport rates, bedload particle-size fractions, as well as bedmaterial characteristics of the study streams (Bunte and Swingle 2008).

Effects of HS-measured bedload transport rates

Results from the nine field studies indicate that the thin-walled HS sampler measured transport rates several orders of magnitude higher than those collected with bedload traps when flows and transport were low (Figure A1). With increasing flows and transport rates, transport rates collected by both samplers approach and may intersect. Based on these results, ratios of transport rates measured with bedload trap and the HS sampler (F_{HS}) at the same flow should be formulated as a function of the transport rate measured by the HS sampler in the basic form of

$$F_{HS} = q_{B,trap} = a \cdot q_{B,HS}{}^{b} \quad (1)$$

where $q_{B\,trap}$ and $q_{B\,HS}$ are the mass-based transport rate per unit stream width (g/m·s) measured with bedload traps and the HS sampler, respectively; a is a coefficient and b an exponent. The function describing how bedload trap-HS transport ratios changes with increasing transport rates is termed inter-sampler transport relationship in this study (Figure 2a).

Effects of bedload particle-size fractions

Fractional bedload rating curves fitted to bedload trap data and the HS sampler for the study sites differ from each other. For bedload traps, they are typically parallel and relatively close to each other. For the HS sampler, fractional rating curves are typically less parallel and further apart with higher transport rates for larger particles (Bunte et al. 2004). These differences will likely

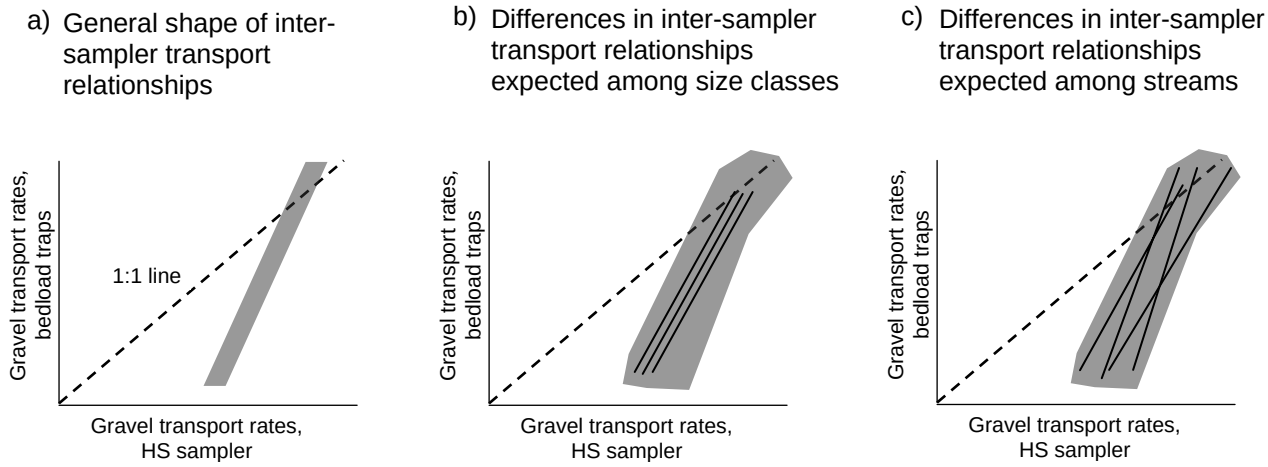

Figure 2: General shape of inter-sampler transport relationships plotted in log-log space (a) and expected differences among particle-size classes (b) and among streams (c).

cause the ratio of transport rates between the two samplers to vary among size fractions. Consequently, inter-sampler transport relationships (Eq. 1) may need to be formulated for individual size fractions (*i*) in the form of (Figure 2b):

$$F_{HS,i} = q_{B\ trap,i} = a_i \cdot q_{B\ HS,i}^{\ bi} \qquad (2)$$

Effects of stream sediment supply: subsurface sediment size and rating curve steepness
Studies have shown that the difference between bedload trap and HS gravel bedload rating curves differ among the study streams (see Figures A1 and A2 in the Appendix). It appears important to identify the parameters that differ among streams and that may cause systematic variability among streams (Figure 2c).

Studies by Bunte et al. (2006) have shown that bedload traps tend to have flatter transport relationships (i.e., lower exponents of fitted power function rating curves) in streams with large amounts of subsurface fines < 8 mm than in stream with fewer subsurface fines. Conversely, rating curve coefficients tend to increase with the percent subsurface fines (see Figure A5 a and b in the appendix as an illustration). High amounts of subsurface fines < 8 mm suggest a high supply of easily transportable sediment, and this causes the lower end of bedload trap rating curves to be elevated, and thus the rating curve slope to be rather flat. Rating curve exponents and coefficients obtained from HS samples differ much less with the amount of subsurface fines. If the difference in gravel rating curve steepness between the two samplers decreases with increasing amount of subsurface fines, the ratios of transport rates between bedload traps and the HS sampler should vary with the amount of subsurface fines as well, probably in a way that the ratio between HS and bedload trap transport rates becomes smaller in streams with high sediment supply. To test this assumption, the study should explore whether inter-sampler transport relationships vary among streams and whether they show similarities for streams that share commonalities of the shape of bedload rating curves as well as sediment supply.

Effects of bedload D_{max} particle size

Earlier study results suggested that the ratio of transport rates should be affected by the size of the largest particles in transport. Comparison of HS and bedload trap sampling results between East Dallas and Hayden Creek shows that the HS sampler is most likely to collect transport rates similar to those from bedload traps when a large amount of small gravel particles that fit into the 3-inch opening are in motion per time. Thus, transport ratios between the two samplers at high flows should approach unity when transport is high and comprised of relatively small gravel. When a large amount of coarse gravel and cobbles are in transport, the HS transport rate should fall below that of bedload traps, as these large clasts cannot enter the 3-inch HS sampler. When small amounts of medium gravel are in motion, inadvertent particle dislocation and entrainment increases HS transport rates beyond those collected with bedload traps. Bedload trap-HS transport relationships should therefore be evaluated for variability within the transported bedload D_{max} particle size.

Accounting for the potential effects of subsurface fines, the rating curve steepness, and the bedload D_{max} particle sizes, inter-sampler transport relationships assume the general form of

$$F_{HS,,sed} = a_{,sed} \cdot q_{B\ HS,sed}{}^{b,sed} \tag{3}$$

where the subscript *sed* denotes the magnitude of rating curve steepness, subsurface fines, bedload D_{max} particle sizes, or a combination of some or all of these factors.

2.2 Effects of sampler behavior

Attributes of sampler design and deployment method affect the differences in rating curves measured by bedload traps and the HS sampler (Figure 1), causing either oversampling or undersampling compared to transport rates collected in a sampler (e.g., bedload traps) that is neither deployed directly in the bed nor shares other design attributes of a 3-inch, thin-walled, wide-flared HS sampler. Figure 3 illustrates how the various sampling behaviors "plot out" in inter-sampler transport relationship graphed in a diagram of bedload trap versus HS transport rates.

Oversampling occurs as the HS sampler:

a) Inadvertently dislocates particles at the sampler entrance when set on the bed. Without support from neighboring particles, dislocated particles are easily entrainable by flow and aided by the sampler's high hydraulic efficiency, these particles are likely to enter the sampler: → oversampling gravel
   The effects of particle dislocation and entrainment increase with the number of verticals per cross-section and the brevity of sampling time.
b) Is not set flatly on the bed and inadvertently scoops an easily entrainable particle as the HS is set on the bed: → oversampling gravel
c) Has a high hydraulic efficiency: → oversampling sand and pea gravel.
d) Is set onto the bed: Particles dislocation and subsequent entrainment, as well as particle scooping and a hydraulic efficiency → oversampling particularly when transport rates are otherwise very low.

Undersampling occurs when the HS sampler

1. is perched on cobbles or coarse gravel in a coarse bed: → undersampling small particles that pass beneath the sampler,
2. is not on the bed sufficiently long to capture infrequently moving (large) particle sizes: → undersampling large particles
3. when particles in transport exceed the sampler opening size: → undersampling large particles
4. when a large particle lodged in front of the sampler blocks the sampler opening: → undersampling any particle size in a specific sample.

Each of these processes individually affects transport relationships between a HS sampler that is deployed directly on the bed (x) and bedload traps (y). Several of these processes may occur in combination during an individual sample or while a sequence of samples is collected over the cross-section. This causes variability in the inter-sampler transport relationship in response to changing conditions of bedload transport and bedmaterial at the time of sampling.

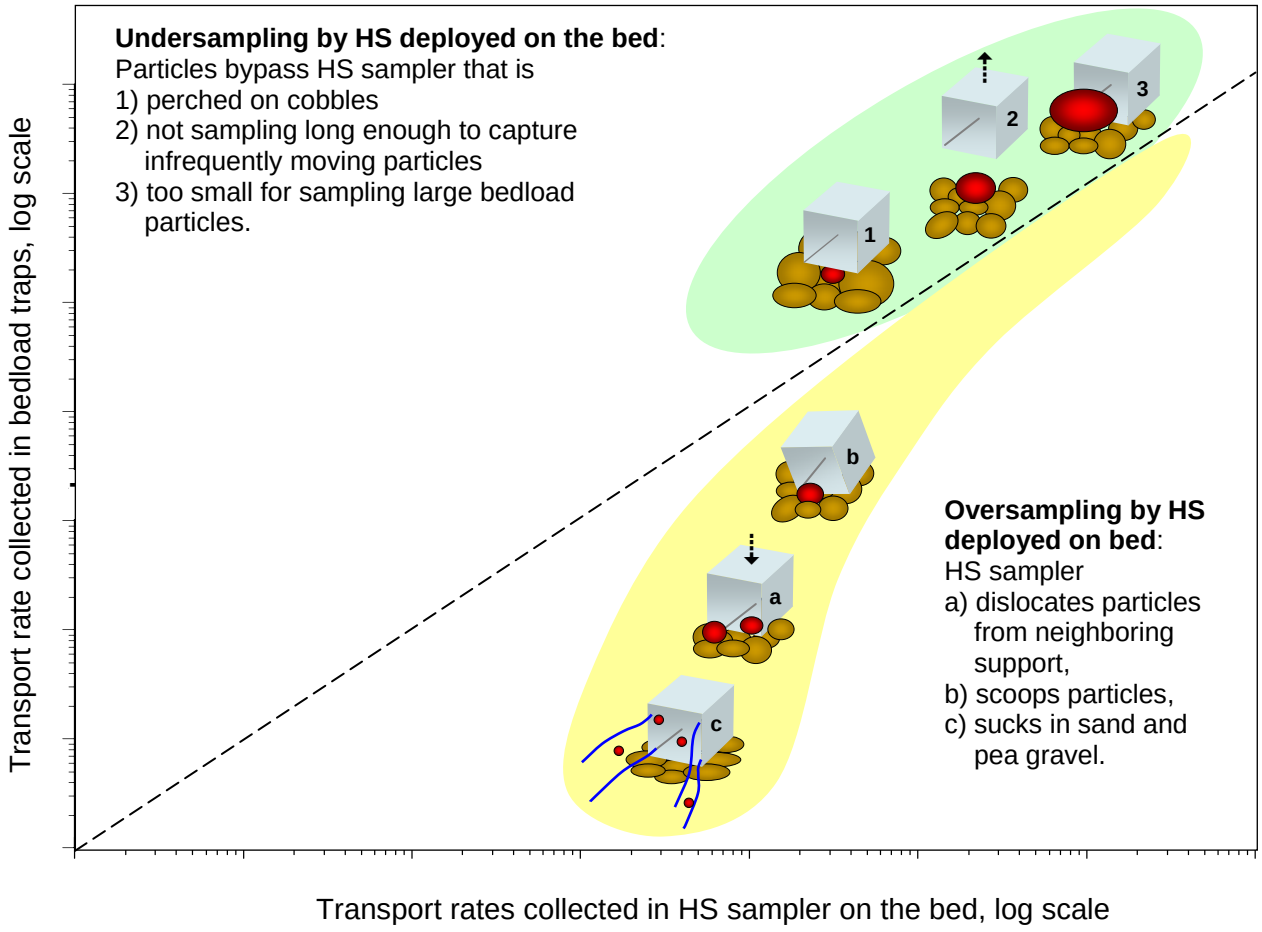

Figure 3: Sampling behaviors of a HS sampler (shown here only with its cube-shaped entry part) and their expected effects on the ratio of transport rates between bedload traps and a HS deployed directly on the channel bed.

3. Methods

3.1 Data collection

Field data were collected at nine study sites in mountain streams with armored, coarse gravel and small cobble beds (Table 1). The sites were located on National Forest land in the northern and central Rocky Mountains (USA) in subalpine and montane zones at altitudes between 2,000 to 3,000 m above sea level. Most of the stream basins experienced some logging, mining and road building several decades ago, but today the basins are comparatively undisturbed and mostly forested. Valley floors are mainly open and vegetated by meadows with shrubs or willow thickets. All sampled streams have a snowmelt highflow regime in which runoff typically

Table 1: Characteristics of the streams near the study sites.

Parameters / Stream; Year sampled	Predo-minant lithology	Basin area (km^2)	Bank-full flow (m^3/s)	Bank-full width (m)	Meas'd range of flow (%Q_{bkf})	Water surface slope (m/m)	Surface		Subsurface % fines		Sub-surface D_{50} (mm)	Predominant stream type
							D_{50} (mm)	D_{84} (mm)	< 2 mm	< 8 mm		
St. Louis Cr., '98	Granite	34	3.99	6.5	26 - 65	0.017	76	163	9	24	41	plane-bed, forced pool-riffle
Little Granite Cr., nr. confluence '99	Sediment-ary	55	5.66	14.3	61 - 131	0.017	59	133	8	16	42	plane-bed, forced pool-riffle
Cherry Cr., '99	Volcanic	41	3.09	9.5	49 - 145	0.025	49	140	11	27	30	plane-bed, forced pool-riffle
E. St. Louis Cr., '01	Granite	8	0.76	3.7	26 - 71	0.093	108	258	6	17	54	step-pool
Little Granite Cr., abv. Boulder Cr. '02	Sediment-ary	19	2.83	6.3	37 - 102	0.012	67	138	10	25	34	plane-bed, forced pool-riffle
E. St. Louis Cr., '03	Granite	8	0.76	3.7	44 - 144	0.093	108	258	6	17	54	step-pool
Halfmoon Cr., '04	Granite	61	6.23	8.6	17 - 77	0.014	49	119	13	29	26	plane-bed, forced pool-riffle
Hayden Cr., '05	Sediment-ary	39	1.92	6.5	28 - 149	0.038	63	164	13	26	36	step-pool, plane-bed, mixed
East Dallas Cr., 07	Volcanic	34	3.7	8.0	10 - 113	0.017	58	128	12	31	21	plane-bed, forced pool-riffle

increases from 10-20 % of bankfull discharge (Q_{bkf}) in early to mid May to 80 - 140% Q_{bkf} between late May and mid June, depending on the annual snowpack and spring weather conditions. Daily fluctuations of flow can be pronounced, varying by up to 50% between daily low flows in the early afternoon and daily peak flows in the early to late evening. The streams are typically incised into glacial or glacio-fluvial deposits. At most sites, the streambed is entrenched into a floodplain such that highflows of l40% Q_{bkf} cause little overbank flooding.

3.1.1 Bedload trap data

At all study sites, gravel bedload was sampled using bedload traps that consist of an aluminum frame 0.3 by 0.2 m in size. Bedload is collected in an attached net 0.9 – 1.6 m long and with a mesh width just below 4 mm. Bedload traps are mounted onto ground plates 0.43 by 0.37 m in size that are anchored on the stream bottom with metal stakes. This deployment set-up not only permits long sampling times but also avoids direct contact of bedload traps with the channel bed.

Four to six bedload traps were installed across each of the study streams spaced 1-2 m apart, typically in a locally wide cross-section. All traps sampled simultaneously, typically for 1 hour per sample, but sampling time was reduced to 30 or even 10 minutes when transport rates were high in order to avoid overfilling the sampler net (Bunte et al. 2008). Four to nine samples of gravel bedload were collected back-to-back on almost all days of the snowmelt highflow seasons that extended over 4 to 7 weeks. Therefore, 2l-196 samples were collected per site with an average number of 92 samples. Sampled flows ranged from low flows of 16% to highflows of 140% of bankfull discharge, but only 5 of the nine study streams exhibited this range.

3.1.2 Helley Smith data

Bedload was sampled at all study sites using a 76 by 76 mm opening, thinwalled Helley-Smith sampler with a 3.22 opening ratio and a 0.25 mm mesh bag. Sampling locations were spaced in 0.4-1.0 m increments across the stream, yielding 12 to 18 verticals that were sampled for 2 minutes each, completing one traverse. At several sites, HS samples were collected in the same cross-section as the bedload traps, and the HS verticals were placed into spaces between the traps. This arrangement permitted simultaneous sampling with bedload traps and a HS sampler, however, individual verticals were not all evenly spaced. At other sites, HS samples were collected in a cross-section about 1.8 m downstream from the traps by an operator standing on a low footbridge (decking height 0.4 – 0.7 m above the water surface). This permitted an even spacing of the HS verticals but required that bedload traps were removed from the ground plates while the HS samplers were collected. One set of HS samples was typically collected in the morning before bedload traps were fastened on the ground plates and one in the evening after the bedload traps were removed. Depending on the length of the field season, about 20 – 80 samples were collected with the HS sampler for each site per season. Most of the HS samples were paired with a bedload trap sample that was collected either immediately before or after the HS sample. Flows were quite similar for the two paired samples in the morning, but could vary by up to 20% for some of the evening samples when flows increased. Transport relationships computed from HS samples in this study usually aligned with HS samples that the USDA Forest Service had obtained at or close to sites in this study in earlier years (mainly between 1993 and 2002, see data sets in Ryan et al. 2002, 2005).

3.2 Data analysis

Two approaches were considered when comparing transport rates collected with bedload traps and the HS sampler. The rating curve approach compares transport rates predicted for each of the two samplers for a specified flow from a fitted rating curve. The paired data approach compares transport rates measured sequentially by the two samplers at a similar flow. Both approaches are applied to data from all study streams.

3.2.1 Rating curve approach

The rating curve approach uses all non-zero gravel transport rates collected at a study site to compute bedload transport rating curves for total and individual size fractions (total and fractional rating curves). Several computational steps are required to predict transport rates for specific flows from both samplers and to establish inter-sampler transport relationships. These steps are explained and repeated at each study stream.

3.2.1.1 Establishing total and fractional transport relationships

a) Plot total gravel and fractional gravel transport rates for each 0.5 phi size class versus discharge for both samplers.

b) Establish rating curves by fitting power function regressions to the total and all fractional transport relationship for both samplers. Power functions were selected because they are frequently used for gravel transport (e.g., Barry et al. 2004, King et al. 2004, Bunte et al. 2008) and are convenient for subsequent computations.

$$q_{B\,trap,i} = g_i \cdot Q^{hi} \tag{4}$$

$$q_{BHS,i} = c_i \cdot Q^{di} \tag{5}$$

where $q_{B\,trap,i}$ and $q_{BHS,i}$ are either the total gravel or fractional gravel transport rates predicted for the i^{th} size class (g/m·s), Q is discharge (m^3/s), g_i and c_i are coefficients, and h_i and d_i are exponents for bedload traps and the HS sampler, respectively.

c) Compute and evaluate the *p*-value[1] for the fitted total and fractional rating curves. *p*-values smaller than 0.05 are typically considered to indicate statistical validity of a fitted relationship. For streams in which many size fractions were in transport, most of the bedload trap rating curves for individual size fractions as well as total gravel transport had *p*-values << 0.05. However, for the one or two largest size classes transported within a given highflow year, small sample sizes and narrow ranges of flow result in rather flat transport relationships for both samplers, and *p*-values were typically >> 0.05, i.e., statistically not significant, and not suitable for comparison of fractional transport rates between the two samplers. For HS samples, *p*-values were generally higher (i.e., somewhat less significant) than for bedload traps because HS samples tended to have larger data scatter and sometimes a slightly smaller range of sampled flows. In order not to exclude several of the HS fractional rating curves from further analysis, *p*-values within the range 0.05 – 0.1 were considered valid. Many of the sites at which HS samples were collected in this

[1] All *p*-values in this report are two-tailed.

study had been sampled by Ryan et al (2002, 2005) a few years earlier when flows reached higher peaks[2] and transport rates extended over wider ranges. However, transport relationships measured in both studies fall within a common envelope, and fitted gravel transport rating curves are similar between both studies. It may be reasoned that many of the HS fractional transport relationships fitted in this studies would have been statistically significant with $p < 0.05$ had there been an opportunity to sample over a larger range of flows.

d) Plot the computed total and fractional transport relationships over the range of flow for which transport of a specified size fraction was observed. The power functions fitted to the fractional transport relationships streams are shown for all study streams in Figure 4**Error! Reference source not found.**. The parameters of the fitted power functions are listed in Table 10 in the Appendix.

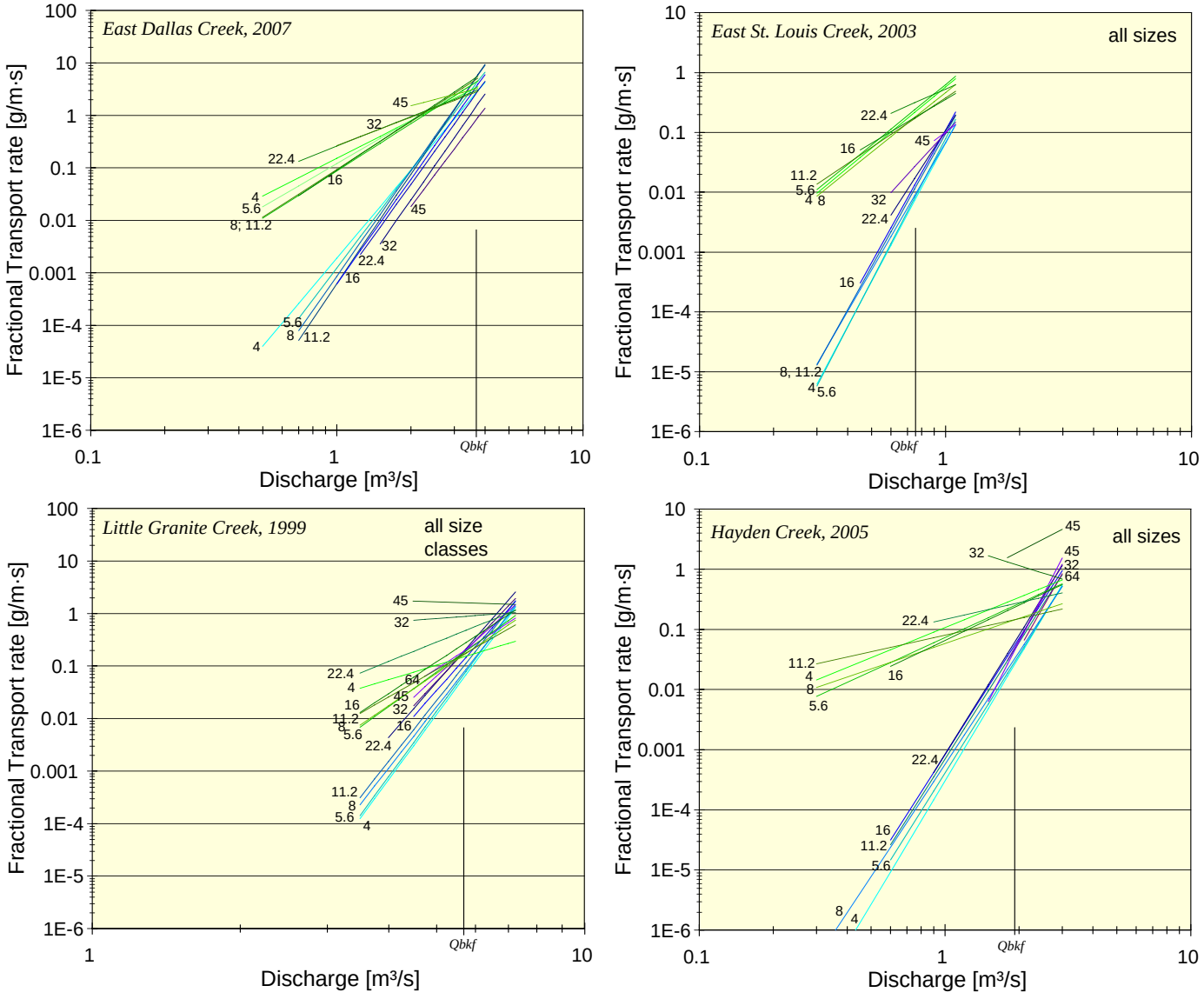

[2] The years 1995, 1996, 1997, and 1999 reached peak flows of 130 - 170% of bankfull. Data for the study presented here were collected between 1998 and 2007; flows peaked within 80 - 100% Q_{bkf} in 1998, 2001, 2002, and 2004.

Fig. 4, cont'd next page

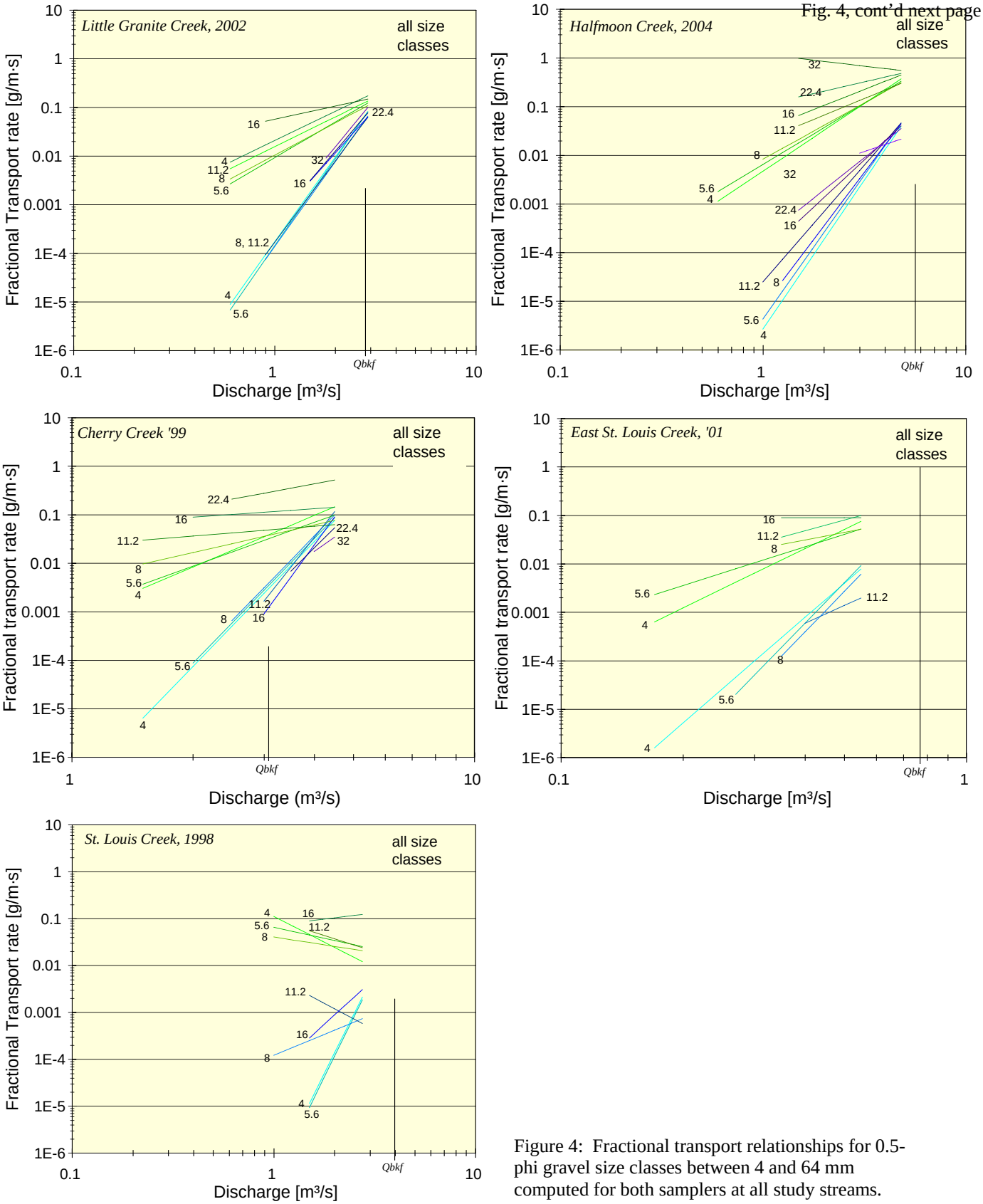

Figure 4: Fractional transport relationships for 0.5-phi gravel size classes between 4 and 64 mm computed for both samplers at all study streams.

3.2.1.2 Bias correction factors

Any prediction of a *y*-estimate from a value of *x* in a power function relationship fitted to data that exhibit scatter suffers an inherent underestimation in the *y*-estimate. The underestimation is zero for perfectly correlated data and increases—typically to a factor of 1.5-5 for the study streams—with the amount of data scatter that is quantified by the standard error of the *y*-estimate. To adjust for the underestimation, the computed *y*-estimate needs to be multiplied by a bias correction factor (*CF*). Several factors are available, e.g., Ferguson (1986, 1987), Duan (1983), and Koch and Smilie (1986). This study used Ferguson's correction factor for the rating curve approach based on Hirsch et al. (1993) who consider Ferguson's correction factor very suitable if the standard error of the *y*-estimate (s_y) is < 0.5 and if sample size (n) is > 30. The corrections factor CF_{Ferg} is computed as

$$CF_{Ferg} = \exp (2.651 \cdot s_y^2) \tag{6a}$$

if the logarithm to the base of 10 (i.e., log) is used for the log-transformation of the *x*- and *y*-data (as was done in this study); s_y is typically provided in a spreadsheet regression table. For log transformations using the natural logarithm,

$$CF_{Ferg} = \exp (s_y^2/2). \tag{6b}$$

Values for CF_{Ferg} typically range between 1 and 3 for fractional transport rates from the HS sampler, and values up to 4 for total bedload transport rates. Values of CF_{Ferg} are somewhat lower for bedload trap data because transport rates collected with bedload traps tend to have less scatter in their relationship with flow than HS samples. In cases when s_y exceeds 0.5 and n drops below 30, Ferguson's bias correction function overcorrects and creates a bias in the opposite direction. To prevent this overcorrection, Hirsch et al. (1993) suggest using the nonparametric smearing function by Duan (1983) for bias correction (CF_{Duan}) which is computed from

$$CF_{Duan} = \frac{\sum_{i=1}^{n} 10\text{^}(e_i)}{n} \tag{7a}$$

when power function regressions are fitted log-transformed data based on decadal logarithms. e_i are the residuals of the predicted *y*-estimate (i.e., the difference between the measured and the predicted *y*-values) that are exponentiated, summed, and divided by the sample size n. For natural logarithms, Duan's correction factor is computed from

$$CF_{Duan} = \frac{\sum_{i=1}^{n} \exp(e_i)}{n} \tag{7b}$$

CF_{Duan} yielded higher values than CF_{Ferg} when the standard error s_y took values of up to 0.6, but the sample size was much larger than 30. In these cases (i.e., when only one of the conditions

described by Hirsch et al. (1993) was fulfilled) the CF_{Ferg} bias correction factor was applied. Transport rates for bedload traps and the HS sampler for specified discharges are then predicted from the power function fitted to fractional transport relationships and multiplied by a correction factor.

$$q_{B\,trap,i} = CF \cdot g_i \cdot Q^{hi} \tag{8}$$

$$q_{BHS,i} = CF \cdot c_i \cdot Q^{di} \tag{9}$$

where g_i is the power function coefficient for the i^{th} size class and h_i is the power function exponent for bedload trap transport relationships. CF is either Ferguson's or Duan's correction factor. c_i and d_i are the power function coefficient and exponents for the i^{th} size class for HS sampler transport relationships. The value of the bias correction factor affects the coefficient, but not the exponent of the predictive function. Similarly, the bias correction factor affects the coefficient of the ratio between bedload trap and HS fractional transport rates.

3.2.1.3 Creating and plotting data pairs

Transport rates are predicted for discharges from the fractional rating curves fitted to HS and bedload trap samples (Eqs. 8 and 9) and paired with each other. The matches include the smallest and the largest flows to which fractional transport rates for both samplers extend, as well as a few flows within the extremes. These data paired values are plotted against each other with $q_{B\,traps,i}$ on the *y*-axis and $q_{B\,HS,i}$ on the *x*-axis (Figure 5). All plotted transport ratios necessarily assume a straight line (in log-log space) that describes the inter-sampler transport relationships between bedload traps and the HS sampler for each size fraction.

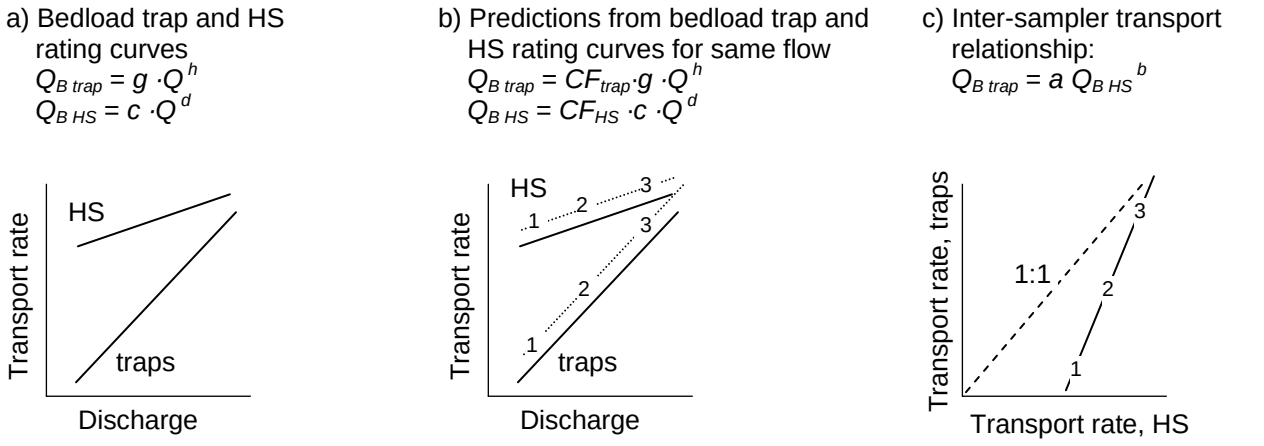

Figure 5: Computation of inter-sampler transport relationship using the rating curve approach: a) Bedload rating curves for bedload trap and HS sampler; b) 1, 2, and 3 are bias-corrected, predicted transport rates from the bedload trap and HS rating curves at the same flows. c) The paired transport rates are plotted versus each other. The fitted power function describes the inter-sampler transport relationship.

3.2.1.4 Formulating inter-sampler transport relationships

To numerically describe fractional inter-sampler transport relationships ($F_{HS,i}$), power function regressions are fitted to two arbitrarily selected data pairs of predicted, log-transformed fractional transport rates for both samplers. Size fractions for which the fitted fractional rating curves for both samplers obtained *p*-values > 0.05 were flagged (some exceptions for $0.05 > p < 0.1$ were allowed). Multiplication by a bias correction factor is not necessary in this step because the power function regression functions fitted to two data pairs have no scatter ($r^2 = 1$).

$$F_{HS,i} = q_{B\,traps,i} = a_i \cdot q_{B\,HS,i}^{\,bi} \tag{10}$$

where a_i and b_i are the power coefficients and exponents for the *i*th size class or the total transport rate. The resulting power functions (F_{HSi}) represent the average ratio of transport rates measured with the two samplers for different particle size fractions and different flows. These functions could be used for adjusting transport rates from a thinwalled, 3-inch HS sampler deployed in mountain gravel-bed streams to transport rates measured with bedload traps.

3.2.1.5 Analyzing inter-sampler transport relationships

Inter-sampler transport relationships are analyzed in various ways. Of interest to this study are analyses of how inter-sampler transport relationships differ among size classes and among study sites. The possibility of systematic differences among streams is assessed by comparing the exponents and coefficients of power functions fitted to inter-sampler transport relationships with parameters describing channel morphology as well as to characteristics of the bedload trap and HS rating curves.

3.2.2 Paired data approach

As an alternative to the rating curve approach, the paired data approach is used to directly compare data pairs of total and fractional transport rates measured with bedload traps and the HS sampler. In this approach, transport rates measured with bedload traps ($q_{B\,trap}$) (*y*-axis) are plotted against those measured with the HS sampler ($q_{B\,HS}$) (*x*-axis) at nearly the same time and the same flow. Regression functions are fitted to the plotted data to describe the inter-sampler transport relationships for all particle sizes and all study streams. To predict an appropriate function for converting HS sampling results to those that would have been measured with bedload traps, parameters of the regression functions are related to parameters of bedmaterial conditions as well as bedload transport characteristics observed in the study streams.

The paired data approach made use of an additional two data sets that were not included in the rating curve approach: samples collected at East Dallas Creek at individual stream locations with particularly fine and coarse beds (i.e., not across the entire stream bed). One bedload trap was deployed at the coarse and the fine bed, and HS samples were collected at two verticals (for 2 min each) in front of the traps after they had been removed (see Bunte and Swingle (2008) for study details). Because bedload was measured locally, while discharge was measured over the cross-section, these data were not suitable for the rating curve approach.

3.2.2.1 Identification of measured data pairs

From all bedload data collected at a specified site, those collected with the HS sampler and bedload traps either concurrently or immediately following each other were identified. When a bedload trap sample was collected both just before and just after the HS sample, these two samples were averaged before being paired with the HS sample. At Little Granite Creek 2002, the number of data sets could be extended by using not only 1-hour samples, but also 10-min bedload trap samples when a HS sample was collected in close temporal proximity. The number of paired data sets when total gravel transport were > 0 for both samplers ranged from 15 to 74 with a mean of 37 for all the study sites. The number of data pairs decreases with increasing particle size such that for the coarsest 1 – 3 particle-size classes mobile in a specified stream there are only five or fewer data pairs.

Data pairs are plotted against each other with bedload trap transport rates ($q_{B\,traps}$) on the *y*-axis and HS-measured transport rates ($q_{B\,HS}$) on the *x*-axis. Values of zero-transport rates for any of the samplers are assigned a transport rate of 1E-6 g/m·s and plotted along the axes (Figure 6 a and b). For a specific size fraction, transport ratios between the two samplers scatter over 1 – 2 orders of magnitude. The scatter decreases towards large transport rates.

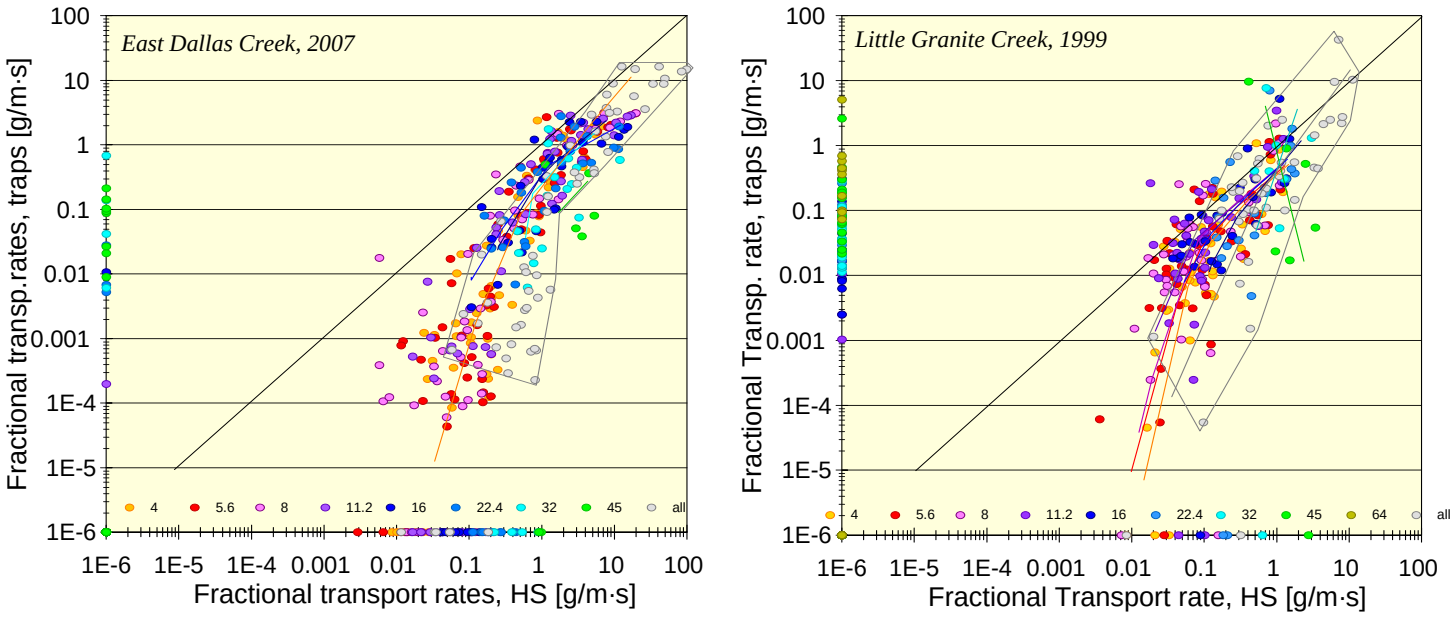

Fig. 6, continued on next page

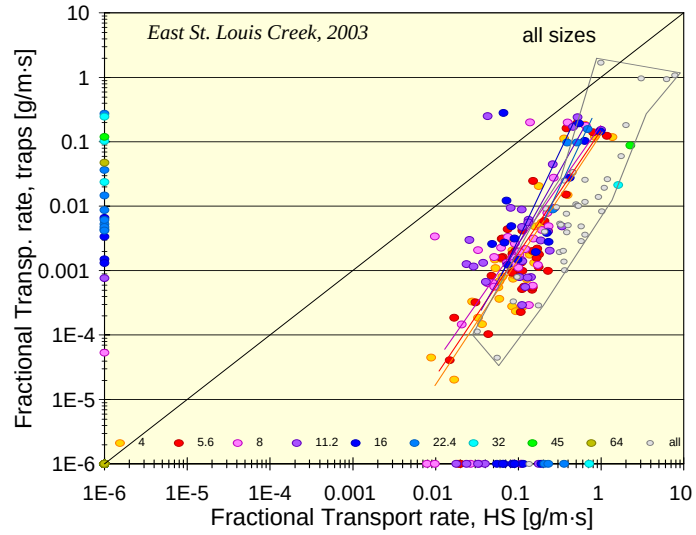

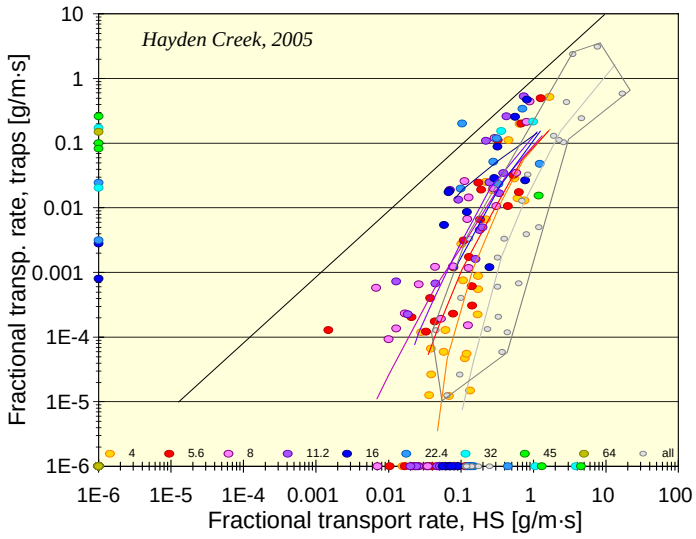

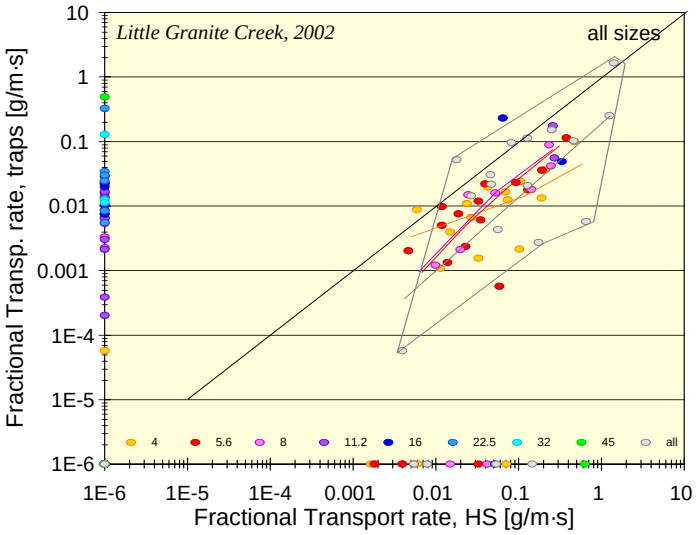

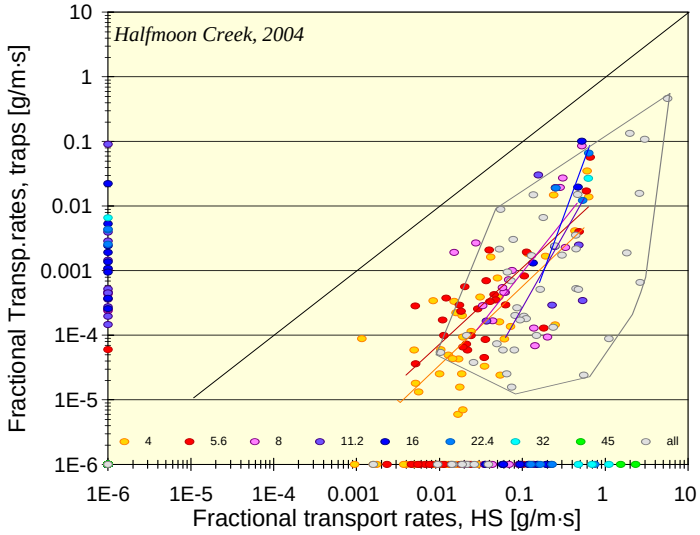

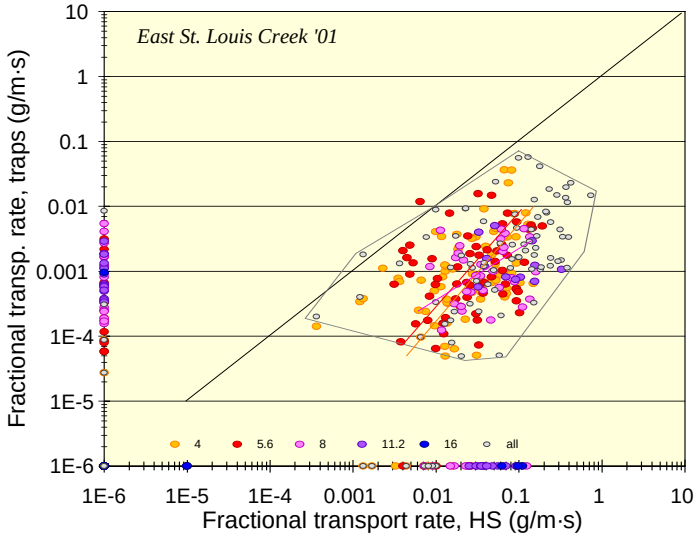

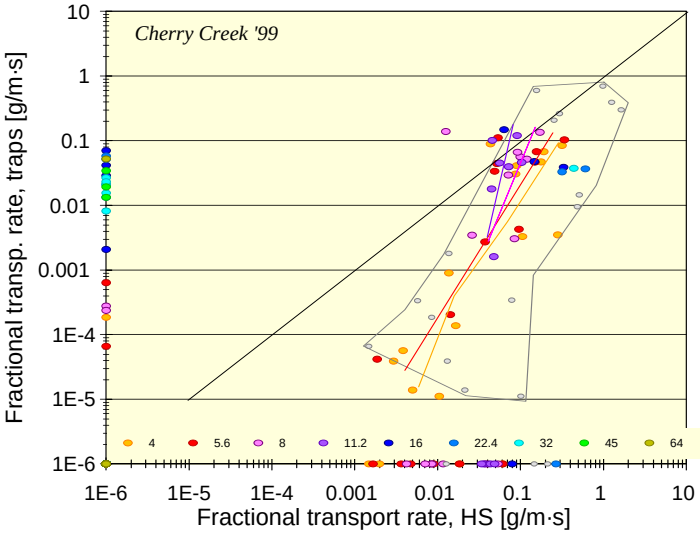

Fig. 6, continued on next page

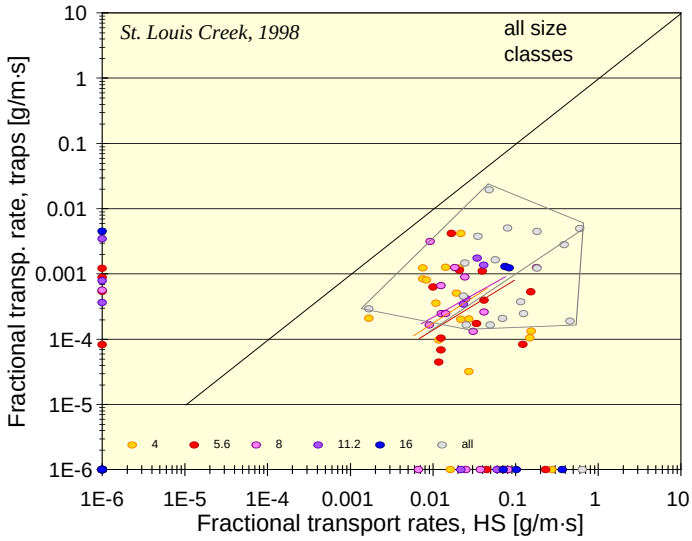

Figure 6a: Paired data approach: measured pairs of total and fractional transport rates collected concurrently with bedload traps and the HS sampler at the nine study sites. Inter-sampler transport relationships shown here are sketched only.

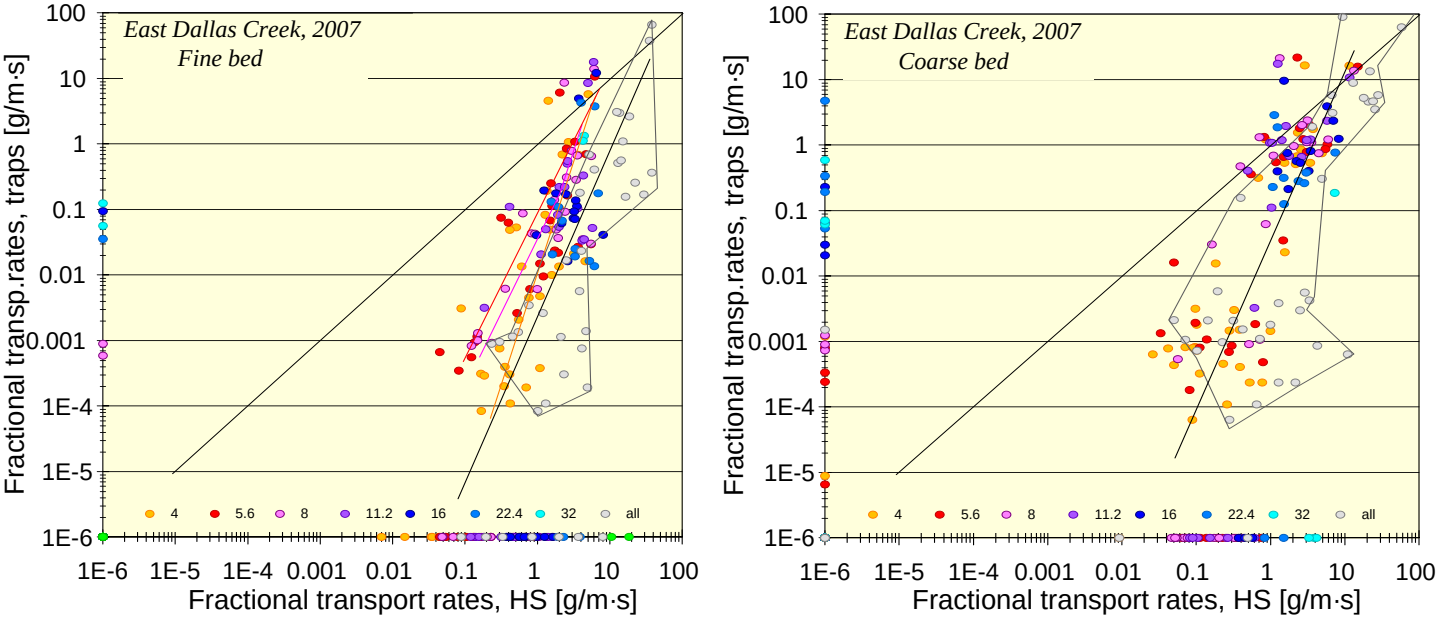

Figure 6b: Paired data approach: measured pairs of total and fractional transport rates collected concurrently with bedload traps and the HS sampler at the two additional stream locations with fine and coarse beds at East Dallas Creek. Inter-sampler transport relationships shown here are sketched only.

3.2.2.2 Identification of patterns in plotted data trends

Stream sites that yielded a large number of data pairs over a large range of transport rates with both samplers show a recurring pattern in the plotted data. Generally, data points for small gravel sizes (4, 5.6, and 8 mm) follow a convex-upward trend. At the lower end, data scatter widely[3], but the data field narrows as the inter-sampler transport ratios approach the 1:1 line or a line parallel to it, creating a data field that has the outline of a downward-facing cornucopia as presented in Figure 7.

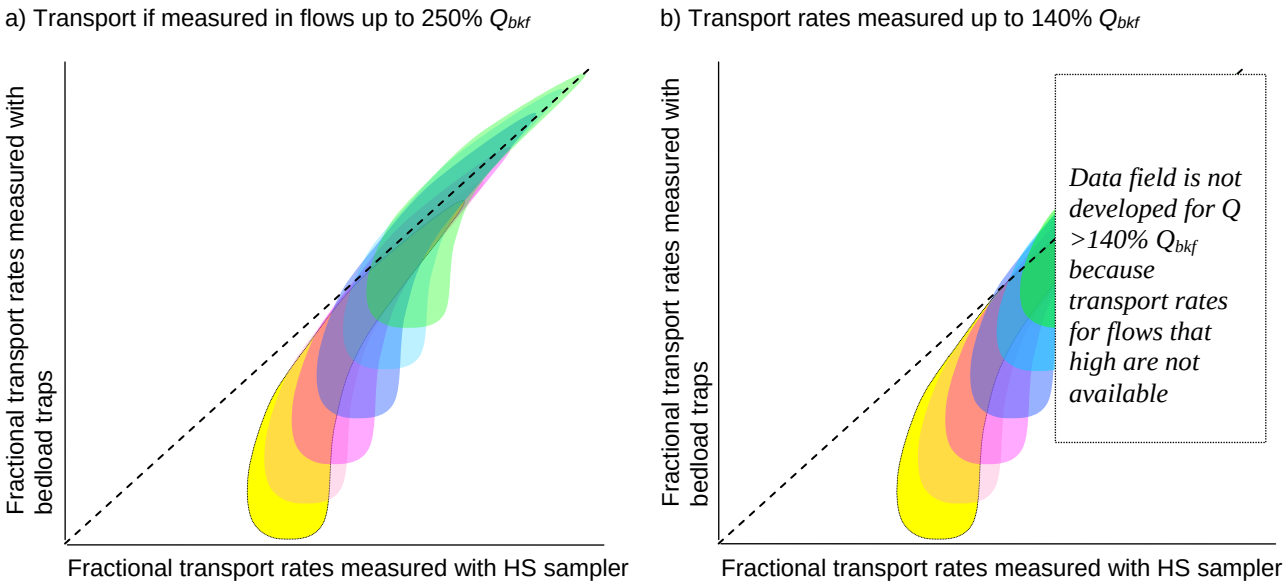

Figure 7: Data fields for inter-sampler fractional transport relationships take the shape of a downward-facing cornucopia. Particle-size classes increase with color spectrum from yellow (small gravel) via red and blue to green (coarse gravel). The trends would likely continue if transport rates were measured up to very high flows (left). Data fields are cropped at the upper portion when sampling is restricted to highflows up to 140% Q_{bkf} (right).

The pattern repeats, shifting upward and towards the right for increasing bedload particle sizes. The trend likely continues up to the 45-64 mm size class, the largest size to fit into the HS opening, if flows reach approximately 250% of bankfull and facilitate collection of 45-64 mm particles over a wide range of transport rates. Flows in the study streams did not exceed 140% of bankfull, thus 45-64 mm particles were just beginning to be collected in both samplers. Consequently, data pairs for the largest particle sizes in motion are scarce, and the upper-right part of the otherwise cornucopia-shaped data field remains undeveloped. A regression function fitted to the "cropped" data field suggests either an overly steep trend for the largest particle size in motion for a given stream, or one that is overly flat.

[3] The plotted data pairs are particularly scattered at Halfmoon Creek where the transport relationships measured with both samplers are already scattered. This is attributed to the multi-peaked hydrograph of the 2004 highflow season that peaked at about 76% of bankfull flow. In a coarse gravel-bed stream where pea gravel is supplied from low lying gravel bars and other instream deposits, this kind of flow patterns leads to hysteresis effects and large differences in transport rates for a specified flow, particularly at low and moderate flows (Thompson 2008).

The problem of undeveloped data fields was not limited to large gravel, but also occurred for smaller gravel when sampled flows did not exceed 80% Q_{bkf}. When only the lower portion of the potential data field exists, the full trend of the data from low to high flows is not developed. A fitted regression is then limited to the low-flow data that plot within a rounded or elongated field. The result is a fitted regression function that is too flat.

3.2.2.3 Fitting regression functions

To determine inter-sampler transport relationships, power functions and polynomial functions were fitted to data pairs from each size fraction as well as to total transport rates. All zero values (i.e., when transport rates for either the HS or the bedload trap or both were zero) were excluded from the data before fitting regressions. The remaining data were log-transformed.

a) **Power function regressions**

When the data field appeared to follow a straight-line shape, power function regressions were fitted to transport rates for each size class (i.e., linear functions fitted to log-transformed data).

$$q_{B\,traps,i} = a_i \cdot q_{B\,HS,i}^{\,bi} \tag{11a}$$

The regression functions are typically statistically significant (p-values << 0.05) for the smaller gravel sizes. Because the analysis is limited to non-zero transport rates for both samplers, the number of data pairs becomes small for the largest size classes in motion at a specific stream. As a result, p-values exceed 0.05, and this limits the possibility to formulate inter-sampler transport relationships for these particle sizes.

In order to formulate an inter-sampler transport relationship with which to adjust measured HS transport rates (F_{HSi}), the fitted power function (Eq. 11) needs to be multiplied by a bias correction factor CF

$$F_{HS,i} = q_{B\,traps,i} = a_i \cdot q_{B\,HS,i}^{\,bi} \cdot CF \tag{11b}$$

The Duan (1983) smearing function (CF_{Duan}) (Eq. 7) is used for the paired data sets because the standard errors s_y of the fitted power functions typically range between 0.6 and 0.8 which makes the Ferguson (1986, 1987) correction factor unsuitable.

b) **Polynomial functions**

In study streams where transport rates were measured with both samplers over a wide range of flows (up to 140% Q_{bkf}), plotted log-transformed data pairs take the shape of a downward-facing cornucopia (Figure 6 and Figure 7). Power functions poorly represent that data, and residuals obtained from a power function fit are not homoscedastically distributed. To better represent the curved, convex upward trend of the plotted data, second order polynomial functions in the form

$$y = ax^2 + bx + c \tag{12}$$

were fitted to the log-transformed data of transport rates from bedload traps (y) and the HS sampler (x). However, obtaining a visually satisfying fit was not straightforward.

In some cases, the data scatter for low values of *x* and *y* caused best-fit polynomial functions to have a concave upward instead of a convex upward trendline (Figure 8A). In another case, a wide *y*-range caused a maximum in the trend near the upper end of the *x*-data range (Figure 8B). Neither of the two features represents the trend of the plotted data. To yield a visually more satisfactory fit to the plotted data, auxiliary data points were generated, one at the lower and one at the upper end of the *x*-range, and in some cases one in the center of the *x*-range. Each auxiliary point was entered approximately10 times to the pool of data to which the polynomial function is fitted. Together with setting a visually determined best-fit *y*-intercept, these measures of guiding the polynomial function improved the visual fit to the plotted data (Figure 8C).

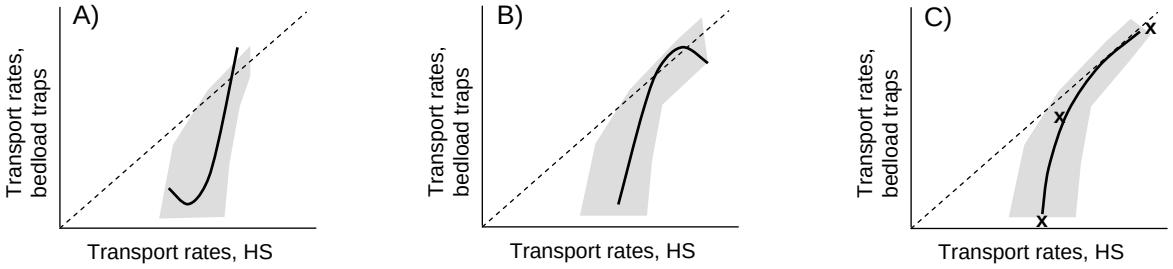

Figure 8: Shapes of second-order polynomial functions obtained by curve-fitting program. The gray-shaded area indicates the plotted field of data. **x** indicates auxiliary data points used to guide the fit.

Guiding the polynomial function did not achieve as much of an asymptotic approach of the fitted function to the 1:1 line (or a parallel to it) as desired. Thus, the fitted polynomial functions should not be extrapolated beyond the range of measured *x*-values (i.e., measured HS transport rates).

Polynomial functions fitted to log-transformed data cannot be easily back-transformed to linear units. Instead, the fitted function is used to predict log *y* for specified log *x*. The values of log *x* and the predicted values for log *y* values are then backtransformed (exponentiated). These predictions also require a bias correction similar to the bias correction required for *y*-values predicted from power functions fitted to log-transformed data in Section 3.2.2.3.a. However, computing the Duan smearing estimate from residuals of the fitted polynomial function was considered invalid because several data points had been added to guide the fit. Also, the correction factor to be applied to the guided polynomial function should be smaller than the one obtained from the power function because the guided polynomial functions had a visually better fit than the fitted power functions. Based on these considerations, Duan's smearing functions computed for the fitted power functions was used as bias correction for the polynomial functions but the computed value was reduced by 20% (= 0.8 CF_{Duan}). The inter-sampler transport relationships for polynomial functions were thus computed from

$$q_{bi\ traps} = (10\ \hat{}(a \log(q_{bi\ HS})^2 + b \log(q_{bi\ HS}) + c)) \cdot 0.8\ CF_{Duan} \quad (13)$$

Fitting polynomial functions was a workable solution. Nevertheless, a curve type that asymptotically approaches the 1:1 line or one of its parallels while facilitating a steep increase for small transport rates would have better represented the plotted data. Several alternatives may be explored in a mathematically more advanced data analysis. Those include hyperbolic functions, a LOWESS fit, and a breakpoint analysis[4].

3.2.2.4 Analyzing inter-sampler transport relationships

Similar to the rating curve approach, inter-sampler transport relationships for fractional and total transport rates were plotted in two different ways: 1) for individual study sites to analyze the difference among size classes and 2) over all sites to analyze the difference among study streams. To assess systematic differences following stream or transport characteristics, exponents and coefficients of the inter-sampler transport relationships were compared to parameters describing channel morphology as well as to exponents and coefficients of the bedload trap and HS rating curves.

4. Results

Results of the data analysis are shown and discussed separately for the rating curve as well as the paired data approach. For each approach, variability of inter-sampler transport relationships is analyzed among size fractions, and particularly among study streams. Different methods are applied to predict a HS adjustment function that best fit a specified study stream.

4.1 Rating curve approach

Fractional inter-sampler transport relationships computed are shown for all study streams (Figure 9). Parameters of the best-fit power functions for fractional the inter-sampler transport relationships are listed in Table 2. Data from St. Louis Creek ’98 are not included in the curve-fitting analysis because sample size and the range of measured flows are too small to show meaningful trends in fractional inter-sampler transport relationships. Fractional inter-sampler transport relationships for the other study streams generally have positive slopes. They intersect the line of perfect agreement (=1:1 line) at high transport rates and fall (mostly) far below the 1:1 line at low transport rates. These results show that the HS sampler collects transport rates several orders of magnitude higher than bedload traps when transport is low and that both samplers collect similar rates when transport is high. The plots in Figure 9 show that the pattern also holds for individual size fractions.

---

[4] A hyperbolic function can better represent data that asymptotically approach some axes than a parabolic function. However, fitting hyperbolic functions in which the axis of symmetry is not parallel to the *x*- or *y*-axes was mathematically too involved to be performed in this study.

Curved log-log relationships between paired transport data from the two samplers might be presented by a LOWESS fit, an iterative procedure called *locally weighted scatter-plot smoothing*. A LOWESS fit is computationally intensive and not suitable for a spreadsheet analysis. Besides, while providing the possibility for a visually pleasing trendline, the LOWESS fit does not yield a simple function to describe the data.

The ratio of transport rates measured with the two samplers might be describable with a breakpoint approach that finds the two least-square linear equations that can be fitted to a curved data set (in this case log-transformed transport data).

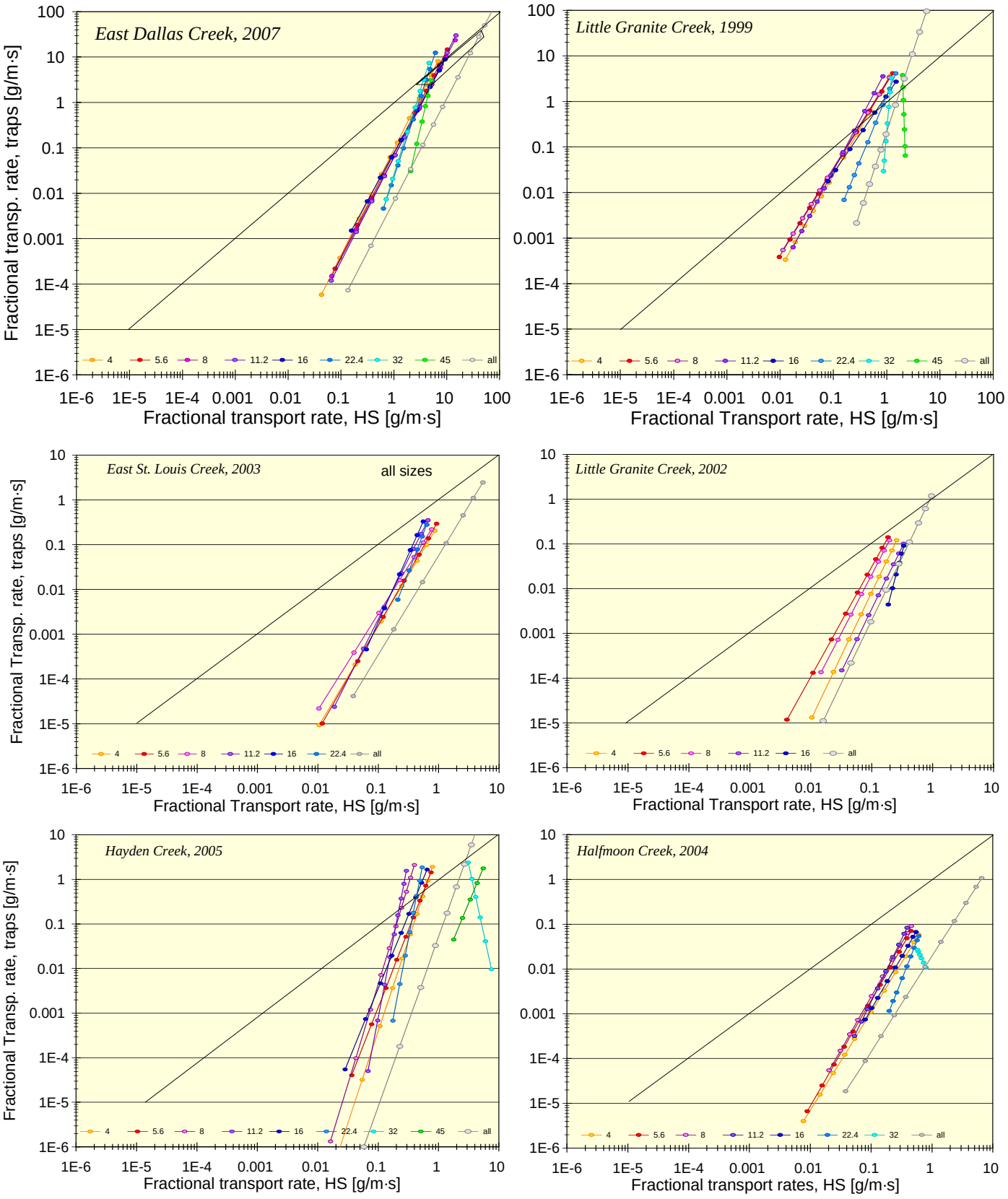

Fig. 9, continued on next page

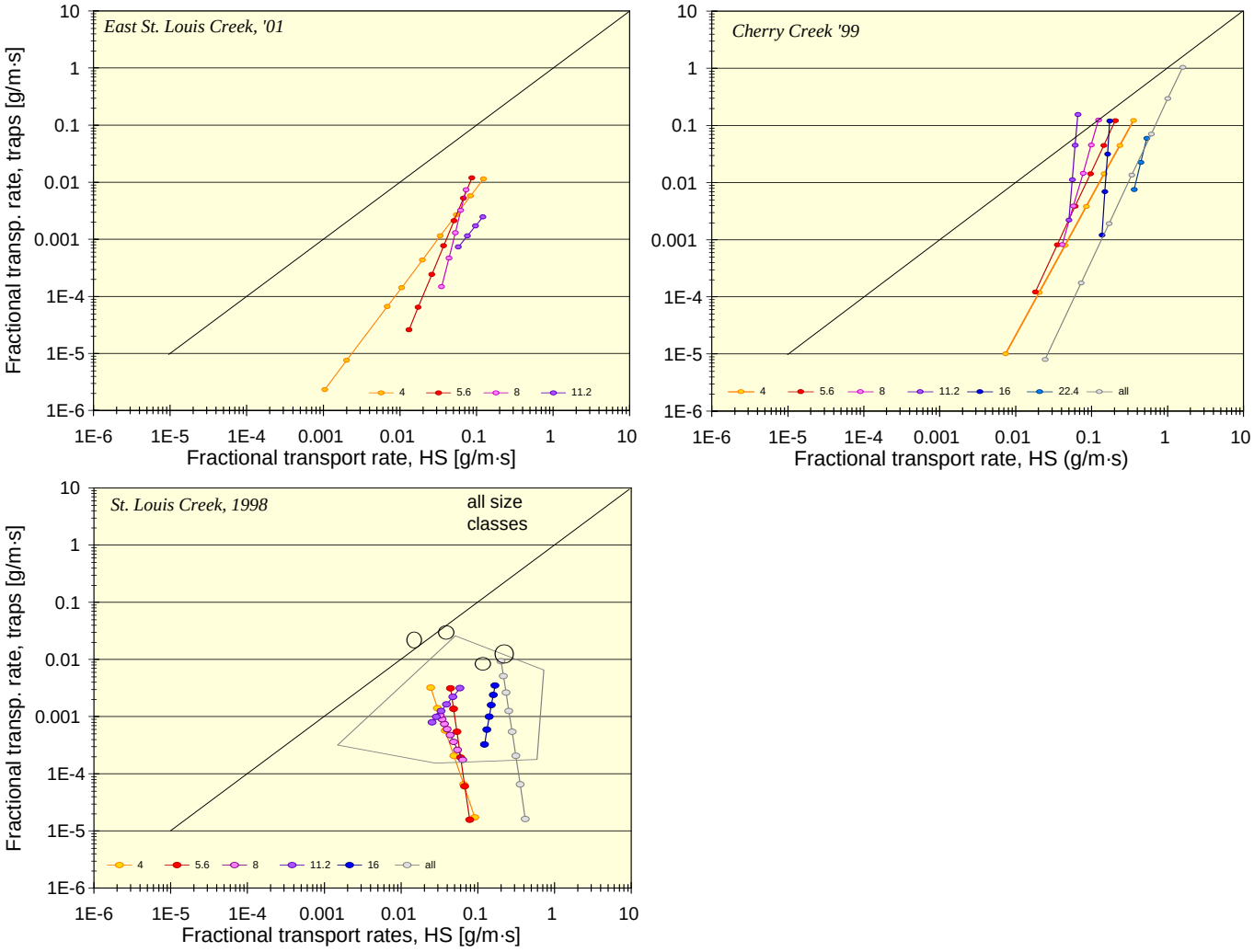

Figure 9: Rating curve approach: fitted inter-sampler transport relationships for individual gravel sizes classes as well as total gravel transport rates at all study streams.

Table 2: Parameters of best-fit power functions describing inter-sampler transport relationships for individual 0.5 phi particle-size fractions.

	4 - 5.6 mm		5.6 – 8 mm		8 - 11.2 mm		11.2 - 16 mm	
Study stream	*a*	*b*	*a*	*b*	*a*	*b*	*a*	*B*
East Dallas Creek	0.0911	2.33	0.0730	2.27	0.0616	2.23	0.0608	2.29
Halfmoon Creek	0.170	2.19	0.449	2.36	0.580	2.39	1.12	2.79
East St. Louis Cr. '03	0.283	2.27	0.351	2.35	0.390	2.14	1.04	2.69
East St. Louis Cr. '01	0.471	1.78	32.3	3.24	8911	5.36	-	-
Cherry Creek	1.48	2.42	10.8	2.84	1611	4.54	5.2E+17	15.7
Little Granite Cr. '99	2.68	2.05	2.49	1.89	2.66	1.89	5.05	2.22
Hayden Creek	4.82	4.11	3.88	3.48	124	4.46	8945	7.08
Little Granite Cr. '02	5.67	2.84	8.58	2.45	8.61	2.62	2.15	2.79

Table 2, continued on next page

Table 2, cont'd.

	16 – 22.4 mm		22.4 - 32 mm		32 – 45 mm		45 - 64 mm	
Study stream	*a*	*b*	*a*	*b*	*a*	*b*	*a*	*b*
East Dallas Creek	0.0760	2.12	0.0224	3.49	0.0249	3.71	7.26E-04	5.10
Halfmoon Creek	0.273	2.34	0.295	3.45	0.00573	-2.87	-	-
East St. Louis Cr. '03	1.94	3.03	1.35	3.50	-	-	-	-
East St. Louis Cr. '01	-	-	-	-	-	-	-	-
Cherry Creek	7.2E+13	19.5	1.61	5.30	-	-	-	-
Little Granite Cr. '99	1.35	1.71	1.31	2.85	0.194	13.9	-	-
Hayden Creek	6.89	3.30	151	7.09	-	-	-	-
Little Granite Cr. '02	24.6	5.16	-	-	-	-	-	-

$r^2 = 1$, and a bias correction factor *CF* is unnecessary (see also Sect. 3.2.1.4). Numbers printed in gray indicate that the fitted regression functions have *p*-values > 0.05, either for samples from bedload traps or, more likely, from the HS sampler (see Table 10, Appendix). Shading in red and blue marks streams classified as the "red" or "blue" groups (see explanation in Section 4.1.3.1).

4.1.1 Variability among bedload particle-size classes

Parallel trends for small gravel

Fractional inter-sampler transport relationships plot approximately parallel, at least for the smaller gravel sizes that are transportable and measurable in both samplers (Figure 9). In four of the study streams (East Dallas Creek, East St. Louis Creek '03, Little Granite Creek '99, and Halfmoon Creek), fractional inter-sampler transport relationships are nearly aligned. This indicates that sampling differences between traps and the HS sampler are similar, at least for the smaller gravel size classes (Figure 9). In the other four streams, transport relationships are "stacked" above each other, separated by a factor of 2-4 for increasingly coarser size classes (Hayden Creek, Little Granite Creek 02, and Cherry Creek). In these streams, the HS sampler collects more fine gravel than bedload traps.

Deviation from parallel trend for coarse gravel: sampling artifact

Inter-sampler transport relationships for the coarsest gravel size-classes that are mobile in a specified stream (typically size classes larger than 16, 22.4, or 32 mm depending on the highflow magnitude) deviate from the parallel trend and become steeper for increasingly larger particles. The slope may become negative. This pattern is most likely a computational artifact occurring when both samplers collected transport rates over a small range. If samples could have been collected in flows up to 250% of bankfull (which in high-elevation Rocky Mountain gravel-bed streams represents approximately the 50-year flood), transport relationships for the largest gravel particles would likely have been flatter and possibly attained slopes similar to or just slightly steeper than those for smaller gravel sizes (see also discussion in Section 3.2.2.2), however only up to the gravel size that fits into the HS opening.

4.1.2 Variability among streams

Inter-sampler transport relationships plotted for individual gravel size classes (Figure 10) as well as total gravel transport rates are combined for all study streams (Figure 11) and show the variability among streams. Analyses of variability among streams were limited to total gravel

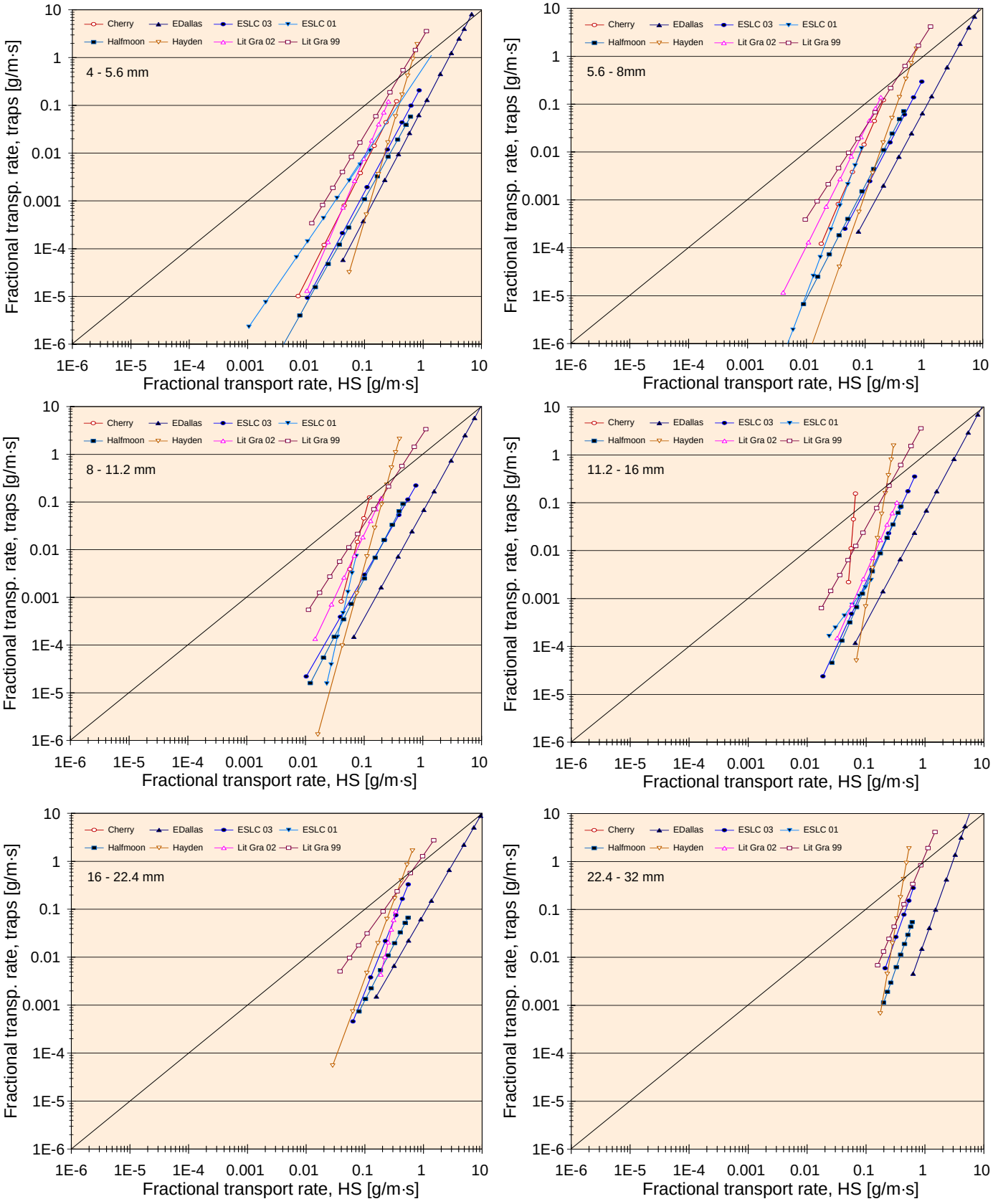

Fig. 10, continued on next page

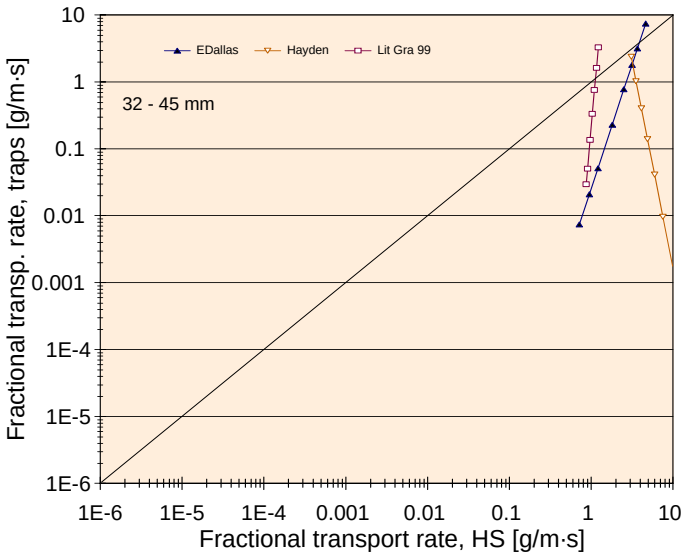

Figure 10: Rating curve approach: fitted inter-sampler transport relationships for individual gravel fractions combined for all study streams. Streams falling into the "red" group are indicated by reddish line colors and open symbols, streams in the "blue" group by bluish line colors and closed symbols (see Section 4.1.3.1 for explanations).

transport rates. The similarity of pattern observed for total transport rates with those for the smallest gravel size classes suggests that analyses could be extended to inter-sampler transport relationships of individual size classes, at least for smaller, well-sampled, gravels.

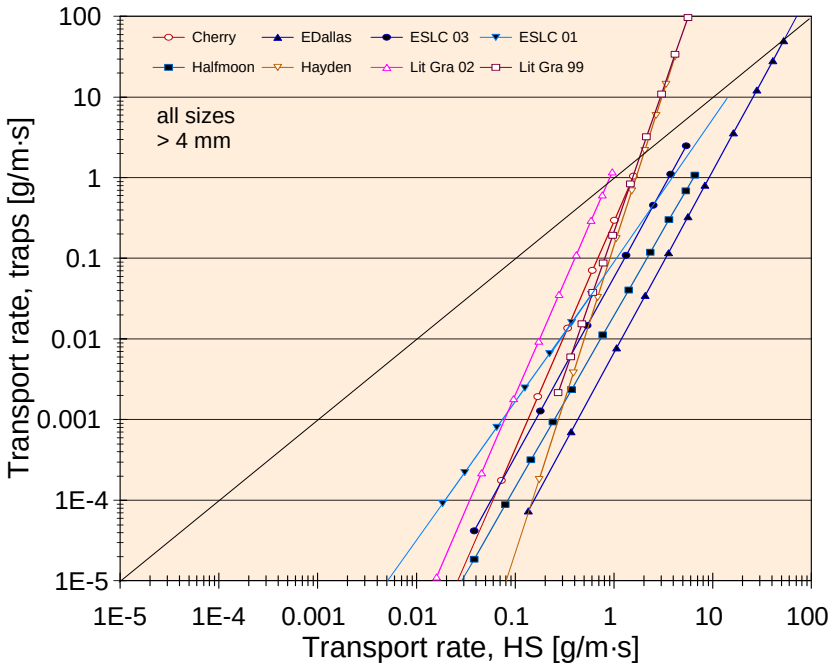

Figure 11: Inter-sampler transport relationships for total gravel transport obtained from rating curve approach plotted for all study streams. Streams within the "red" group have reddish line colors and open symbols, streams in the "blue" group have bluish line colors and closed symbols.

Trendlines for all the inter-sampler relationships of total gravel transport measured at low flows appear to originate within the range of 1E-5 to 1E-4 g/m·s for bedload traps and 0.01 – 0.1 g/m·s for the HS sampler (Figure 11). From this common starting point, inter-sampler transport relationships disperse for individual streams, assuming different steepness (*b*-exponents), different *a*-coefficients, and different intersections with the 1:1 line (Table 3). Several variables describing channel and bedmaterial characteristics as well as bedload transport were tried to predict the steepness, coefficients, and intersections with the 1:1 line of the inter-sampler transport relationships.

Table 3: Parameters of best-fit power functions as well as intersection with 1:1 line of inter-sampler transport relationships for total gravel transport rates and of inter-sampler bedload D_{max} relationships.

	Total gravel transport			Bedload D_{max} size			
Study stream	*a*	*b*	*1:1 line*	*a*	*b*	*1:1 line*	
East Dallas Creek	0.00659	2.26	54.5	1.97	0.0364	29.9	
Halfmoon Creek	0.0191	2.13	33.1	1.37	0.280	32.1	blue group
East St. Louis Cr. '03	0.0573	2.22	10.4	1.85	0.160	14.1	
East St. Louis Cr. '01	0.0870	1.72	29.7	1.18	0.739	5.52	
Cherry Creek	0.285	2.82	1.99	3.22	0.00417	11.9	
Little Granite Cr. '99	0.210	3.55	1.85	2.17	0.0489	13.2	red group
Hayden Creek	0.0498	3.81	2.91	2.27	0.0182	23.6	
Little Granite Cr. '02	1.30	2.82	0.87	8.65E-5	5.15	4.53	

$r^2 = 1$, and a bias correction factor *CF* is unnecessary (see also Sect. 3.2.1.4). All bedload rating curves from which inter-sampler transport relationships were derived have *p*-values >> 0.05 (see Table 10, Appendix). Shading in red and blue marks streams classified as the "red" or "blue" group (see explanation in the text below).

4.1.2.1 Channel and bedmaterial characteristics

The channel and bedmaterial characteristics such as bankfull flow, basin area, bankfull stream width, stream gradient, surface D_{50} and D_{84} sizes, the percent surface and subsurface sediment < 2 and < 8 mm, as well as the subsurface D_{50} and D_{84} sizes did not show a statistically significant correlation with the exponents or coefficients of power functions describing inter-sampler relationships for total gravel transport rates. However, the steepness of these fitted power functions was found to decrease for streams that are well armored[5] (Eq. 15). The correlation is statistically significant ($p < 0.05$) and suggests that exponents of the inter-sampler transport relationship (*b*) may be predictable from the extent of bed armoring (D_{50surf}/D_{50sub}).

[5] Armoring is the ratio D_{50surf}/D_{50sub}. In the study streams, a high degree of armoring was typically caused by high percentages of subsurface fines < 8 mm. Thus, armoring and the % subsurface fines < 8 mm are positively related. Size distributions of surface and subsurface sediment are affected by the methods used to sample bedmaterial, sample size, and methods of particle-size measurements (Bunte and Abt 2001; Bunte et al. 2009b). In this study, a sampling frame was used for pebble counts, and more than 400 particles were collected over the bankfull width of a reach; particle sizes were measured using a template; several large subsurface samples were collected per site using a plywood shield to shelter a 2 by 2 ft (0.36 m^2) area from flow.

$$b = 5.73\ (D_{50surf}/D_{50sub})^{-1.21} \quad (14)$$

with $r^2 = 0.69$, $n = 8$, $p = 0.0112$, $s_y = 0.071$

4.1.2.2 Effects of gravel transport characteristics

Conditions of gravel transport in a specified stream can be described by the steepness and coefficients of the gravel bedload rating and the flow competence curves measured with bedload traps. The study found that inter-sampler transport relationships are affected by a stream's transport and flow competence curves. Inter-sampler transport relationships intersect the 1:1 line at lower values in streams with steep bedload trap flow competence curves ($r^2 = 0.53$, $p = 0.041$), while inter-sampler transport relationships decrease in steepness with increasing rating curve coefficients in a marginal way ($r^2 = 0.39$, $p = 0.0971$) (Table 11, Appendix). Streams with steeper rating and flow competence curves tend to have relatively large differences between bedload trap and HS measurements, while in streams with less steep rating and flow competence curves both samplers measure more similar results.

4.1.2.3 Effects of HS sampling results

It would be beneficial if HS correction functions could be predicted directly from HS sampling results, without bedload trap measurements. However, none of the HS rating or flow competence curve parameters showed a relationship with *b*-exponents and *a*-coefficients of inter-sampler transport relationships, nor with intersections at the 1:1 line (Table 13, Appendix).

4.1.3 Segregation of inter-sampler transport relationships into groups

Section 4.1.2.3 indicated that steeper inter-sampler transport relationships and lower intersections with the 1:1 line occur in poorly armored streams. These streams also have steep bedload transport rating and flow competence curves (Bunte et al. 2006) (Figure A5, left). However, the relationships were not sufficiently defined to predict inter-sampler transport relationships for individual streams. The one exception was the parameter armoring that has a moderately well defined correlation ($r^2 = 0.69$, $p = 0.0112$, Eq. 15**Error! Reference source not found.**) but is laborious to measure in coarse-bedded streams. In order to simplify the prediction of inter-sampler transport relationships that are best suited for a specified stream, predictions were attempted for stream groups that share common characteristics, rather than for individual streams.

4.1.3.1 Visual segregation into two groups

Based on the steepness and the point of intersection with the 1:1 line, inter-sampler relationships for total gravel transport can be visually segregated into two groups: one group with relatively steep inter-sampler transport relationships (plotted in reddish colors and with a reddish shading in Figure 12: Cherry Creek, Hayden Creek Little Granite Creek '99, and Little Granite Creek '02) and one with flatter relationships (plotted in bluish colors and a bluish shading: East Dallas Creek, East St. Louis Creek '01, East St. Louis Creek '03, and Halfmoon Creek). Inter-sampler transport relationships of the steep (red) group have exponents of 2.8 – 3.8 and intersect the 1:1 line around 1 - 3 g/m·s, i.e., the two samplers obtain similar sampling results during moderate

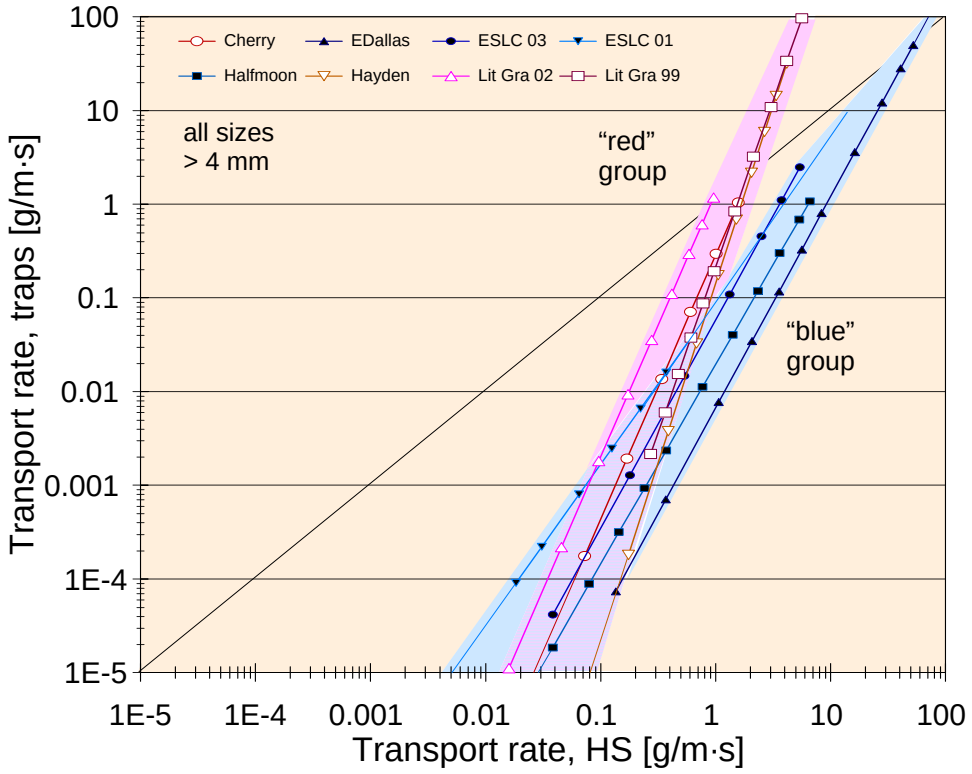

Figure 12: Inter-sampler transport relationships for total gravel transport obtained from rating curve approach plotted for all study streams. Streams falling into the "red" group are indicated by reddish line colors, open symbols, and red shading, streams in the "blue" group by bluish line colors, closed symbols, and blue shading.

transport (Table 3). Within the flat (blue) group, exponents range from 1.7 – 2.3 and intersections of the 1:1 line from 10 - 55 g/m·s, i.e., both samplers provide similar results when transport is high. A *t*-test with a 0.05 confidence level showed that the mean exponents, coefficients, and intersections with the 1:1 line computed for each of the two stream groups are significantly different among the two groups, and this supports the validity of the visual segregation. For fractional inter-sampler transport relationships, segregation into two groups is visually justifiable for the three (or four) smallest gravel size classes, but deviates for larger gravel sizes, most likely because inter-sampler transport relationships are not computed accurately when particle size classes are not sampled over a sufficiently wide range of transport rates.

4.1.3.2 Average inter-sampler transport relationships for both stream groups

Fractional and total gravel transport

To attain group-averaged inter-sampler transport relationships, the arithmetic means of the four exponents and the geometric means of the four coefficients were computed of the blue and red groups (Table 4) and plotted (Figure 13 a and b). Only inter-sampler transport relationships derived from rating curves with *p*-values < 0.05 (<0.1 in a few exceptions) were included in the

computation. These group-averages were computed for both fractional and total transport rates. Exponents and coefficients in Table 4 provide adjustment functions to convert fractional and total transport rates collected with a 3-inch, thin-walled, HS sampler to those collected with bedload traps in streams falling into the blue and red groups. The group-averaged inter-sampler transport relationship for total gravel transport rates are (Table 4):

$$F_{HS} = q_{B\,traps} = 0.249 \cdot q_{B\,HS}^{\,3.25} \quad \text{(red group: less armoring, less subsurface fines, Steeper rating and flow competence curves)} \tag{15}$$

and

$$F_{HS} = q_{B\,traps} = 0.0282 \cdot q_{B\,HS}^{\,2.08} \quad \text{(blue group: more armoring, more subsurface fines, flatter rating and flow competence curves)} \tag{16}$$

Table 4: Exponents and coefficients of inter-sampler transport relationship for individual size classes, total gravel transport rate, and the bedload D_{max} size averaged over the four streams falling into the "red" and "blue" stream groups.

		> 4 mm	>5.6 mm	>8 mm	>11.2 mm	>16 Mm	>22.4 mm	total gravel transport	D_{max} mm	Avg. for any 0.5 phi size class	
Geom. mean	a-coeff.	0.213	0.781	0.241	0.414	0.343	0.207	0.0282	0.168	**0.325**	"blue" stream group
Arith. mean	b-exp.	2.14	2.56	2.25	1.94	1.87	2.61	2.08	1.59	**2.23**	
CV(%)	a-coeff.	143	145	965	174	207	434	1789	334	**68.1**	
CV(%)	b-exp.	11.6	18.0	69.1	67.6	69.8	66.7	11.9	23.9	**13.7**	
Geom. mean	a-coeff.	3.23	5.48	46.2	-	-	-	0.249	0.00423	**9.35**	"red" stream group
Arith. mean	b-exp.	2.85	2.67	3.38	-	-	-	3.25	3.20	**2.97**	
CV(%)	a-coeff.	8.24	5.43	2.69	-	-	-	233	28574	**6.55**	
CV(%)	b-exp.	31.3	25.1	39.3	-	-	-	15.5	43.2	**12.5**	

Bedload D_{max} particle sizes

Inter-sampler bedload D_{max} relationships were combined for all study streams in Figure 14 (left). The exponents, coefficients, and intersections with the 1:1 line were checked for possible relatedness to exponents and coefficients of bedload rating and flow competence curves measured with both samplers (Table 12, Appendix). No statistically significant relationships were found with bedload trap measurements. However, *b*-exponents of the inter-sampler bedload D_{max} relationships at the study streams are negatively related to the HS-measured flow competence exponent ($r^2 = 0.64$; $p = 0.0176$), while the *a*-coefficients are positively related the HS-measured flow competence exponent ($r^2 = 0.77$; $p = 0.0044$) (Table 14, Appendix). HS sampling characteristics appear to affect the inter-sampler bedload D_{max} relationships.

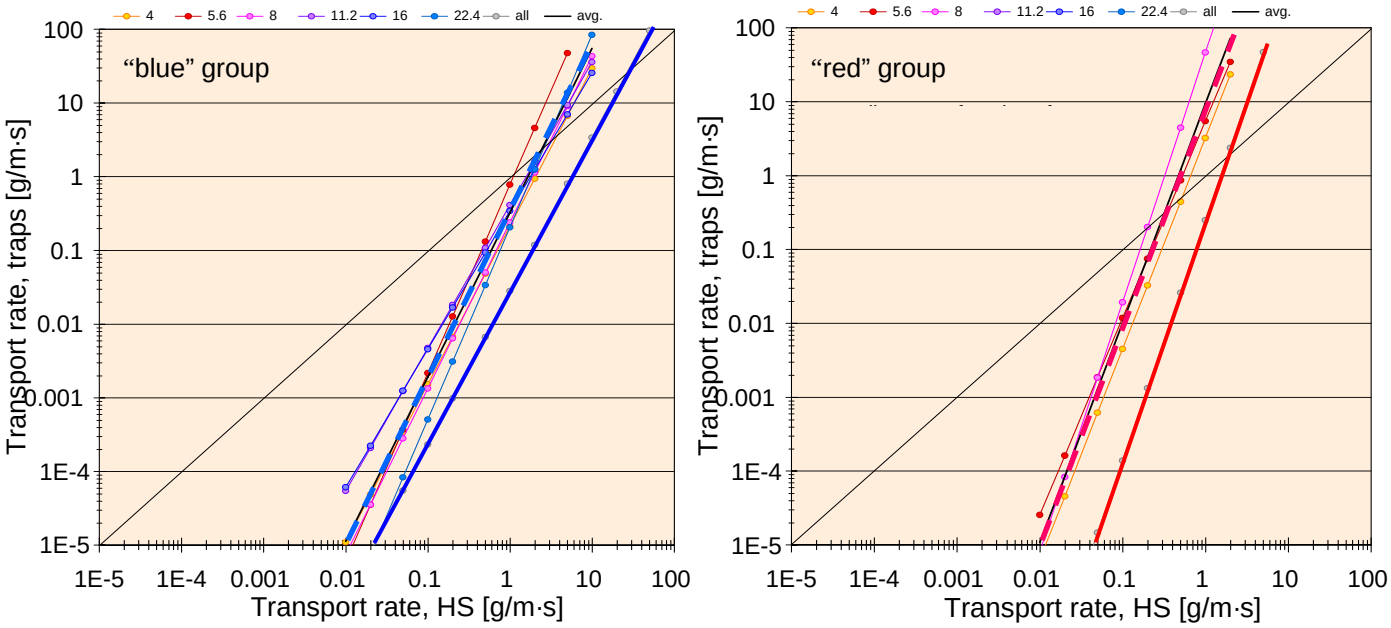

Figure 13: Fractional inter-sampler transport relationships averaged over the four "blue" (left) and "red" (right) streams. The color scheme used to mark individual size fractions follows the one used for size fractions throughout the study. The dashed thick blue and red lines indicate the average inter-sampler transport relationship applicable to any 0.5 phi gravel size fraction over the four "blue" and "red" streams. Solid thick blue and red lines show group-averaged inter-sampler transport relationships for total gravel transport.

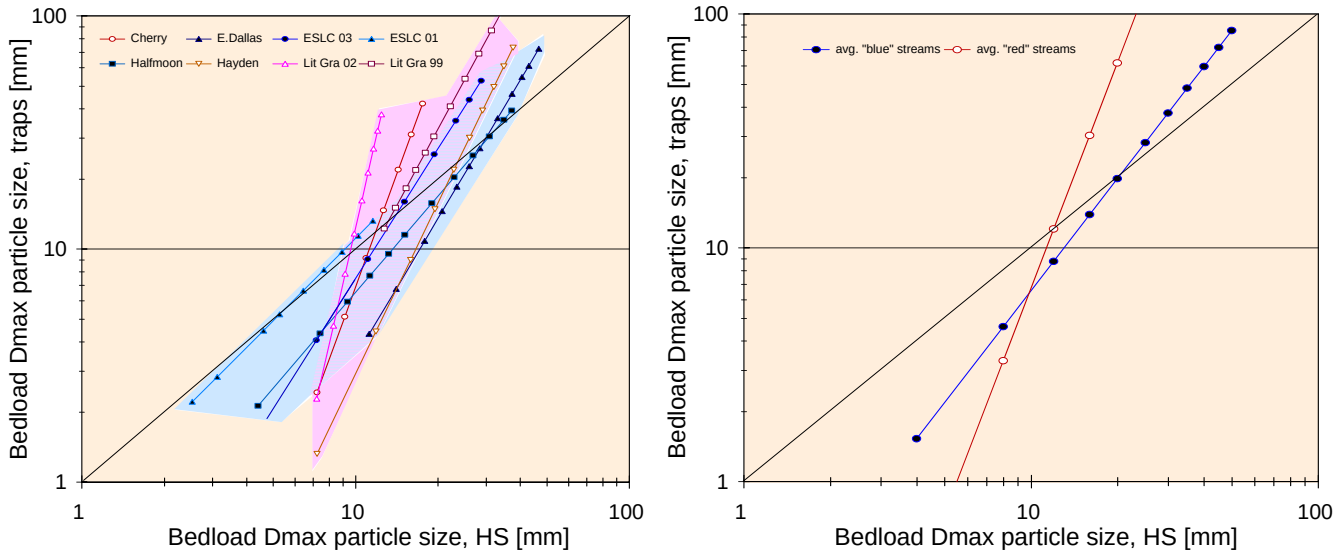

Figure 14: Inter-sampler relationships of bedload D_{max} particle sizes collected with bedload traps and the HS sampler at all study sites (left). Red and blue shading highlights streams of the "red" and "blue stream groups. Bedload D_{max} particle size relationships averaged over study streams within "red" and "blue" stream groups (right).

Segregation of inter-sampler bedload D_{max} relationships computed into two groups is less obvious than for inter-sampler transport relationships. However, a significant difference in *a*-coefficients as well as *b*-exponents between streams falling in the red and the blue groups suggests that a separation into two stream groups is appropriate (Figure 14, right). It is further supported that the streams falling into the "red" and "blue" groups are the same for inter-sampler relationships of both bedload D_{max} particle sizes and total gravel transport rates. Streams that have flatter inter-sampler relationships for bedload D_{max} particle sizes (blue group) have flatter inter-sampler transport relationships. By contrast, streams in the red group have steeper inter-sampler relationships for bedload D_{max} particle sizes and show steeper transport relationships (Table 4) (compare Figure 14 (left) with Figure 11).

Exponents of the inter-sampler relationships for bedload D_{max} sizes were averaged arithmetically over the two stream groups; coefficients were averaged geometrically. The averaged exponents and coefficients in Table 4 provide adjustment functions for the "red" and "blue" stream groups to convert D_{max} particle sizes collected with a 3-inch, thin-walled, HS sampler to those that might have been collected with bedload traps.

$$F_{HS} = D_{max,traps} = 0.00423 \cdot D_{max,HS}^{3.20} \qquad \text{(red group)} \qquad (17)$$

and

$$F_{HS} = D_{max,traps} = 0.168 \cdot D_{max,HS}^{1.59} \qquad \text{(blue group)} \qquad (18)$$

4.1.3.3 Averaging over all size classes within the two stream groups

Inter-sampler fractional transport relationships averaged over the two stream groups fell within a narrow band for all individual size classes (Figure 13), suggesting that within the two groups inter-sampler transport relationships are relatively similar for all 0.5 phi size fractions. The relative similarity suggests that exponents and coefficients of inter-sampler transport relationships may be averaged over all size fractions to attain an inter-sampler transport relationship applicable to any 0.5 size fraction, i.e., one relationship for the steep (red) stream group and one for the flat (blue) stream group (see Figure 13 and the last column in Table 4). The resulting correction functions for any 0.5 phi size class are:

$$F_{HS} = q_{B\,trap,f} = 9.35 \cdot q_{B\,HS,f}^{2.97} \qquad \text{(red group: less armoring, less subsurface fines, Steeper rating and flow competence curves)} \qquad (19)$$

and

$$F_{HS} = q_{B\,trap,f} = 0.325 \cdot q_{B\,HS,f}^{2.23} \qquad \text{(blue group: more armoring, more subsurface fines, flatter rating and flow competence curves)} \qquad (20)$$

These relationships may serve to convert fractional gravel transport rates of any 0.5 phi size class collected with the HS sampler to those that might have been collected with bedload traps for streams in the blue and red groups, respectively. The correction functions for a 0.5 size class (Eq. 19 and 20) differ by more than one order of magnitude from the group-averaged inter-sampler transport relationship for total gravel transport rates (Eqs. 15 and 16) (Figure 13).

4.1.3.4 Bedmaterial and bedload conditions in "red" and "blue" streams

Average values of bedmaterial parameters for the "blue" and "red" stream group were evaluated for statistical difference based on whether the 95% confidence interval around the group means overlapped. Mean values of bed armoring were statistically different between the two groups. Similarly, the arithmetic mean of exponents and the geometric mean of coefficients of bedload rating and flow competence curves measured with bedload traps are statistically different between the "red" and the "blue" stream groups. The midpoints between the means for the two stream groups were considered threshold values to indicate whether inter-sampler transport relationship of the "red" or "blue" group should be used for adjustment of HS-sampled transport rates. For HS samples, only the coefficients of the bedload rating and flow competence curves were statistically different between the red and blue stream groups.

The threshold values for bedmaterial and bedload conditions are compiled in Table 5 and may be used to categorize a study stream as either a "red" or "blue" stream. For example, for a coarse-bedded mountain stream with armoring of less than 1.96, and a HS-measured rating curve coefficient < 0.094, conversion functions obtained for the "red" stream group might be used to adjust HS sampling results. Threshold values in Table 5 are applicable in a strict sense only if the highest four values of any parameter fall into one group while the lowest ones fall into the other. Because this is rarely the case, each threshold has some variability. The user should therefore consider threshold values of several parameters before classifying a study stream.

If the characteristics of a study stream do not fall clearly into one of the stream groups, the user might compare the characteristics of the stream with those listed in Table 1. For conversion of HS sampling results, the inter-sampler transport relationships determined for a specific stream might then be used.

4.1.3.5 Using a correction function to adjust a HS rating curve

To arrive at an adjusted HS rating curve for the study streams, the exponent *b* and coefficient *a* of the respective inter-sampler transport relationships (i.e., correction function) is applied to the measured HS power function rating curve ($Q_{B\,HS} = c \cdot Q^{b}$) to yield

$$q_{B\,traps} = F_{HS} = a \cdot (c \cdot Q^{d})^{b} \tag{21}$$

The exponents and coefficient of the adjusted HS rating curve can then be computed analytically or be obtained via a curve-fitting analysis. Comparing adjusted HS rating curves with those measured using bedload traps shows that for three of the "blue" stream groups, adjusted HS rating curves deviate less than a factor of 2 from the measured bedload trap rating curve. The deviation was more than one order of magnitude for East St. Louis Creek '01, for which the

Table 5: Bedmaterial characteristics and conditions of bedload transport that determine the stream group and the respective inter-sampler relationships (rating curve approach).

	Streams in "red" group	Stream in "blue" group
<u>For bedmaterial conditions of:</u>		
Armoring ($D_{50\,surf}/D_{50\,sub}$)	< 2.0	> 2.0
<u>For bedload conditions measured with bedload trap:</u>		
Exponent of bedload rating curve	> 8.9	< 8.9
Coefficient of bedload rating curve	< 1.1E-4	> 1.1 E-4
Exponent of flow competence curve	> 1.9	< 1.9
Coefficient of flow competence curve	< 5.30	> 5.30
Bedload D_{max} (mm) at 50% Q_{bkf}	< 11	> 11
Gravel transport rate (g/m·s) at 50% Q_{bkf}	< 0.001*	> 0.001*
Bedl. D_{max} (mm) at gravel transp. rate of 1 g/m·s	> 40	< 40
<u>For bedload conditions measured with HS sampler:</u>		
Exponent of bedload rating curve	< 3.4*	> 3.4*
Coefficient of bedload rating curve	< 0.094	> 0.094
Exponent of flow competence curve	> 0.91*	< 0.91*
Coefficient of flow competence curve	< 9.7	> 9.7
Bedload D_{max} (mm) at 50% Q_{bkf}	< 13*	> 13*
Gravel transport rate (g/m·s) at 50% Q_{bkf}	< 0.15*	> 0.15*
Bedl. D_{max} (mm) at gravel transp. rate of 1 g/m·s	< 18*	> 18*
<u>Inter-sampler transport relationships that may be used to adjust HS measurements:</u>		
For any size 0.5 phi size fraction	Eq. 19: $q_{B\,traps,f} = 9.35\ q_{B\,HS,f}^{2.97}$	Eq. 20: $q_{B\,traps,f} = 0.325\ q_{B\,HS,f}^{2.23}$
For total gravel transport rates	Eq. 15: $Q_{B\,traps} = 0.249\ Q_{B\,HS}^{3.25}$	Eq. 16: $Q_{B\,traps} = 0.0282\ Q_{B\,HS}^{2.08}$
For bedload D_{max} particle size class	Eq. 17: $D_{max\,traps} = 0.00423\ D_{max\,HS}^{3.20}$	Eq. 18: $D_{max\,traps} = 0.168\ D_{max\,HS}^{1.59}$

* Difference between red and blue stream group not statistically significant. Red and blue shading refers to "red" and "blue" stream groups.

original HS rating curve was measured over a small range of flows. These results are encouraging but also emphasize the importance of using HS measurements that extend over a wide range of flow. A user must note that inter-sampler transport relationships presented in this study were obtained in mountain-gravel bed streams. The adjustment functions suggested for conversion of HS sampling results should therefore be applied to streams with similar characteristics as the study streams.

Summary for rating curve approach

Inter-sampler transport relationships were computed for all streams and for all particle size classes as well as for total transport rates and the bedload D_{max} sizes. The variability of fractional inter-sampler transport relationships among size classes is generally less than expected, although some streams indicate that the difference between the two samplers is greatest for the smallest gravel sizes.

Inter-sampler transport relationships vary among streams. The relationships are flatter in streams that are well armored and have high amounts of subsurface fines < 8 mm; the correlation with armoring is sufficient to serve as a prediction. Bedload transport characteristics as measured with bedload traps also affect inter-sampler transport relationships; the intersection with the 1:1 line decreases with the steepness of flow competence curves. For example, at Little Granite Creek (1999) with a flow competence curve exponent of 2.98, both samplers yield similar results at a relatively low transport of about 1 g/m·s, whereas at East Dallas Creek with a flow competence curve exponent of 1.32, similar results for both samplers are obtained at a transport rate of about 26 g/m·s. Similarly, inter-sampler transport relationships are steeper for streams with lower rating curve coefficients. At Little Granite Creek (1999) with a bedload trap rating curve coefficient of 7.3E-12, the inter-sampler transport relationship has an exponent of 3.5, while at East St. Louis Creek (2001) with a rating curve coefficient of 3.9, the exponent of the inter-sampler transport relationship was 2.1. Inter-sampler transport relationships were unrelated to transport measurements made with a HS sampler, making it very difficult to determine conversion functions based on HS measurements alone.

Inter-sampler transport relationships can be visually and statistically segregated into two groups: one with flatter trendlines that intersect the 1:1 line at high values (blue group) and one with steeper trendlines that intersect the 1:1 line at lower values (red group). This allows inter-sampler transport relationships to be reduced to two cases: those applicable to the “red” and those to the “blue” stream group. The similarity of fractional inter-sampler transport relationships among individual size classes and within each of the two stream groups suggests that one inter-sampler transport relationship may apply to any 0.5 phi gravel size fraction. This reduces the number of inter-sampler transport relationships needed to convert HS sampling results to those that might have been collected with bedload traps to six: one for fractional transport rates of any 0.5 size class, one for total gravel transport, and one for bedload D_{max} particle sizes for each the “red” or the “blue” stream group.

Several bedmaterial parameters as well as the exponents and coefficients of bedload rating and flow competence curves measured with bedload traps (and to some degree also measured with a HS sampler) were statistically different for streams falling in to the “red” and “blue” stream groups. The blue group occurs in streams with more armoring, higher amounts of subsurface fines < 8 mm, and steeper bedload rating and flow competence curves. This segregation opens the possibility of placing a study stream either into the “red” or the “blue” stream group. The respective inter-sampler transport relationship is then selected, and its coefficient and exponent are applied to the measured HS rating curve.

4.2 Paired data approach

Power and polynomial functions that were fitted to plotted data pairs (see Figure 6) describe the inter-sampler transport relationships for fractional and total transport rates obtained at each study stream from the paired data approach. At sites with relatively small sample sizes and narrow ranges of measured transport rates, power functions provided a visually acceptable fit to the plotted data (East St. Louis Creek '03, Cherry Creek, Little Granite Creek '02, and Halfmoon Creek). Polynomial functions were visually more satisfying at sites with larger sample sizes and a wider range of sampled transport rates (East St. Louis Creek '01, East Dallas Creek, Hayden Creek, and Little Granite Creek '99) (Figure 15).

Inter-sampler transport relationships obtained from the paired data approach or intersect the 1:1 line at moderate to high transport rates and fall below the 1:1 line when transport is low (Figure 15). Regression functions for data sets with low sample size or a narrow range of measured transport rates have flatter slopes (Little Granite Creek '02, East St. Louis Creek '01, and Halfmoon Creek) than other streams. There are two explanations for the flatness: one is that the data range was too narrow to reflect the well developed, steep trend otherwise seen in inter-sampler-transport relationships (see Figure 7). Another is that a fitted straight function tends to be overly flat in data sets that extend over a narrow x-range and have a lot of scatter.

Fitted power functions were statistically significant ($p < 0.05$) for the two smallest size classes (4 – 5.6 and 5.6 – 8 mm) as well as for total gravel transport rates, but not necessarily for the coarsest gravel sizes. The goodness-of-fit for the polynomial functions is difficult to assess because guiding the function (Section 3.2.2.3) makes statistical measures of fit such as r^2 and *p*-values meaningless. Inter-sampler transport relationships are formulated using the *a*- and *b*-parameters from fitted power functions and have the form $F_{HS} = Q_{B,traps} = a\ Q_{B,HS}^{\ b}$ (Table 6). For fitted polynomial functions (Eq. 13), the *a*-, *b*-, and *c*-coefficients in Table 6 need to be used with Eq. 14.

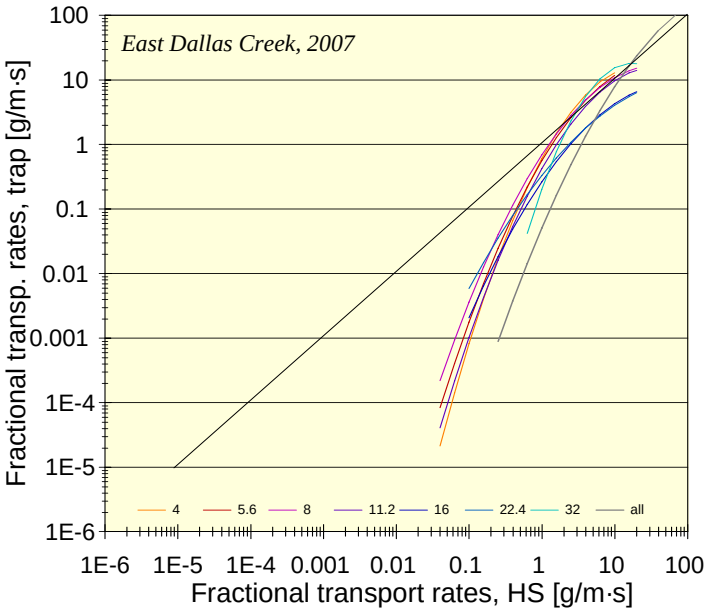

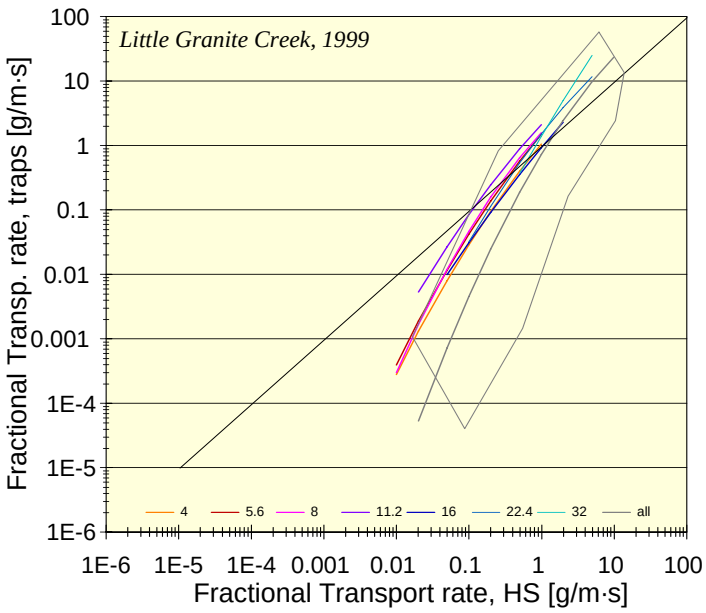

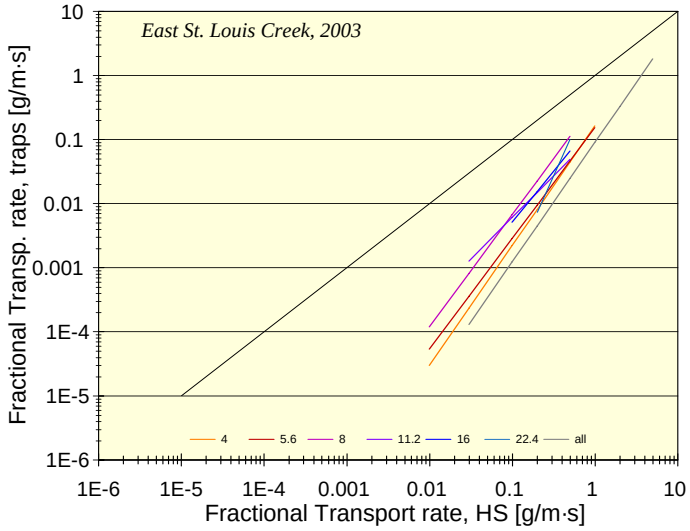

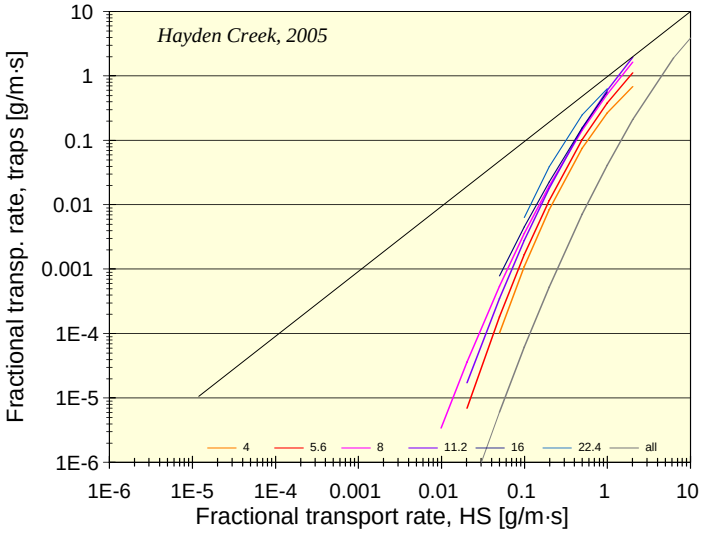

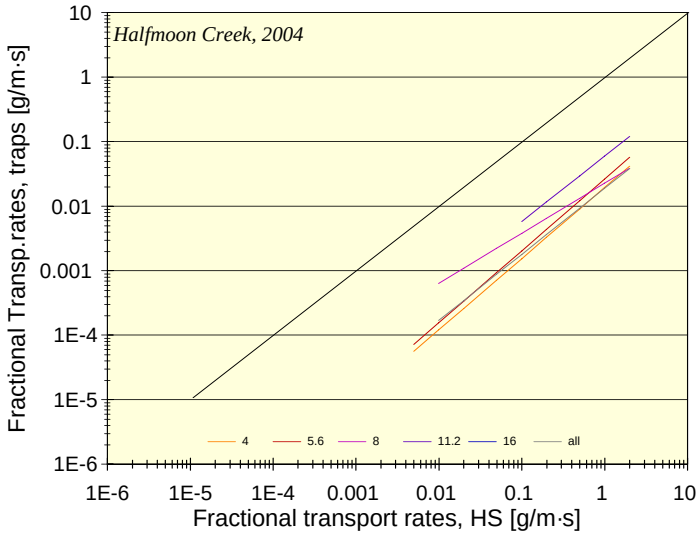

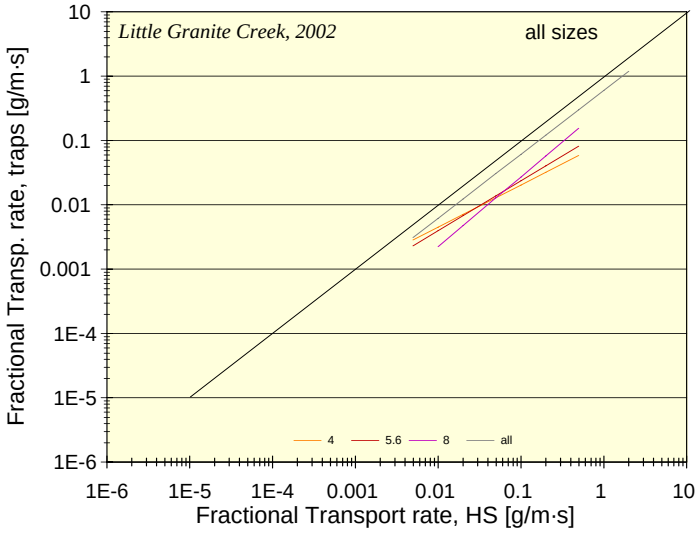

Fig. 15, continued on next page

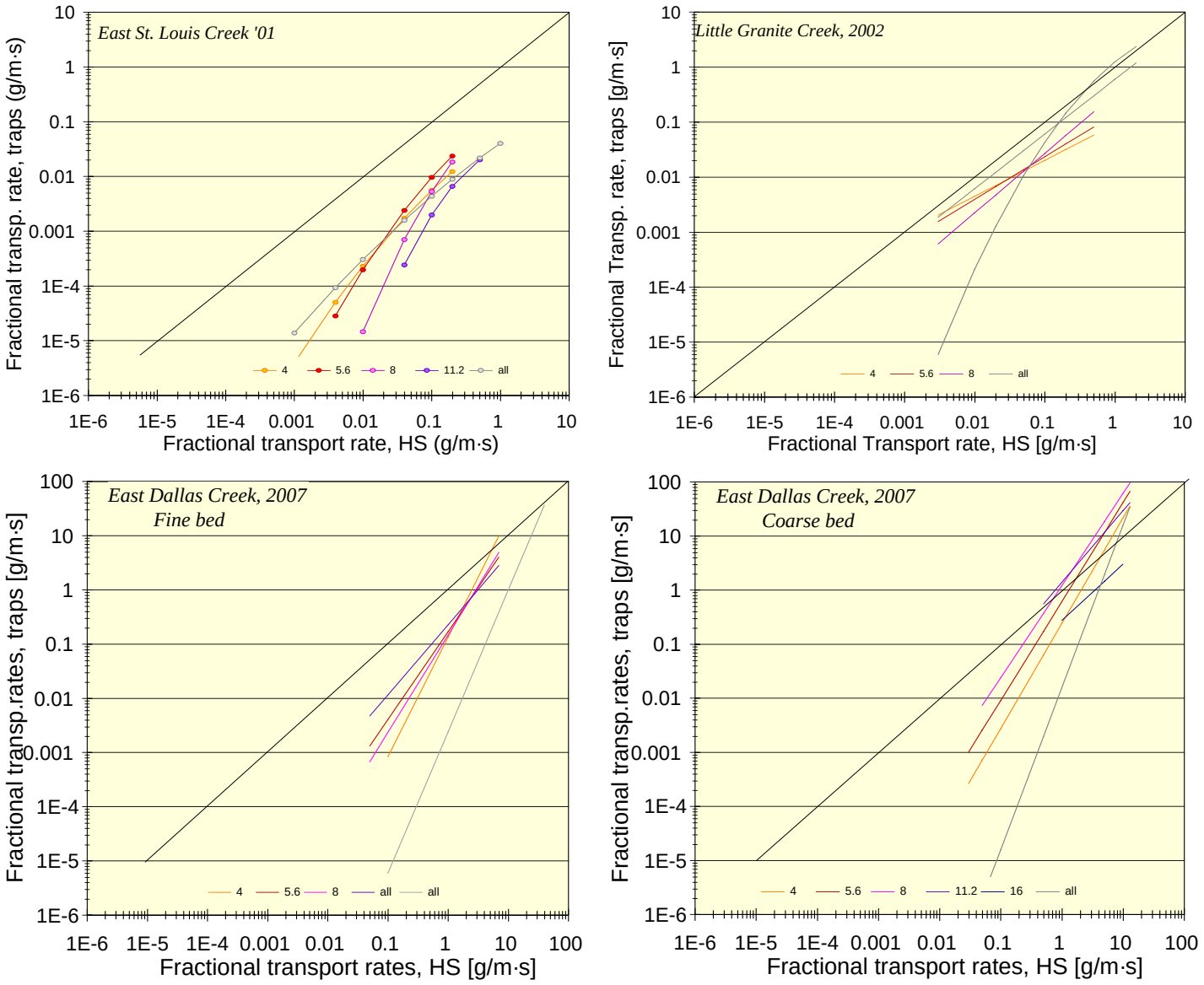

Figure 15: Paired data approach: fitted inter-sampler transport relationships for individual gravel sizes classes and total gravel transport at all study streams.

Table 6: Parameters of power functions (*a*-coefficient and *b*-exponent, no value for *c*) and polynomial functions (*a*-, *b*-, and *c*-coefficients) fitted to inter-sampler transport relationships for individual size fractions and total gravel transport rates using the paired data approach. Also given are number of non-zero samples (*n*), coefficient of variation (r^2), *p*-value (*p*), the standard error of the *y*-estimate (s_y), as well as bias correction factors after Ferguson (1986, 1987) (CF_F) and Duan (1983) (CF_D) obtained for fitted power functions.

		Streams in "blue" stream group						Streams in "red" stream group			
Size class (mm)	Para-meter	East Dallas Cr.	E. Dallas fine bed	E. Dallas coarse bed	Half-moon Cr.	E. St. Louis Cr. '03	Hayden Cr.	E. St. Louis Cr. '01	Cherry Cr.	Little Granite Cr. '99	Little Granite Cr. '02
4-5.6	*n*	53	30	34	35	38	24	72	14	40	14
	a	-0.772	0.0141	0.0533	0.00752	0.113	-0.809	-0.193	0.7	-0.226	0.066
	b	2.1	2.21	1.95	1.1	1.87	1.58	0.808	1.8	1.34	0.656
	c	-0.55	-	-	-	-	-0.91	-1.5	-	-0.2	-
	r^2	0.76	0.52	0.67	0.53	0.81	0.75	0.22	0.73	0.54	0.41
	p-value	<<	<<	<<	<<	<<	<<	<<	<<	<<	0.013
	s_y	0.69	0.96	0.96	0.66	0.39	0.73	0.56	0.8	0.59	0.43
	CF_F	3.47	11.2	11.2	3.13	1.5	4.17	2.27	5.57	2.53	1.65
	CF_D	2.7	9.58	4.58	2.58	1.45	2.72	2.22	3.99	2.09	1.4
5.6 - 8	*n*	53	24	23	28	37	19	60	10	41	14
	a	-0.59	0.0382	0.100	0.0146	0.08	-0.653	-0.304	1.26	-0.237	0.102
	b	1.91	1.62	1.83	1.11	1.73	1.7	0.776	1.64	1.32	0.775
	c	-0.65	-	-	-	-	-0.56	-1.2	-	-0.1	-
	r^2	0.76	0.63	0.65	0.6	0.64	0.79	0.08	0.75	0.53	0.44
	p-value	<<	<<	<<	<<	<<	<<	0.029	0.0012	<<	0.009
	s_y	0.77	0.78	0.99	0.52	0.51	0.53	0.57	0.64	0.67	0.48
	CF_F	4.72	4.92	13.3	2.06	2.01	2.08	2.35	2.95	3.34	1.83
	CF_D	3.14	4.47	6.15	1.8	1.91	1.75	2.3	2.31	2.36	1.38
8-11.2	*n*	49	22	17	19	31	19	31	8	39	7
	a	-0.544	0.0363	0.186	0.00804	0.132	-0.431	-0.6	0.0595	-0.331	0.269
	b	1.74	1.80	1.70	0.775	1.75	1.73	0.764	0.227	1.2	1.08
	c	-0.55	-	-	-	-	-0.5	-1	-	-0.05	-
	r^2	0.81	0.67	0.53	0.31	0.59	0.72	0.03	0.02	0.46	0.82
	p-value	<<	<<	<<	0.013	<<	<<	0.33	0.76	<<	<<
	s_y	0.73	0.70	0.99	0.72	0.53	0.63	0.44	0.7	0.63	0.31
	CF_F	4.17	3.70	13.4	3.95	2.09	2.86	1.68	3.64	2.83	1.29
	CF_D	3.08	4.10	6.52	2.81	2.86	2.07	1.55	1.97	2.22	1.22
11.2-16	*n*	39	17	14	13	25	14	11	7	36	2
	a	-0.627	0.0529	0.402	0.018	0.0567	-0.519	-0.765	5.57	-0.202	-
	b	1.99	1.29	1.32	1.01	1.3	1.81	0.445	1.87	1.2	-
	c	-0.6	-	-	-	-	-0.4	-1.5	-	0.0	-
	r^2	0.82	0.33	0.32	0.28	0.45	0.69	0.05	0.2	0.39	-
	p-value	<<	0.0156	0.0358	0.065	<<	<<	0.49	0.32	<<	-
	s_y	0.6	0.77	0.76	0.8	0.6	0.58	0.32	0.62	0.65	-
	CF_F	2.57	4.79	4.58	5.52	2.59	2.41	1.31	2.77	3.02	-
	CF_D	2.1	4.31	3.49	3.31	2.13	1.89	1.27	1.74	2.64	-
16 - 22.4	*n*	28	14	10	4	13	10	0	3	26	2
	a	-0.449	0.0496	0.239	-	0.125	-0.339	-	-	-0.125	-
	b	1.68	1.08	1.04	-	1.59	1.76	-	-	1.35	-
	c	-0.7	-	-	-	-	-0.4	-	-	-0.15	-
	r^2	0.7	0.11	0.59	-	0.69	0.36	-	-	0.62	-
	p-value	<<	0.238	0.00982	-	<<	0.068	-	-	<<	-
	s_y	0.46	0.77	0.26	-	0.46	0.66	-	-	0.42	-
	CF_F	1.75	4.76	1.19	-	1.74	3.14	-	-	1.61	-
	CF_D	1.66	4.78	1.15	-	1.6	1.78	-	-	1.63	-

Size class (mm)	Para-meter	East Dallas Cr.	E.Dallas fine bed	E. Dallas coarse bed	Half-moon Cr.	E. St. Louis Cr. '03	Hayden Cr.	E. St. Louis Cr. '01	Cherry Cr.	Little Granite Cr. '99	Little Granite Cr. '02
22.4 - 32	n	24	2	9	3	4	7	0	22	18	0
	a	-0.334	-	-	-	0.642	-0.916	-	-	-0.241	-
	b	1.42	-	-	-	2.86	1.09	-	-	1.43	-
	c	-0.6	-	-	-	-	-0.3	-	-	-0.2	-
	r^2	0.57	-	-	-	0.81	0.03	-	-	0.29	-
	p-value	<<	-	-	-	0.1	0.705	-	-	0.021	-
	s_y	0.48	-	-	-	0.3	0.5	-	-	0.68	-
	CF_F	1.65	-	-	-	1.14	1.59	-	-	3	-
	CF_D	1.86	-	-	-	1.27	1.96	-	-	3.35	-
32 - 45	n	16	0	1	1	1	2	0	2	8	0
	a	-1.28	-	-	-	-	-	-	-	-0.121	-
	b	3.16	-	-	-	-	-	-	-	1.88	-
	c	-1	-	-	-	-	-	-	-	-0.2	-
	r^2	0.35	-	-	-	-	-	-	-	0	-
	p-value	0.015	-	-	-	-	-	-	-	0.88	-
	s_y	0.6	-	-	-	-	-	-	-	0.68	-
	CF_F	2.6	-	-	-	-	-	-	-	3.43	-
	CF_D	2.52	-	-	-	-	-	-	-	2.75	-
All gravel size classes	n	53	32	33	39	38	25	74	16	41	15
	a	-0.459	1.39E-03*	0.0117[#]	0.00393	0.0339	-0.413	-0.0946	0.144	-0.348	-0.424
	b	2.65	2.09*	1.78[#]	1.02	1.87	2.41	0.871	1.47	1.86	1.040
	c	-1.70	-	-	-	-	-1.78	-1.70	-	-0.40	-0.10
	r^2	0.79	0.64	0.63	0.37	0.77	0.79	0.24	0.59	0.59	0.45
	p-value	<<	<<	<<	<<	<<	<<	<<	<<	<<	0.006
	s_y	0.75	1.01	1.19	0.88	0.5	0.74	0.62	1.19	0.7	0.8
	CF_F	4.36	15.1	43.9	7.65	1.94	4.25	2.75	42.1	3.66	5.39
	CF_D	3.17	4.42	10.7	4.81	2.67	3.08	2.54	7.08	2.28	2.58

<< indicates a value << 0.05; Gray print indicates *p*-values ≥ 0.1. Pale red and blue shading indicates classification as "red" or "blue" stream group (see explanation in the text). *A slight alteration of the *a*-coefficient to 5.50E-04, and the *b*-exponent to 2.61 improved the visual fit to the plotted data. [#]A slight alteration of the *a*-coefficient to 0.00316, and the *b*-exponent to 3.00 improved the visual fit to the plotted data.

4.2.1 Variability among particle size classes

Fractional inter-sampler transport relationships tend to shift upwards toward the 1:1 line for increasingly coarser particle-size classes. The "stacked" trend is best developed at sites where measurements extend over a wide range of transport rates and provide a large *n* for many size fractions. In this case, fractional inter-sampler transport relationships differ by a factor of up to 2 – 4 between neighboring size classes, and maximally by to a factor of 10 (Figure 15). These results suggest that HS sampling results exceed those from bedload traps to a higher degree for fine gravel than for coarse gravel. However, for the coarsest size classes (for which only a few data pairs exist), fractional inter-sampler transport relationships tend to cross or deviate in some other way from the otherwise parallel upward trend.

It is difficult at this point to pinpoint whether different trends for the coarsest particles is merely a computational artifact caused by a small and narrow range of measured transport rates, or whether inter-sampler transport relationships for coarse particles actually follow a different trend.

Based on results where a large number of samples had been collected over a wide range of flows and transport rates, it is expected that the trend displayed for the smallest gravel size classes would continue for the coarser size classes as well. However, as soon as the size of transported gravels approaches the size of the HS sampler opening, the trend would be expected to change.

4.2.2 Variability among streams

Inter-sampler transport relationships are combined over all study streams (Figure 16) to show variability among streams. The variability among streams for a specified gravel size fraction is notably larger than the variability among gravel fractions for a specified stream (Figure 15). Fine gravel as well as total gravel transport (last plot of Figure 16) show a similar pattern of variability among streams. Based on this similarity, and based on not knowing the true inter-sampler

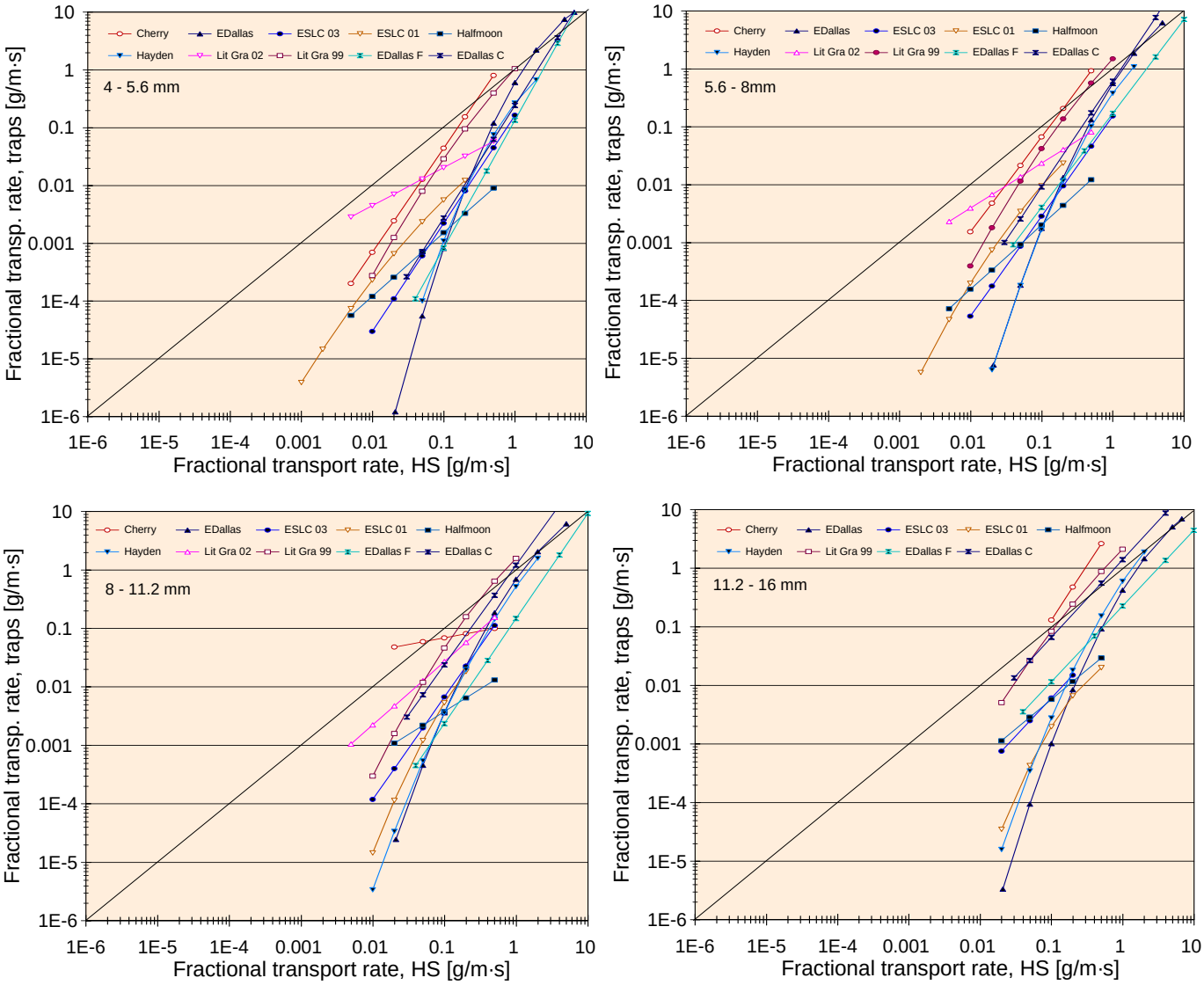

Figure 16 continued on next page

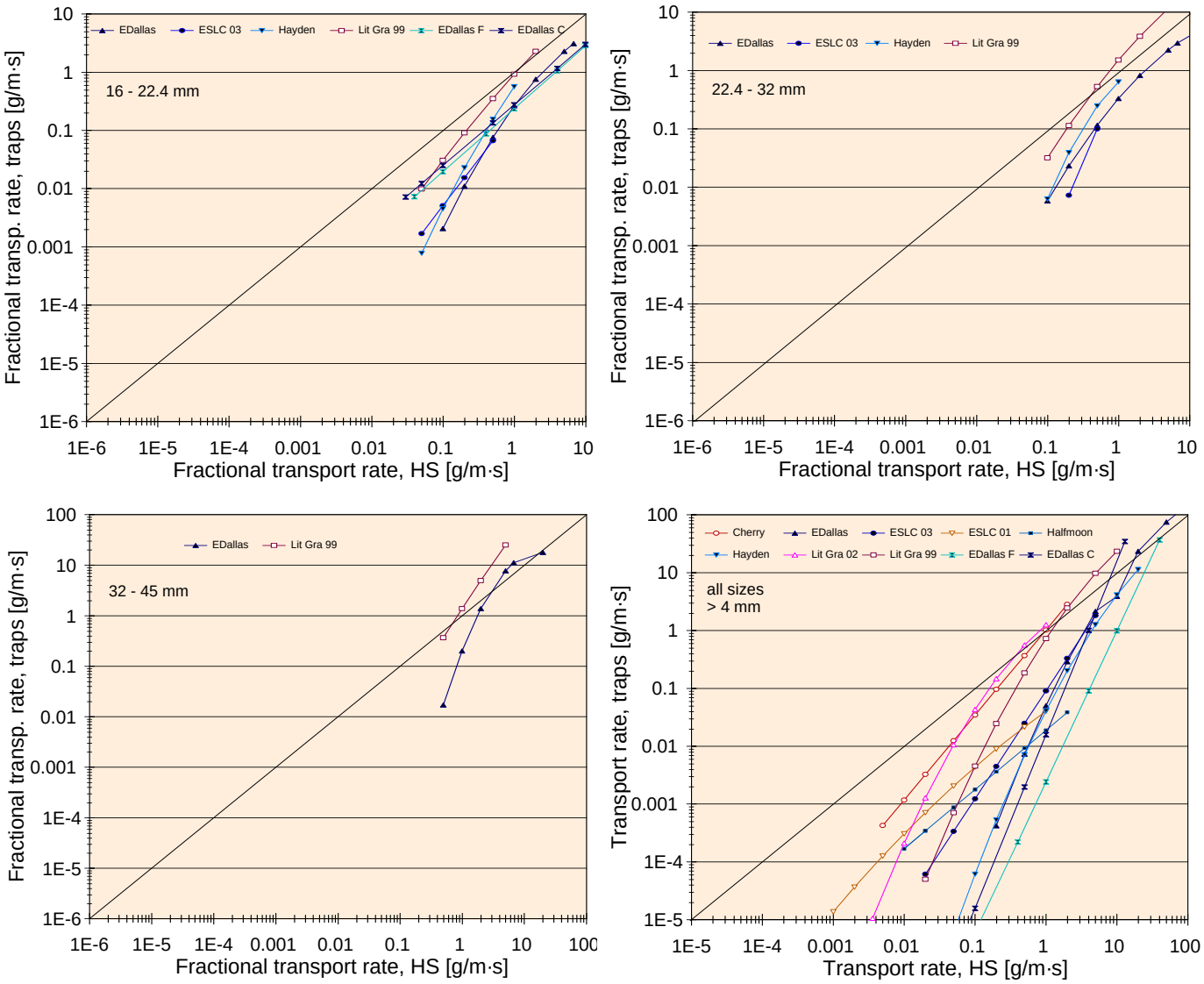

Figure 16: Paired-data approach: inter-sampler transport relationships for individual gravel size classes as well as total gravel transport rates (last plot) combined for all study streams. Streams classified as the "red" group are indicated by reddish line colors and open symbols; streams in the "blue" group by bluish line colors and closed symbols (see explanation in text).

transport relationships for the coarsest size classes, analyses of variability among streams were limited to total gravel transport rates in this study. Had all study streams provided a large number of samples collected over a wide range of transport rates (i.e., in flows up to 200% of bankfull), it is expected that trends displayed for the smallest size classes and for total transport rates would continue in a similar fashion for coarser size classes, until the sampling limitation imposed by the small HS opening size sets in.

Inter-sampler relationships for total gravel transport appear to have a common origin for all streams in the vicinity of the 1:1 line at about 100 g/m·s, i.e., when transport is high. There, transport relationships disperse for lower transport rates and take different courses for individual streams. Given the wide range of different inter-sampler transport relationships, a user should ideally be able to select an adjustment function suitable to a specific study stream. Two methods are considered: One approach assigns a group-average adjustment function to a stream that meets some general criteria of bedmaterial and transport characteristics (Section 4.2.2.1.ff). The other approach focuses on predicting individual adjustment factors to a study stream based on bedload characteristics measured with bedload traps and a HS sampler in that stream (Section 4.2.2.5).

4.2.2.1 Segregation into two stream groups

Inter-sampler transport relationships for total gravel transport visually fall into two groups (Figure 17). Inter-sampler transport relationships for the "red" group plot close to the 1:1 line and approach or intersect the 1:1 line at transport rates (around 1 – 2 g/m·s). Inter-sampler transport relationships from the "blue" group plot further away from the 1:1 line and intersect at 8 g/m·s and higher. Three of the four streams that had been categorized as "red" and "blue" groups in the rating curve approach (Section 4.1.3.1) remained in these groups in the paired data approach. The exceptions are East St. Louis Creek '01 that moved from the "red" group in the

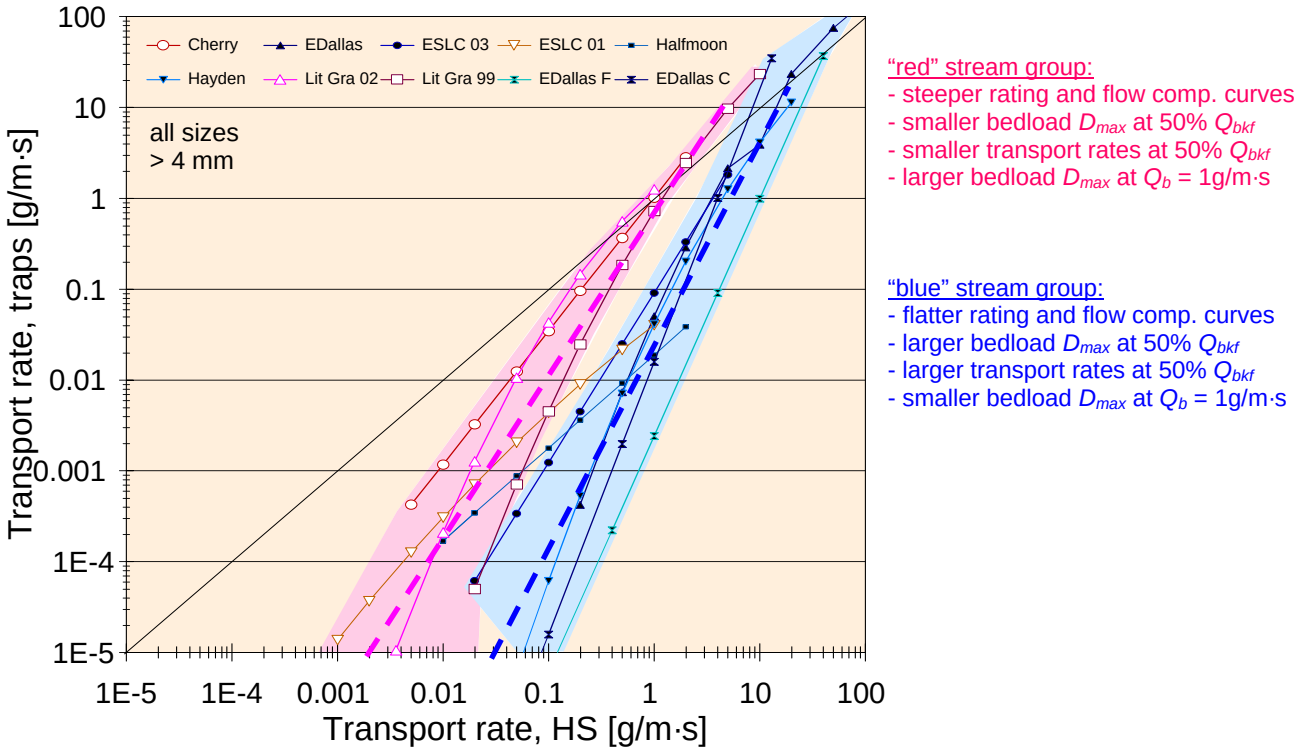

Figure 17: Paired-data approach: Inter-sampler transport relationships for total gravel transport combined for all study streams. Streams falling into the "red" group are indicated by open symbols and reddish line colors, streams in the "blue" group by closed symbols and bluish line colors. Thick dashed lines are functions that visually average over the trendlines of the "red" and "blue" stream groups.

rating curve approach to the "blue" group in the paired data approach, and Hayden Creek that moved from the "blue" to the "red" group. The "red" group of inter-sampler transport relationships is generally flatter than those in the "blue" group. The steepness of inter-sampler transport relationships in the "red" group is the main difference between the paired data and the rating curve approach ("red" group flatter than "blue" group in paired data approach but steeper than the "blue" group in the rating curve approach).

Inter-sampler transport relationships in the rating curve approach could be described by commonalities in their *a*-coefficients and *b*-exponents of the fitted power functions. This approach is not applicable when a combination of power and polynomial functions are used to describe inter-sampler transport relationships. Therefore, inter-sampler transport relationships in the paired data approach were quantified by the bedload trap transport rates associated with HS-measured transport rates of 0.1 and 1.0 g/m·s. (i.e., the intersections with vertical lines at HS-measured transport rates of x = 0.1 and x = 1 g/m·s). These two transport rates were selected because they were measured with the HS sampler for nearly all size fractions and streams (thus did not require extrapolation).

Inter-sampler relationships for total gravel transport from the "red" group intersect the line x = 0.1 g/m·s within the range of 0.004 – 0.06 g/m·s, indicating that HS sampler collected transport rates 0.5 – 1.5 orders of magnitude higher than those collected with bedload traps. At transport rates of 1 g/m·s, both samplers collect similar transport rates. In the "blue" group, sampling differences between the two samplers are larger for small transport rates (2-4 orders of magnitude of x = 0.1 g/m·s) but decrease during higher transport (1-2 orders of magnitude at x = 1 g/m·s) and approach near-unity at high transport (10 g/m·s) (Figure 17). The group-averaged bedload trap-measured transport rates at x = 0.1 g/m·s and x = 1.0 g/m·s are significantly different between the two stream groups, suggesting that inter-sampler transport relationships among the two stream groups are statistically different.

4.2.2.2 Bedmaterial and bedload conditions in "red" and "blue" streams

Streams categorized as "red" or "blue" can be distinguished based on whether the 95% confidence interval around the group mean values for parameters of bedmaterial and bedload transport overlap. When there was no overlap, the two stream groups were considered different with respect to a specified parameter, and the value equidistant to both group means served as a threshold to differentiate among groups. The computed threshold values[6] are presented in Table 7 and allow a user to classify a study stream as either "red" or "blue". Stream groups in the paired data approach did not differ in their bankfull flow (Q_{bkf}), bankfull width (w_{bkf}), stream gradient (S), the surface D_{50} and D_{84} sizes, the subsurface D_{50} size (D_{50sub}), the % surface and the % subsurface sediment < 2 and < 8 mm, or bed armoring. The same evaluation showed that several bedload transport characteristics were significantly (α = 0.05) different between the "red" and the "blue" stream groups. Bedload rating and flow competence curves measured with both samplers were generally less steep for "blue" streams and had higher coefficients than the "red" streams. In "blue" streams, both samplers collected significantly larger gravel transport rates and bedload D_{max} sizes at 50% of bankfull flow. A discharge of 50% Q_{bkf} was selected because it did

[6] Threshold values are associated with some variability except those printed in bold. The user should therefore consider threshold values for several parameters before classifying a stream.

not require extrapolating bedload rating and flow competence curves above the measured range in study streams where bankfull flows were not obtained. Also significantly different between stream groups was the bedload D_{max} particle size collected at a fixed transport rate of 1 g/m·s.

Table 7: Bedmaterial characteristics and conditions of bedload transport that determine the stream group and the respective inter-sampler relationships for the paired data approach.

	Streams in "red" group	Stream in "blue" group
<u>For bedload conditions measured with bedload trap:</u>		
Exponent of bedload rating curve	> 8.9	< 8.9
Coefficient of bedload rating curve	< 1.1E-4	> 1.1 E-4
Exponent of flow competence curve	> 1.9	< 1.9
Coefficient of flow competence curve	< 5.30	> 5.30
Bedload D_{max} at 50% Q_{bkf}	< 11 mm	> 11 mm
Gravel transport rate at 50% Q_{bkf}	< 0.001 g/m·s	> 0.001 g/m·s
Bedl. D_{max} at gravel transp. rate of 1 g/m·s	> 40 mm	< 40 mm
<u>For bedload conditions measured with HS sampler:</u>		
Exponent of bedload rating curve	< 3.4*	> 3.4*
Coefficient of bedload rating curve	< 0.094	> 0.094
Exponent of flow competence curve	> 0.91*	< 0.91*
Coefficient of flow competence curve	< 9.7	> 9.7
Bedload D_{max} at 50% Q_{bkf}	**< 13 mm**	**> 13 mm**
Gravel transport rate at 50% Q_{bkf}	**< 0.15 g/m·s**	**> 0.15 g/m·s**
Bedl. D_{max} at gravel transp. rate of 1 g/m·s	< 18 mm	> 18 mm
<u>Inter-sampler transport relationships (F_{HS}) that may be used to adjust HS measurements of total gravel transport:</u>		
Power functions visually fitted over all trendlines	Eq. 22: $Q_{B\,trap} = 0.635\ Q_{B\,HS}^{1.73}$	Eq. 23: $Q_{B\,trap} = 0.0305\ Q_{B\,HS}^{2.29}$
Power functions fitted to all individual data pairs	Eq. 24: $Q_{B\,traps} = 4.80^{\#} \cdot 0.120\ Q_{B\,HS}^{1.25}$	Eq. 25: $Q_{B\,traps} = 3.90^{\#} \cdot 0.0191 Q_{B\,HS}^{1.75}$
Power functions visually fitted to all individual data pairs	Eq. 26: $Q_{B\,traps} = 0.316\ Q_{B\,HS}^{1.50}$	Eq. 27: $Q_{B\,traps} = 0.0234\ Q_{B\,HS}^{2.25}$
Power function visually fitted to average over results from all approaches and submethods	Eq. 30 (avg. over Eqs. 22, 24, 26) $Q_{B\,traps} = 0.532\ Q_{B\,HS}^{1.58}$	Eq. 29 (avg. Eq.16, 23, 25, 27) $Q_{B\,traps} = 0.0235\ Q_{B\,HS}^{2.10}$

* and gray print: Difference between red and blue stream group not statistically significant; **Bold Print:** Threshold value between groups is considered precise; # Duan (1983) bias correction factor. Red and blue shadings refer to "red" and "blue" stream groups (see text for explanation).

4.2.2.3 Computation of group-average inter-sampler transport relationships

The inter-sampler transport relationships determined from the paired data approach cannot be easily mathematically averaged because the *a*-and *b*-parameters of the fitted power functions are not directly comparable to those from the fitted polynomials. To attain group-averaged inter-sampler transport relationships, three methods of integration were applied.

1) A straight-line (i.e., power function) was fitted to visually average the inter-sampler transport relationships for the "red" and for the "blue" stream group (Figure 17). This approach places approximately equal weight to the trendline of each stream within a group. Power functions subsequently fitted to the visually fitted straight lines yielded the equations

$$Q_{B\,trap} = F_{HS} = 0.635\ Q_{B\,HS}^{\ 1.73} \qquad \text{"red" streams} \qquad (22)$$

and

$$Q_{B\,trap} = F_{HS} = 0.0305\ Q_{B\,HS}^{\ 2.29} \qquad \text{"blue" streams} \qquad (23)$$

2) For a statistically more defensible approach, power functions were fitted to individual data pairs of measured transport ratios within the "red" and within the "blue" stream group (Figure 18). This approach places equal weight to each data measured pair. The power functions yielded the equations:

$$Q_{B\,trap} = F_{HS} = 0.1207\ Q_{B\,HS}^{\ 1.252} \qquad \text{"red" streams} \qquad (24)$$

with $n = 146$, $r^2 = 0.59$, $s_y = 0.87$, and $CF_{Duan} = 4.80$

and

$$Q_{B\,trap} = F_{HS} = 0.01913\ Q_{B\,HS}^{\ 1.745} \qquad \text{"blue" streams } \textit{(excluding East Dallas Creek, fine and coarse bed)} \qquad (25)$$

with $n = 155$, $r^2 = 0.76$, $s_y = 0.79$, and $CF_{Duan} = 3.90$

Predictions of inter-sampler transport relationships for streams falling into the "red" or "blue" groups based on Eqs. 24 and 25 need to be multiplied by the Duan (1983) smearing estimate (CF_{Duan}). Visually, Eqs. 24 and 25 do not fit the plotted data well.

3) As an alternative, straight lines that visually integrate over individual data pairs within the "red" and "blue" stream groups (Figure 18) are offered. They are described by the power function equations

$$Q_{B\,trap} = F_{HS} = 0.316\ Q_{B\,HS}^{\ 1.50} \qquad \text{"red" streams} \qquad (26)$$

$$Q_{B\,trap} = F_{HS} = 0.0234\ Q_{B\,HS}^{\ 2.25} \qquad \text{"blue" streams} \qquad (27)$$

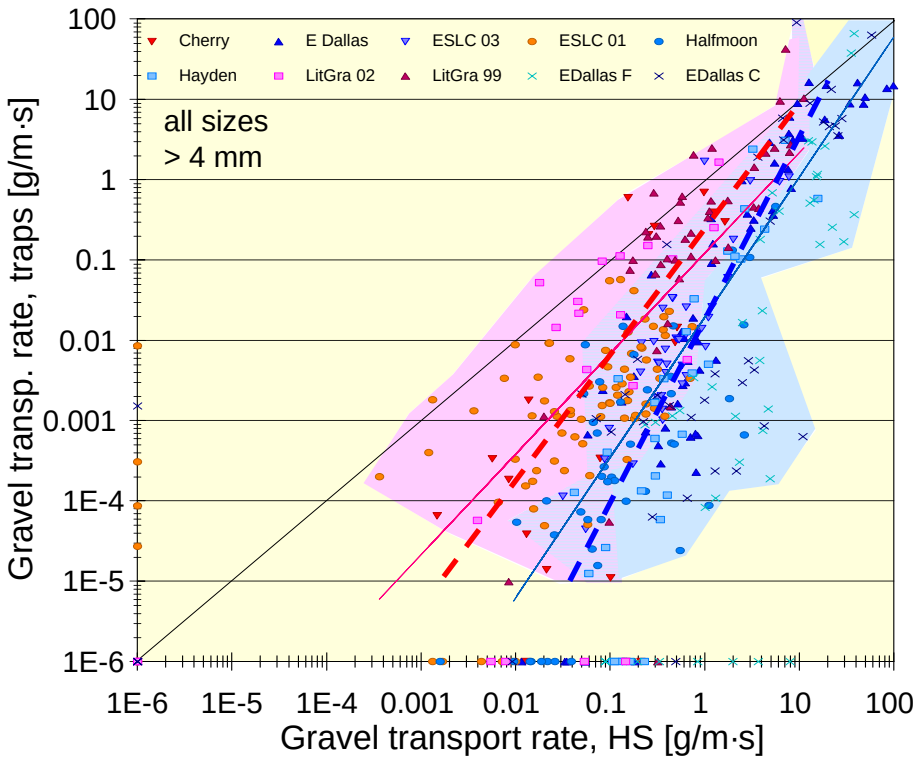

Figure 18: Ratios of total gravel transport rates measured with bedload traps *vs*. the HS for all study streams combined. Red and blue shading marks the field of data collected in "red" and "blue" streams. Thin red and blue lines indicate power functions fitted to data from all "red" and all "blue" streams (Eqs. 24 and 25). Dashed thick red and blue lines indicate functions that visually integrate over the "red" and "blue" stream groups (Eqs. 26 and 27).

The three functions are combined in Figure 19. The segregation of the two groups is maintained indicating that the variability between the two stream groups is larger than the variability among the three functions fitted to integrate over streams within a group. It is difficult to evaluate which of the three integrating methods provides the preferred inter-sampler transport relationship to be used for correction of HS samples.

4.2.2.4 Using the correction function to adjusted a HS rating curve

Equations 22 – 27 can be applied to adjust either individual HS measurements of gravel transport or a measured HS transport relationship after the study stream has been classified as a "red" or "blue" based on threshold values of bedload conditions (Table 7). To arrive at an adjusted HS rating curve for a study stream, transport rates are measured with a HS sampler over a range of flows, and a rating curve is fitted to the data. The exponent *b* and coefficient *a* of the respective inter-sampler transport relationships (i.e., one of Eqs. 22 – 27) are then applied to the study stream's power function rating curve ($Q_{B\,HS} = c{\cdot}Q^{d}$) and multiplied by a bias correction factor *CF* (to be computed from the data scatter of field measurements) to yield

$$q_{B\,traps} = F_{HS} = CF_{Duan}{}^{*} \cdot a \cdot (CF \cdot c{\cdot}Q^{d})^{b} \qquad (28)$$

where the asterisk * denotes that CF_{Duan} is to be applied if a user chooses to use regression Eqs. 24 and 25. The exponents and coefficient of the adjusted HS rating curve can be computed analytically or be obtained via a curve-fitting analysis using two data points.

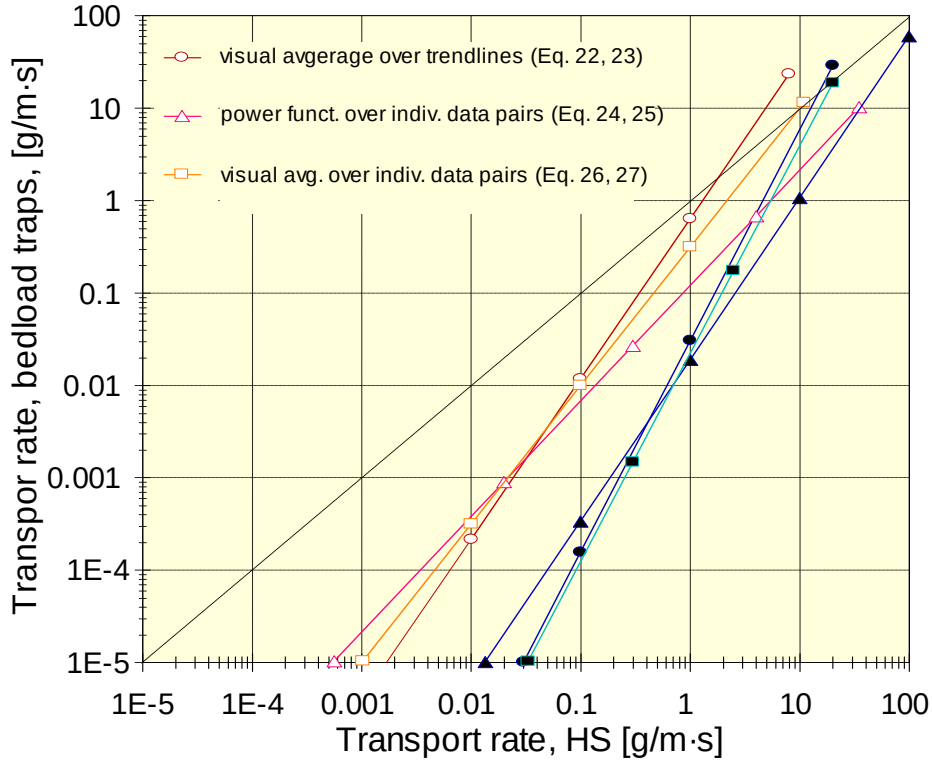

Figure 19: Inter-sampler transport relationships for total gravel transport (= HS correction functions) obtained from various methods of integrating over the "red" and "blue" groups in the paired data approach. Numbers on graphs refer to equation numbers. Inter-sampler transport relationships from the "red" stream group are plotted in reddish colors and those from the "blue" stream group in bluish colors.

4.2.2.5 Correction factors directly related to HS transport characteristics

This study also explored whether adjustment functions for individual streams (as opposed to stream groups) could be predicted from HS-measured transport characteristics. If a well-defined relationship existed between inter-sampler transport relationships and the bedload characteristics measured at a particular stream, a user could select a more representative HS correction function.

Parameters determining the magnitude of difference between HS and bedload traps

To explore the possibility of providing adjustment functions that are more closely matched to an individual stream, bedload trap transport rates associated with HS-measured transport rates of 0.01, 0.1 and 1 g/m·s were regressed against transport characteristics measured with bedload traps as well as the HS sampler in the study streams. The transport characteristics included exponents and coefficients of the bedload rating and flow competence curves as well as gravel transport rates and the bedload D_{max} particle sizes collected at 50% Q_{bkf}, and the bedload D_{max} particle sizes collected at a transport rate of 1 g/m·s. All except two of these parameters had been identified as

statistically different between the "red" and the "blue" stream groups (Table 7). Data from East Dallas Creek at the fine and coarse bed locations were included in these analyses. Power function regressions were used in all cases.

Effects of rating and flow competence curve characteristics

Bedload trap transport rates associated with HS-measured transport rates of 0.01, 0.1, and 1.0 g/m·s were not consistently correlated to parameters of the rating and flow competence curves measured with either bedload traps or the HS sampler. Statistically significant correlations were found only with the steepness of the bedload trap-measured flow competence curve as well as the coefficient of the HS-measured rating curve (Table 15 and Table 16, both in the Appendix) (r^2-values of 0.50 and 0.49, respectively).

Effects of transport rates and bedload D_{max} sizes collected at 50% Q_{bkf} and Q_b = 1 g/m·s

Bedload trap transport rates associated with HS-measured transport rates of 0.1, and 1.0 g/m·s were better correlated with transport rates and the bedload D_{max} particle size measured at a specific discharge. Values of r^2 were 0.57 and 0.60, respectively, for the negative correlation with the bedload trap transport rates collected at 50% Q_{bkf} (Figure 20, Table 9). Correlations were stronger with the HS-measured gravel transport rate at 50% Q_{bkf} (r^2-values of 0.67 and 0.81). Similarly, the bedload trap transport rates associated with HS-measured transport rates of 0.1, and 1.0 g/m·s decreased with the HS-measured D_{max} particle size at 50% Q_{bkf} (r^2-values of 0.69 and 0.55) and to a lesser degree with the bedload D_{max} particle sizes collected in bedload traps at 50% Q_{bkf} (r^2-values of 0.48 and 0.50). Bedload trap transport rates associated with HS-measured transport rates of 0.1, and 1.0 g/m·s were weakly correlated with the bedload trap D_{max} particle sizes collected at a transport rate of 1 g/m·s (Figure 21; Table 8), but not with the HS-measured D_{max} particle size at 1 g/m·s. The bedload trap transport rates associated with HS-measured transport rates of 0.01 g/m·s were not significantly related to any of the parameters discussed.

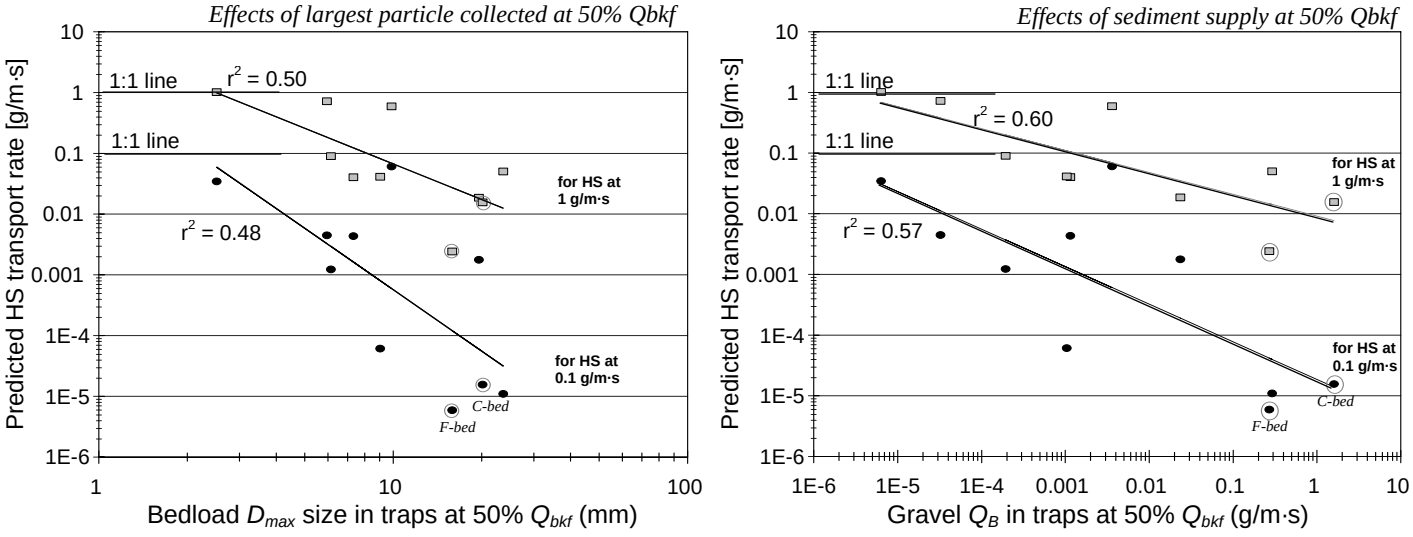

Figure 20 continued on next page

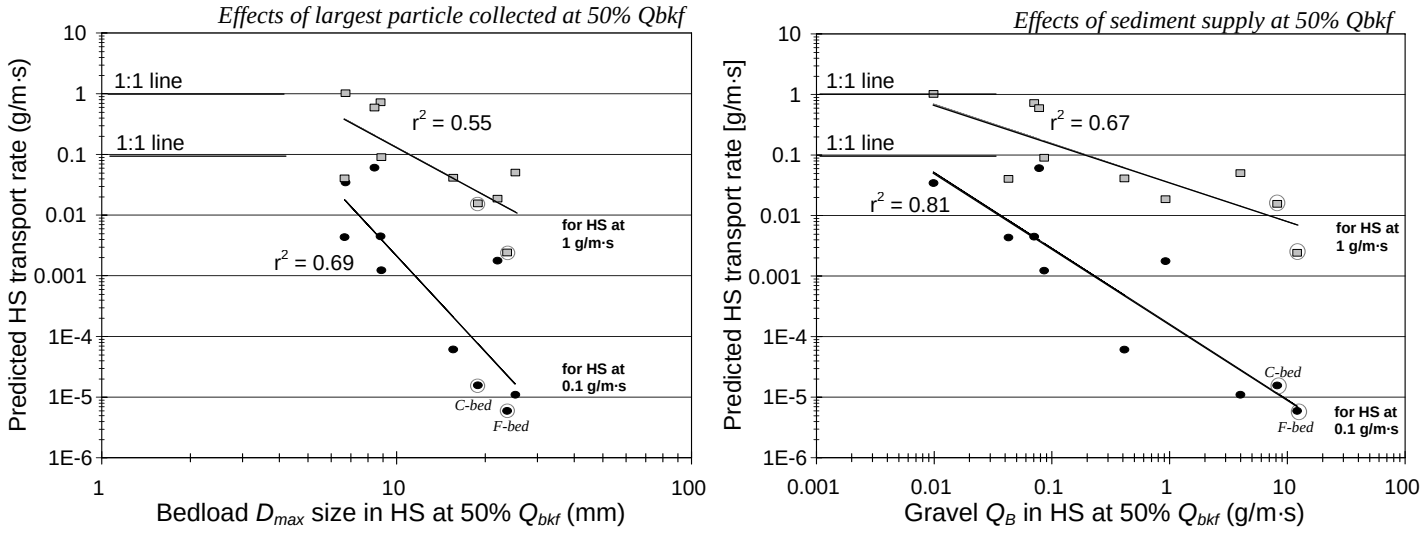

Figure 20: Effects of D_{max} bedload particle size and transport rates collected at 50% of bankfull flow with bedload traps (top plots) and the HS sampler (bottom plots) on transport rates predicted for the HS sampler from bedload trap measurements when HS collected transport rates of 0.1 and 1.0 g/m·s. Data points for sites with fine and coarse beds at East Dallas Creek are marked by dashed circles.

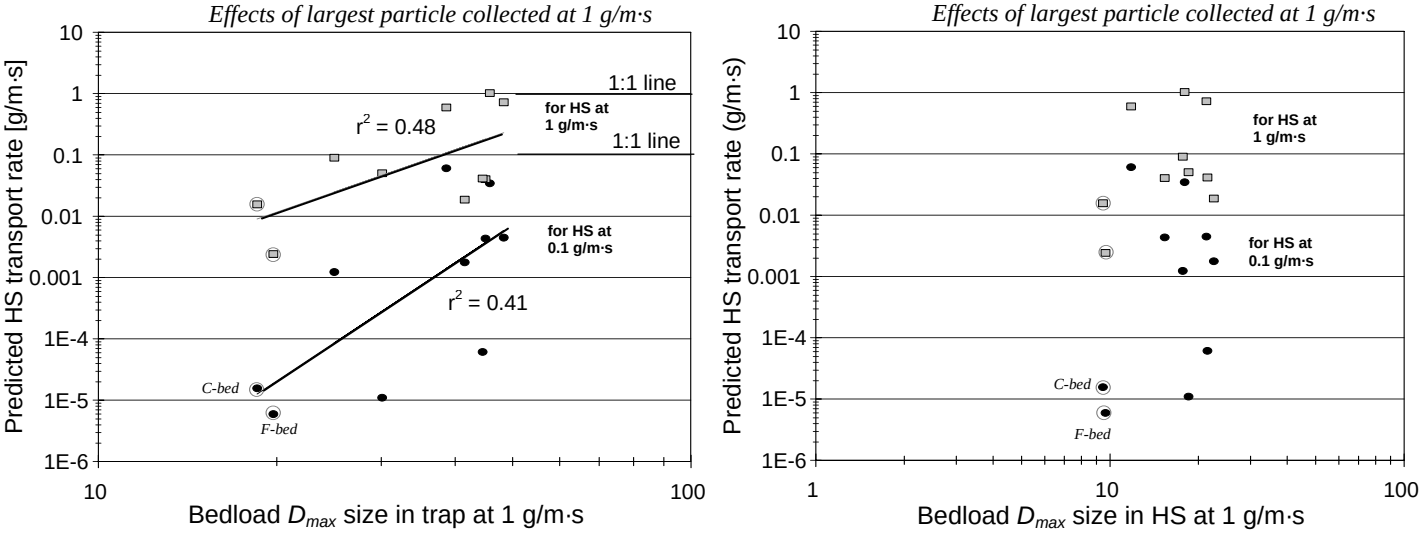

Figure 21: Effects of bedload D_{max} particle size and transport rates collected at 50% of bankfull flow with bedload traps (top plots) and the HS sampler (bottom plots) on transport rates predicted for the HS sampler from bedload trap measurements when HS collected transport rates of 0.1 and 1.0 g/m·s. Data points for sites with fine and coarse beds at East Dallas Creek are marked by dashed circles.

Table 8: HS transport rate predicted from inter-sampler transport relationships for transport rates of 0.01, 0.1, and 1.0 g/m·s.

		a-coefficient	*b*-exponent	r^2	*N*	*p-value*[#]	s_y	CF_{Duan}
Predicted from bedload trap measurements:								
for 0.01 g/m·s	*transp. rates* at 50% Q_{bkf}	7.78E-06	-0.363	0.11	8	0.423	1.68	
	bedload D_{max} at 50% Q_{bkf}	9.01E-03	-2.13	0.16	8	0.330	1.63	
for 0.1g/m·s	***transp. rates* at 50% Q_{bkf}**	**1.88E-05**	**-0.619**	**0.57**	**10**	**0.0121**	**1.03**	**11.6**
	bedload D_{max} at 50% Q_{bkf}	1.32	-3.36	0.48	10	0.0257	1.12	13.7
	D_{max} at 1g/m·s	9.36E-14	6.41	0.48	10	0.0275	1.13	7.03
for 1 g/m·s	***transp. rates* at 50% Q_{bkf}**	**9.20E-03**	**-0.361**	**0.60**	**10**	**0.0089**	**0.56**	**1.94**
	bedload D_{max} at 50% Q_{bkf}	6.01	-1.95	0.50	10	0.0214	0.62	2.10
	D_{max} at 1g/m·s	4.73E-07	3.38	0.41	10	0.0465	0.68	2.13
Predicted from HS measurements:								
for 0.01 g/m·s	*transp. rates* at 50% Q_{bkf}	8.02E-06	-1.32	0.44	8	0.0743	1.33	
	bedload D_{max} at 50% Q_{bkf}	5.53	-4.53	0.40	8	0.0931	1.38	
for 0.1g/m·s	***transp. rates* at 50% Q_{bkf}**	**1.63E-04**	**-1.25**	**0.81**	**10**	**0.0004**	**0.68**	**3.06**
	***bedload* D_{max} at 50% Q_{bkf}**	**370**	**-5.24**	**0.69**	**10**	**0.0027**	**0.86**	**6.83**
	D_{max} at 1g/m·s	1.02E-07	3.14	0.09	10	0.398	1.49	
for 1 g/m·s	***transp. rates* at 50% Q_{bkf}**	**3.52E-02**	**-0.647**	**0.67**	**10**	**0.0038**	**0.51**	**1.59**
	bedload D_{max} at 50% Q_{bkf}	58.2	-2.65	0.55	10	0.0140	0.59	1.76
	D_{max} at 1g/m·s	1.18E-04	2.31	0.15	10	0.265	0.82	

Values printed in gray have *p*-values > 0.05 and are statistically not (or only marginally) significant. Values printed in bold have *p*-values < 0.001 and indicate well-correlated relationships.

The correlations of transport rates measured by bedload traps when the HS sampler collected 1.0 and 0.1 g/m·s with transport characteristics provide two important results. 1) The relationship between bedload trap and HS transport measurements is affected by a stream's transport and bedload D_{max} characteristics (as measured with bedload traps). 2) The relatively well-defined correlations with HS measurements offer the opportunity of predicting inter-sampler transport relationships from HS measurements.

Similar results from correlation analyses and segregation into "red" and "blue" stream groups

Results from the correlation analyses are generally in line with those obtained from classifying streams into two groups. Figure 20 illustrates that HS and bedload trap measurements differ most at sites where bedload transport is well developed at 50% of bankfull flow and comprises medium or larger gravel as the D_{max} particle size. This is characteristic of "blue" streams. By contrast, HS and bedload trap measurements differ least at sites where at 50% of bankfull flow bedload transport is still poorly developed and comprises maximally pea gravel, attributes characteristic of "red" streams. Also, HS and bedload trap measurements differ most at sites where only medium gravel is mobile at a transport rate of 1 g/m·s ("blue" streams), and differ least where at a transport rate of 1 g/m·s coarse gravels are mobile ("red" streams) (Figure 21).

Computations of adjusted HS transport rates

The analyses offer conversion of two HS-sampled transport rates, at 0.1 and 1.0 g/m·s, to those collected with bedload traps. Based on a field-measured HS transport rates at 50% Q_{bkf}, the transport rate that bedload traps would have when the HS measured 0.1 and 1.0 g/m·s can be

computed from the functions provided under "predicted from HS measurements" in Table 8. For example, if a HS collected 0.3 g/m·s at 50% of bankfull flow, then the HS-measured transport rates of 0.1 and 1.0 g/m·s should be adjusted to 0.0007 and 0.08 g/m·s, respectively. Similarly, if a HS collected bedload D_{max} particles of 10 mm, HS-measured transport rates of 0.1 and 1.0 g/m·s should be adjusted to 0.002 and 0.13 g/m·s, respectively. Note that these results need to be multiplied by the Duan (1983) smearing estimate (i.e., by a factor of about 2 in most cases, but a factor of >10 in some cases, see last column of Table 8) to adjust for the inherent underprediction of *y* from *x* in power functions fitted to scattered data.

Figure 17 can be used for predictions of adjusted HS-transport rates over a wider transport rate. It is believed that if adjusted HS transport rates are predicted directly from bedmaterial and bedload characteristics observed in a study stream, results may be more representative of that stream than those obtained from applying one of the correction functions devised for streams categorized either as the "red" or "blue" stream group. Unfortunately, computation of adjusted HS transport rates using the proposed relationships in Table 8 do not provide continuous conversion functions (similar to those listed in Table 5) that can be applied to measured HS transport rates in order to yield the adjusted HS rating curve (Eq. 28). However, a user could devise a continuous function by regressing adjusted HS transport rates *vs*. measured HS transport rates of 0.1 and 1.0 g/m·s.

4.3 Comparison of rating curve and paired data approach

A variety of different inter-sampler transport relationships were computed for total gravel transport for each of the two stream groups (Table 5 and Table 7). The rating curve approach yielded one group-average inter-sampler relationship (Eqs. 15 and 16) per stream group. The paired data approach yielded three results per group depending on the method used to integrate over the streams within each group (Eqs. 22 – 27). All results are combined in Figure 22. The question arises how results vary among computational methods, whether correction functions from both approaches can be used interchangeably for adjusting HS sampling results to those obtained from bedload traps, and whether there is reason to believe that one approach and its results may be more desirable.

4.3.1 Similarities in results from both approaches

Segregation into two groups with similar streams per group

Both the rating curve and the paired data approach clearly suggest that inter-sampler transport relationships segregate into two groups. The lines along which stream groups split are similar for the two approaches. Three of the four streams that fell into the "red" or the "blue" stream group are the same between the two approaches, while two streams switched groups. The similarity among the approaches validates the segregation. While the mean group characteristics of bedload transport vary slightly between the two approaches, threshold values distinguishing between the two group averages are independent of grouping.

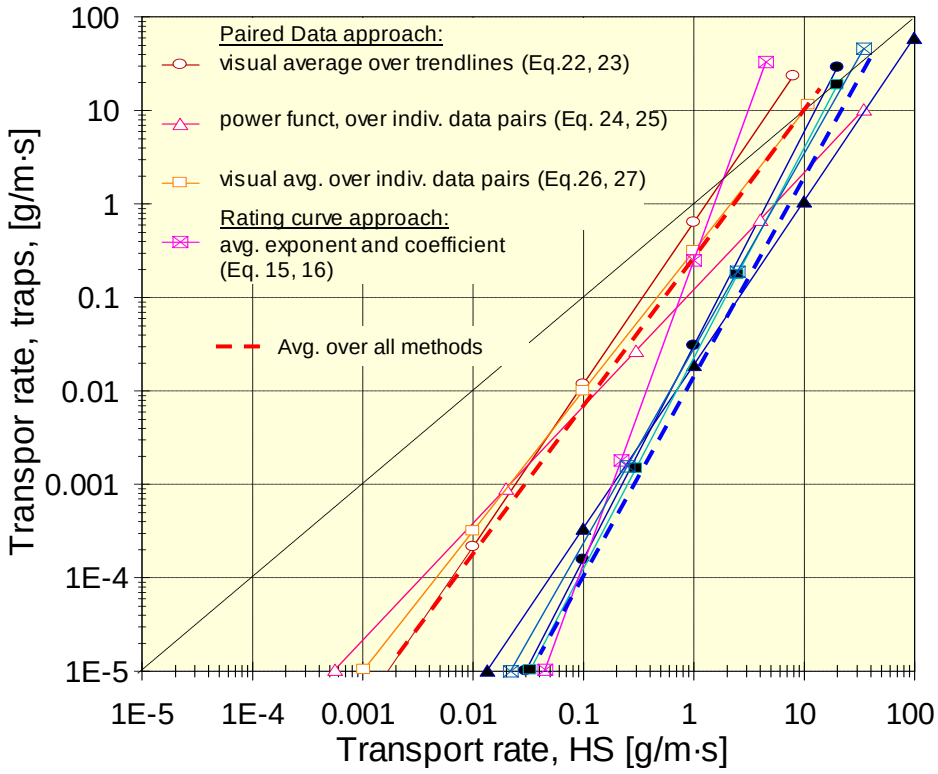

Figure 22: Comparison of inter-sampler transport relationships for total gravel transport (= HS correction functions) within the "red" and "blue" group obtained from various methods applied to the rating curve and paired data approaches. Numbers on graphs refer to equations. Inter-sampler transport relationships from the "red" stream group are plotted in reddish colors and those from the "blue" stream group in bluish colors. Thick dashed lines indicate group averages over all approaches.

Inter-sampler transport relationships differ little among size classes

Inter-sampler transport relationships were computed for individual size fractions for the rating curve and the paired data approach (Figure 9, Figure 10, and Figure 15). Both approaches indicate that inter-sampler differences tend to be slightly larger for small gravel particles compared to larger gravel. However, this trend is neither pronounced nor visible for all study streams. The general similarity among fractional inter-sampler transport relationships in the rating curve approach suggested that the same function may be applied for adjustment of all individual 0.5 phi size fractions (Figure 13).

Similar inter-sampler transport relationships for "blue" streams

Both the rating curve and the paired data approach indicated similar inter-sampler transport relationships for the "blue" stream group, suggesting that methodological differences are not critical when computing correction functions in streams characterized by relatively high transport rates of small to mid-sized gravel. Based on this finding, it appears reasonable to integrate all approaches and submethods (i.e., over Eqs. 15, 23, 25, and 27) and arrive at one inter-sampler

transport relationship to be used for adjustment of HS gravel transport rates for streams in the "blue" group (Figure 22):

$$Q_{B\,trap} = F_{HS} = 0.0235\, Q_{B\,HS}^{\,2.10} \qquad \text{"blue" streams} \qquad (29)$$

Eq. 28 can be used to apply Eq. 29 for correction of a HS-measured gravel bedload rating curve.

4.3.2 Differences in results from both approaches

Inter-sampler transport relationships computed from the rating curve and paired data approach showed several differences. Differences between the two approaches were largest for streams in the "red" group and when the range of transport rates available for analysis was narrow.

Variability among streams follows different patterns in the two approaches

The two approaches indicate a different pattern of variability among streams. In the rating curve approach, inter-sampler transport relationships for "red" and "blue" stream groups differ mostly at their upper ends, i.e., when transport rates are high. In the paired data approach, inter-sampler transport relationships for "red" and "blue" stream groups differ mostly at their lower ends, when transport rates are low. Field experience suggests similarity among samplers when transport is high and large differences (that vary in magnitude among streams) when transport is low. Results from the paired data approach align with field experience rather than the rating curve results.

Different computational response to narrow ranges of measured transport rates

The rating curve and paired data approaches lead to different inter-sampler transport relationships when data available for analysis are limited to a narrow range of transport rates. The rating curve approach creates overly steep inter-sampler transport relationships that may yield negative exponents. In the paired data approach, by contrast, overly flat inter-sampler transport relationships resulted from narrow data ranges. The two approaches differ less when samples used for analysis extend over a wide range of transport rates.

Inter-sampler transport relationships from rating curve approach appear overly steep, particularly for "red" streams

Inter-sampler transport relationships computed from the rating curve approach are straight and steep. By comparison, inter-sampler transport relationships from the paired data approach are either straight and less steep or steep during small transport rates and flatten to approach the 1:1 line when transport is high. For "blue" streams that transport relatively large amounts of small to mid-sized gravel, these differences cause only moderate disagreements in the inter-sampler transport relationships computed from the two approaches. However, the differences are pronounced for "red" streams that typically transport less, but coarser gravel. The "red" stream group is closer to the 1:1 line and intersects at lower transport rates than "blue" streams for both

approaches. However, in the rating curve approach, inter-sampler transport relationships of the "red" group are steeper than the "blue" group; in the paired data approach, the "red" stream group was flatter than the "blue" group.

The steep "red" inter-sampler transport relationships from the rating curve approach indicate that the HS sampler collects at least three orders of magnitude more gravel than bedload traps when transport is low (0.05 g/m·s), and the 1:1 line is intersected at relatively low transport rates of 2 g/m·s. Consequently at transport above 2 g/m·s, the rating curve approach indicates that the HS collects less gravel than bedload traps, up to an order of magnitude less when transport is high. Undersampling by the HS occurs when bedload contains many coarse particles that exceed the size of the HS opening, when sampling time is too short to representatively collect infrequently moving large gravel, or when the HS is perched on cobbles and fine gravel passes under the sampler (see Figure 3). However, the degree of undersampling of the HS computed by the rating curve approach appears to be exaggerated.

Based on the greatly differing results between the rating curve and paired data approach for streams in the "red" group, it is concluded that results from the two approaches cannot be used interchangeably for "red" streams. Together with the interpretation that the rating curve approach exaggerated the degree of undersampling by the HS sampler at high transport, it is not prudent to include the rating curve results when computing the HS correction function for the "red" stream group. Instead, the three correction functions obtained by integrating over the streams within the "red" group in the paired-data approach (Figure 22) (i.e., over Eqs. 22, 24, and 26) were visually averaged. The fitted grand-average correction function can be described as

$$Q_{B\,trap} = F_{HS} = 0.532\ Q_{B\,HS}^{\ 1.58} \qquad \text{"red" streams} \qquad (30)$$

Eq. 28 is used to apply Eq. 30 to a HS-measured rating curve.

5. Discussion

The discussion will address the evaluation of the rating and paired data approaches and include recommendations. Also, recommendations for future study needs will be presented.

5.1 Evaluation of the rating curve and paired data approaches

The rating and paired data approach both have advantages and disadvantages that are discussed below. The advantages and disadvantages are then weighed using a numerical comparison that highlights data requirements, the efforts and accuracy of preliminary computations, as well as the effort and accuracy of the resulting inter-sampler transport relationships (Table 9). The scores for each item ranged between -1 (negative attribute), -0.5 (somewhat negative), 0 (neutral), +0.5 (somewhat beneficial), and + 1 (beneficial attribute), offering five evaluation choices.

5.1.1 Rating curve approach

The major advantage of the rating curve approach is that the computation is straightforward and its results are statistically defensible. The rating curve approach involves all data collected with bedload traps and the HS sampler at a study stream. Using all samples increases the data range, but it may complicate the relationship between the two samplers if the relationship of transport rates versus discharge has scatter or hysteresis. Fitting rating curves to data sets is a laborious step. Another disadvantage in the rating curve approach is that inter-sampler transport relationships tend to become overly steep in "red" streams where transport is low at low flows and includes cobbles at high flows. Overly steep inter-sampler transport relationships also occur when sample size and/or the range of measured transport rates are small.

5.1.2 Paired data approach

The paired data approach requires concurrently measured data. Because hysteresis and other effects causing variability in the relationships between transport rates and flow have little if any effect on the paired data approach, limiting computations to measured data pairs ensures that data used to create data pairs are of high-quality. However, the number of pairs with non-zero transport rates from both samplers rapidly decreases for the coarsest size classes in motion, as the coarsest particle size in motion may not be simultaneously contained in the bedload trap or the HS sample, and scarcity of data pairs for the coarsest particles is of concern.

Transport relationships of data pairs from bedload traps *vs.* the HS sampler have a curved trend in some streams, and this feature requires a curvilinear function. A guided polynomial function, fitted curve segments, or a computationally involved LOWESS fit may be used. All of these procedures are time-consuming and result in functions more difficult to engage in subsequent computations than power functions. Visually fitted procedures are prone to some degree of operator variability. However, with plotted data extending over several log cycles, functions fitted by multiple operators should not vary by more than approximately half a log unit (i.e., a factor of about ±3.2) in *x* and *y*-direction. This degree of variability is often less than the error introduced by a statistical regression that is visually too flat or does not account for the proper curvature of the plotted data. Another argument that supports operator guidance is that the plotted data have a context, such as the relationship to neighboring size classes (that may have a wider range of sampled transport rates) or similarity with streams in which a wider range of transport rates and particle sizes was collected. Being aware of these relationships, an operator can often make a valid estimate of the data trend up to approximately half a log unit beyond the plotted data and use this information to guide the fit.

An advantage of the paired data approach is that its inter-sampler transport relationships align better with field observations. Transport rates and collected particle sizes differ among the two samplers when transport rates are small. Transport rates from the two samplers approach each other with increasing transport, and their ratios remain in the vicinity of the 1:1 line during high transport. The paired data approach is able to reflect this relationship.

The paired data approach offers the added possibility of using transport rates and the bedload D_{max} size collected in the HS sampler at 50% of bankfull flow to predict the bedload trap transport rate associated with the HS collected rate of 0.1 and 1.0 g/m·s. The ability to predict

correction factors for individual streams is likely to represent conditions in a study stream better than classification of a study stream into one of two stream groups and applying group-average correction functions.

Table 9: Evaluation and scoring of various attributes within the rating curve and the paired data approach.

Computational component		Rating curve approach	Score	Paired data approach	Score
Source data	Requirements	All bedload samples for which flow is known; but data quality may be hampered by hysteresis	+0.5	Only concurrently measured data pairs; results in fewer data but excludes hysteresis effects	0
	Effect of limitations	Rating curves may expand information beyond measured range (or introduce error).	0	Non-zero data pairs become scarce for infrequently transported large particles.	-1
Preliminary Computation	Time and effort	Fitting rating curves is an extra step.	-1	Compilation of data pairs not too laborious.	0
	Accuracy	Fitting rating curves can be error prone	-1	Little or no error involved in creating data pairs.	+0.5
Inter-sampler transport relationships:	Time and effort of computations	Simple computation	+1	For curved data trends: Visually fitting curves or guiding a polynomial fit is laborious.	-1
	Potential for operator guidance	Operator cannot guide the fit.	-1	Operator guidance justified because operators "knows" expected trends.	+1
	For large *n* and wide range of measured transport rates	Somewhat steep results.	-0.5	Somewhat flat results, but correctable by guiding the fit.	+0.5
	For small *n* or narrow range of measured transport rates	Overly steep and even negative results.	-1	Results too flat, but somewhat correctable by guiding the fit.	+0.5
	Statistical rigor	Statistically defensible.	+1	Guiding polynomial introduces some degree of operator variability.	-0.5
	Perceived accuracy of result	Potentially inaccurate, particularly when *n* and/or range of measured transport rates are small.	-1	A known, small degree of inaccuracy; but no major errors.	+0.5
	Applicability of results	User can differentiate among "red" and "blue" stream group and select a group-specific adjustment function. Adjustment functions cannot be determined based on HS sampling results alone.	0	User can differentiate among "red" and "blue" stream group and select a group-specific adjustment function; User can adjust HS transport rates based on measurements made with either traps or HS.	+1
Total score			-3.0		+1.5

Positive and negative evaluations are visually enhanced by light green and light purple shadings, respectively.

It is concluded that the paired data approach was more suitable for this study (see also scoring in Table 9). The relative small error introduced by operator variability when guiding or fitting inter-sampler transport relationships outweighs the potentially large error introduced by the rating curve approach that offers no operator guidance. However, the selection of the study approach may be influenced by the source data, particularly if concurrently measured data pairs are scarce. The rating curve approach can be improved by using functions with multiple segments or a curved function to optimize the rating curve fit. Both approaches yield poor results in streams that have a narrow range of measured transport rates as well as a large amount of data scatter, but a salient operator can salvage the data by guiding or handfitting functions.

5.2 Future study needs

Several topics for future work arise from the analyses in this study. They include 1) the need for more field data, 2) the need for more extensive computations (e.g., using curved or segmented regression functions and extending computations to individual size fractions), 3) the need for analyzing the effects and variability among computational methods, and 4) the need for validation of computed results. These points are discussed below.

More field data needed to improve accuracy of correction functions

Only 5 of the 9 study streams have a wide data range that extends from around 15% to 140% of bankfull flow, and one of these streams (Cherry Creek) has a small sample size. Inter-sampler transport relationships are not well developed when the range of sampled flows, and thus the range of measured transport rates, is narrow. The resulting inter-sampler transport relationships are overly steep in the rating curve approach and overly flat in the paired data approach. Consequently, the computed inter-sampler transport relationship may not be truly representative of the conditions of bedmaterial and bedload transport in that particular stream. When the measured range of transport rates is narrow, data are lacking particularly for medium and large gravel. Data sets collected over a wide range of transport rates are needed to establish accurate inter-sampler transport relationships for medium and coarse gravel, and to differentiate between differences due to computational artifacts and those due to transport mechanisms of coarse particles or the way that coarse particles are trapped in a sampler.

Formulate correction functions for individual particle-size fractions

Analyses of how inter-sampler transport relationships from both approaches were related to and predictable from parameters of bedmaterial and bedload transport were limited to total gravel transport. The study indicated that the variability among size fractions is comparatively low, and that some streams have somewhat larger inter-sampler transport ratios for smaller gravel. To improve correction of HS transport rates, the analyses should be extended to involve individual particle-size fractions in future studies. To include particle size fractions of medium and coarse gravel in these computations, more data sets are needed that extend over a wide range of flows and transport rates.

Cover stream types other than mountain gravel-bed streams

Results from this study pertain to armored coarse gravel and cobble beds typical of mountain gravel-bed streams. The wide variability of computed inter-sampler transport relationships

among these streams suggests that correction functions are stream-type specific, and that correction functions computed in this study should not be applied to streams other than the types analyzed in this study. To expand the applicability of correction functions, studies are needed in other kinds of streams, such as streams with fine gravel beds, cobble beds that transport mostly sand, and mixed sand-gravel beds. It could likewise be advisable to conduct studies where samples from a HS sampler are compared to those from samplers not affected by HS-typical restrictions other than bedload traps.

Select curved or segmented functions, if necessary, to improve the fit

The rating curve approach was based on power functions that were fitted to bedload rating curves. Fitting power functions is a common practice (e.g., Barry et al. 2004; King et al. 2004, Bunte et al. 2008), and they are convenient for subsequent computations. However, power functions (straight lines in log-log space) do not necessarily provide the best fit in all situations. If a HS sampler collects large amounts of fine gravel at low flow during otherwise very low transport rates, a knickpoint appears in the rating curve at flows less than half bankfull (not to be equated with the breakpoints observed in linear plots at around 80% of bankfull flow (Ryan et al. 2002, 2005)). A change in rating curve steepness can be addressed by fitting curved functions, such as polynomial functions, by using a LOWESS fit, or by fitting two (or more) power function segments. A better representation of the rating curve would improve inter-sampler transport relationships computed from the rating curve approach. However, using curved functions increases the computational effort and, in case of a LOWESS fit, exceeds spreadsheet capabilities. While straight rating curves fitted to the relationship of transport versus discharge necessarily result in straight inter-sampler transport relationships, curved rating curves result in curved inter-sampler transport relationships. Curved inter-sampler transport relationships represent the true trend of plotted data pairs better in some streams, as could be seen from the paired data approach.

Comparison of methods for computing group averages

In this study, group-averaged inter-sampler transport relationships were computed in several ways depending on the data source: 1) The rating curve approach suggested that arithmetic and geometric averaging over the exponents and coefficients, respectively, from fitted power functions was a suitable method. In the paired data approach, 2) fitted inter-sampler transport relationships were visually averaged over the streams within a stream group, 3) power function curves were fitted over all data within a group without regard to individual streams, and 4) functions fitted by eye to integrate over all data within a group without regard to individual streams. Computational differences within a stream group were less different than results between the two stream groups. Nevertheless, the consequences of selecting either one of these methods should be further explored.

Validate correction functions

The adjustment functions computed in this study have not been validated in streams that are not part of this study. To assess the accuracy of the proposed correction functions, they should be applied to data sets where HS samples can be paired either with bedload trap samples or with data from another sampler that is not subject to HS-typical restrictions, such as a vortex or pit sampler. However, care must be taken to ensure that bedload and bedmaterial conditions in a validation stream meet those of the study streams.

6. Summary

This study computed transport relationships between bedload traps and a HS sampler based on field data obtained from intensive sampling with both samplers in nine mountain gravel-bed study streams. The computed inter-sampler transport relationships generally display a similar pattern, with transport rates of the HS being orders of magnitude lower than those collected with bedload traps, but approaching or intersecting the 1:1 line at high transport. However, the computed inter-sampler transport relationships vary not only between the two computational approaches, but also among streams, and to a smaller degree among bedload particle-size fractions. Results from this study are limited to coarse-bedded, armored, mountain gravel-bed streams.

The rating and paired data approaches suggested that inter-sampler transport relationships computed for the study streams segregate into two groups. Inter-sampler transport relationships in the group called "red" in this report stayed relatively close to the 1:1 line and intersected at relatively low flows. The "blue" group remained further away from the 1:1 line (i.e., larger difference in transport rates between the two samplers when transport was low) and approached the 1:1 line at higher flows. Three of the four streams comprising each group were identical in the two approaches. Compared to "blue" streams, streams in the "red" group transported smaller amounts of fine gravel at low flows but coarser gravel at high flows. Such ("red") streams exhibit generally steep rating and flow competence curves, smaller bedload D_{max} particle sizes and transport rates at a moderate flow of 50% Q_{bkf}, but larger bedload D_{max} particles at a fixed transport rate of 1 g/m·s. Threshold values are provided to differentiate these parameters into the "red" and "blue" stream groups, and they permit a user to identify the appropriate group for a specific study stream.

The inter-sampler transport relationships identified for the "blue" stream group are relatively similar for the two approaches, as well as among the various submethods employed in the paired data approach used to average over the streams within the group. This suggested that any of the approaches may be used interchangeably and justified formulating one HS correction function for "blue" streams:

$$Q_{B\,trap} = F_{HS} = 0.0235\, Q_{B\,HS}^{\,2.10} \qquad \text{"blue" streams} \qquad (29)$$

The inter-sampler transport relationships computed within the "red" (steeper) stream group differ between the two approaches. In the rating curve approach, the "red" group had steeper inter-sampler transport relationships than the "blue" group; in the paired data approach, the "red" group of inter-sampler transport relationships was flatter than the "blue" group. The rating curve result averaged over the "red" stream group is considerably steeper than any of the three group-average results obtained by the paired data approach. The rating curve and the paired data approach cannot be used interchangeably for streams in the "red" group (i.e., when transport rates are low at low flows, and particles are coarse at high flow). Because the rating curve result deviated from the general trend of inter-sampler transport relationships obtained for the "red" group in the paired data approach, the rating curve result was excluded when formulating the average HS correction function for "red" streams which was given as

$$Q_{B\,trap} = F_{HS} = 0.532\, Q_{B\,HS}^{\,1.58} \qquad \text{"red" streams} \qquad (30)$$

Whether the rating curve or paired data approach should be selected for determining inter-sampler transport relationships, and therefore HS correction functions, depends on the kind of data available and conditions in a study stream. The rating curve approach is best applied when bedload transport-discharge relationships for both samplers can be accurately defined by a power function (always problematic for the coarsest size classes for which relatively few samples exist). If a fitted power function does not accurately reflect the rating curve over the entire range of measured flows, then the resulting inter-sampler transport relationship may not be accurate. Determining properly fitting rating curves can be challenging, requiring the use of polynomial functions, LOWESS fits, or function segments.

The paired data approach avoids the time-consuming and error-prone step of fitting rating curves and fits regression functions directly to pairs of bedload samples collected concurrently with bedload traps and HS, provided that data pairs exist in sufficient quantity. Ratios of bedload trap transport rates versus those collected with a HS sampler may assume either a straight trend (in log-log space), or a curved trend. Curve-fitting difficulties again arise for curved inter-sampler transport relationships, requiring either guided polynomial functions (as used in this study) or the computationally more involved methods of fitting function segments, or a LOWESS fit.

For the present study, the paired data approach appears to have yielded more accurate results, not least because it immediately made clear that curved functions (in log-log space) were needed to appropriately represent the trend of inter-sampler transport relationships. The advantage gained by presenting plotted data in a visually satisfying way outweighs inaccuracies introduced by the potential for operator subjectivity when guiding a polynomial fit and by the lack of statistical rigor.

Acknowledgements
Field work to collect the data used in this study could not have been accomplished without the efforts of Kurt Swingle. The field studies were funded by the USDA Forest Service Stream Systems Technology Center. We thank John Potyondy for encouragement and good advice.

The project described in this publication was supported by Grant/Cooperative Agreement Number 08HQGR0142 from the United States Geological Survey. Its contents are solely the responsibility of the authors and do not necessarily represent the official views of the USGS. The views and conclusions contained in this document are those of the authors and should not be interpreted as representing the opinions or policies of the U.S. Government. Mention of trade names or commercial product does not constitute their endorsement by the U.S. Government.

7. References

Barry, J. J., J. M. Buffington, and J. G. King, 2004. A general power equation for predicting bed load transport rates in gravel bed rivers, *Water Resources Research*, 40, W10401, doi:10.1029/2004WR003190.

Beschta, R.L., 1981. Increased bag size improves Helley-Smith bed load sampler for use in streams with high sand and organic matter transport. In: *Erosion and Sediment Transport Measurement.* IAHS Publ. no. 133: 17-25.

Bunte, K. and S.R. Abt, 2001. Sampling Surface and Subsurface Particle-Size Distributions in Wadable Gravel- and Cobble-Bed Streams for Analysis in Sediment Transport, Hydraulics, and Streambed Monitoring. USDA Forest Service, Rocky Mountain Research Station, Fort Collins, CO, *General Technical Report* RMRS-GTR-74, 428 pp. [Online] Available: http://www.fs.fed.us/rm/pubs/rmrs/gtr_74.html

Bunte, K. and S.R. Abt, 2005. Effect of sampling time on measured gravel bed load transport rates in a coarse-bedded stream. *Water Resources Research*, *41*, W11405, doi:10.1029/2004WR003880.

Bunte, K. and K.W. Swingle, 2008. Bedload traps and the Helley-Smith sampler deployed on the bed and on ground plates: Sampling results from East Dallas Creek, CO. Report submitted to Stream Systems Technology Center, USDA Forest Service, Rocky Mountain Research Station, Fort Collins, CO, 104 pp.

Bunte, K., S.R. Abt, and K.W. Swingle, 2006. Predictability of bedload rating and flow competence curves from bed armoring, stream width and basin area. Proceedings of the Eighth Federal Interagency Sedimentation Conference, April 2-6, 2006 in Reno, NV., Session 4A-2, 9 pp. [CD ROM] and [Online] Available: http://pubs.usgs.gov/misc_reports/FISC_1947-2006/html/pdf.html

Bunte, K., K. Swingle, and S.R. Abt, 2007a. Guidelines for using bedload traps in coarse-bedded mountain streams: Construction, installation, operation and sample processing. General Technical Report RMRS-GTR-191, Fort Collins, CO, U.S. Department of Agriculture, Forest Service, Rocky Mountain Research Station, 91 pp. [Online] Available: http://www.fs.fed.us/rm/pubs/rmrs_gtr191.pdf

Bunte, K., K.W. Swingle and S.R. Abt, 2007b. Adjustment Needed for Helley-Smith Bedload Samples Collected at low Transport Rates on Coarse Gravel Beds. Abstract. *Eos Trans. AGU*, 88(52), Fall Meet. Suppl., Abstract H41A-0132. [Online] Available: http://www.agu.org/meetings/fm07/waisfm07.html

Bunte, K., K.W. Swingle and S.R. Abt, 2009a. Necessity and difficulties of field calibration of signals from surrogate techniques in gravel-bed streams: possibilities for bedload trap samples. U.S. Geological Survey Scientific Investigations Report (*in press*).

Bunte, K., S.R. Abt, J.P. Potyondy, and S.E. Ryan, 2004. Measurement of coarse gravel and cobble transport using a portable bedload trap. *Journal of Hydraulic Engineering* 130(9): 879-893.

Bunte, K., S.R. Abt, J.P. Potyondy and K.W. Swingle, 2008. A comparison of coarse bedload transport measured with bedload traps and Helley-Smith samplers. *Geodinamica Acta* 21(1/2): 53-66 (supplement, Gravel-Bed Rivers VI Meeting)

Bunte, K., S.R. Abt, K.W. Swingle, and J.P. Potyondy, 2009b. Comparison of three pebble count protocols (EMAP, PIBO, and SFT) in two mountain gravel-bed streams. *Journal of the American Water Resources Association, in press.*

Childers, D., 1991. Sampling differences between the Helley-Smith and BL-84 bedload samplers. In: *Proceedings of the Fifth Federal Interagency Sedimentation Conference, March 18-21, 1991, Las Vegas, NV.,* Subcommittee of the Interagency Advisory Committee on Water Data, p. 6.31-6.38.

Childers, D., 1999. Field comparison of six-pressure-difference bedload samplers in high energy flow. U.S. Geological Survey, *Water Resources Investigations Report* 92-4068, Vancouver, WA, 59 pp.

Druffel, L., W.W. Emmett, V.R. Schneider, and J.V. Skinner, 1976. Laboratory hydraulic calibration of the Helley-Smith bedload sediment sampler. *U.S. Geological Survey Open-File Report* 76-752, 63 pp.

Duan, N., 1983. Smearing estimate: a nonparametric retransformation method. *Journal of the American Statistical Association* 87: 605-610.

Emmett, W.W., 1980. A Field Calibration of the Sediment Trapping Characteristics of the Helley-Smith Bedload Sampler. *Geological Survey Professional Paper* 1139, Washington, DC.

Emmett, W.W., 1981. Measurement of bed load in rivers. In: *Erosion and Sediment Transport Measurements*, IAHS Publ. no. 133: 3-15.

Emmett, W.W., 1984. Measurement of bedload in rivers. In: *Erosion and Sediment Yield: Some Methods of Measurement and Modelling.* R.F. Hadley and D.E. Walling (eds.), Geo Books, Norwich, Great Britain, p. 91-109.

Ferguson, R.I., 1986. River loads underestimated by rating curves. *Water Resources Research* 22(1): 74-76.

Ferguson, R.I., 1987. Accuracy and precision of methods for estimating river loads. *Earth Surface Processes and Landforms* 12: 95-104.

Gaudet, J.M., A.G. Roy and J.L. Best, 1994. Effects of orientation and size of Helley-Smith sampler on its efficiency. *Journal of Hydraulic Engineering* 120 (6): 758-766.

Gray, J.R., R.H. Webb and D.W. Hyndman, 1991. Low-flow sediment transport in the Colorado River. *Proceedings of the Fifth Federal Interagency Sedimentation Conference*, March 18-21, 1991, Las Vegas, Nev., Subcommittee on Sedimentation of the Interagency Advisory Committee on Water Data, p. 4.63-4.71.

Helley, E.J. and W. Smith, 1971. Development and calibration of a pressure-difference bedload sampler. USDI, Geological Survey, Water Resources Division, Open File Report, Menlo Park, California, 18pp.

Hirsch, R.M., D.R. Helsel, T.A. Cohn and E.J. Gilroy, 1993. Statistical analysis of hydrological data. In: *Handbook of Hydrology*, Maidment, D.R. (ed.) McGraw-Hill, New York.

Horowitz, A.J., 2003. An evaluation of sediment rating curves for estimating suspended sediment concentrations for subsequent flux calculations. *Hydrological Processes* 17: 3387–3409, DOI: 10.1002/hyp.1299.

Hubbell, D.W., H.H. Stevens, J.V. and J.P. Beverage, 1985. New approach to calibrating bed load samplers. *Journal of Hydraulic Engineering* 111(4): 677-694.

Hubbell, D.W., H.H. Stevens Jr., J.V. Skinner, and J.P. Beverage, 1987. Laboratory Data on Coarse-Sediment Transport for Bedload-Sampler Calibrations. *U.S. Geological Survey Water-Supply Paper* 2299*:* 1-31. http://pubs.er.usgs.gov/pubs/wsp/wsp2299/

Johnson, C.W., R.L. Engleman, J.P. Smith and C.L. Hansen, 1977. Helley-Smith bed load samplers. *Journal of the Hydraulics Division, ASCE,* 103 (HY10): 1217-1221.

King, J.G., W.W. Emmett, P.J. Whiting, R.P. Kenworthy and J.J. Barry, 2004. *Sediment transport data and related Information for Selected Coarse-Bed Streams and Rivers in Idaho*. USDA Forest Service, Rocky Mountain Research Station, General Technical Report RMRS-GTR 131, 26 pp. [Online] Available: http://www.fs.fed.us/rm/pubs/rmrs_gtr131.html

Koch, R.W. and G.M. Smillie, 1986. Bias in hydrologic prediction using log-transformed prediction models. *Water Resources Bulletin* 22(5): 717-723.

Kuhnle, R.A., 1992. Fractional transport rates of bedload on Goodwin Creek. In: *Dynamics of Gravel Bed Rivers*. P. Billi, R.D. Hey, C.R. Thorne and P. Tacconi (eds.), John Wiley, Chichester, p.141-155.

O'Brien, J.S., 1987. A case study of minimum streamflow for fishery habitat in the Yampa River. In: *Sediment Transport in Gravel-Bed Rivers*. C.R. Thorne, J.C. Bathurst and R.D. Hey (eds.), John Wily and Son, Chichester, UK, p. 921-948.

O'Leary, S.J. and R.L. Beschta, 1981. Bed load transport in an Oregon Coast Range stream. *Water Resources Bulletin* 17(5): 886-894.

Pitlick, J.C., 1988. Variability of bed load measurement. *Water Resources Research* 24(1): 173-177.

Ryan, S.E., 2005. The use of pressure-difference samplers in measuring bedload transport in small, coarse-grained alluvial channels, in: Proc. Federal Interagency Sediment Monitoring Instrument and Analysis Workshop**,** September 9-11, 2003, Flagstaff, Arizona, J.R. Gray, ed.: *U.S. Geological Survey Circular* 1276, 78 p. available on the Web, accessed August 21, 2008, at http://water.usgs.gov/osw/techniques/sediment/sedsurrogate2003workshop/listofpapers.html

Ryan, S.E. and L.S. Porth, 1999. A field comparison of three pressure-difference bedload samplers. *Geomorphology* 30: 307-322.

Ryan, S.E. and C.A. Troendle, 1997. Measuring bedload in coarse-grained mountain channels: procedures, problems, and recommendations. In: *Water Resources Education, Training, and Practice: Opportunities for the Next Century*. American Water Resources Association Conference, June 29-July 3, Keystone, CO, p. 949-958.

Ryan, S.E., L.S. Porth and C.A. Troendle, 2002. Defining phases of bedload transport using piecewise regression. *Earth Surface Processes and Landforms*, 27(9): 971-990.

Ryan, S.E., L.S. Porth and C.A. Troendle, 2005. Coarse sediment transport in mountain streams in Colorado and Wyoming, USA. *Earth Surface Processes and Landforms* 30: 269–288. DOI: 10.1002/esp.1128

Sterling, S.M. and M. Church, 2002. Sediment trapping characteristics of a pit trap and the Helley-Smith sampler in a cobble gravel-bed river. *Water Resources Research* 38(6), 10.1029/2000WR000052, 2002.

Thomas, R.B. and J. Lewis, 1993. A new model for bed load sampler calibration to replace the probability-matching method. *Water Resources Research* 29 (3): 583-597.

Thompson, D.M., 2008. The influence of lee sediment behind large bed elements on bedload transport rates in supply-limited channels. *Geomorphology* 99: 420–432

Vericat, D., M. Church and R.J.Batalla, 2006. Bed load bias: Comparison of measurements obtained from using two (76 and 152 mm) Helley-Smith samplers in a gravel bed river. *Water Resources Research* 42, W01402, doi:10.1029/2005WR004025.

Wilcox, M.S., C.A. Troendle and J.M. Nankervis, 1996. Bedload transported in gravelbed streams in Wyoming. Proceedings of the Sixth Federal Interagency Sedimentation

Conference, March 10-14, Las Vegas, Nevada. Interagency Advisory on Water Data, Subcommittee on Sedimentation, Vol. 2: VI.28-VI.33.

Appendices

A. Figures provided for illustration of information in Section 1

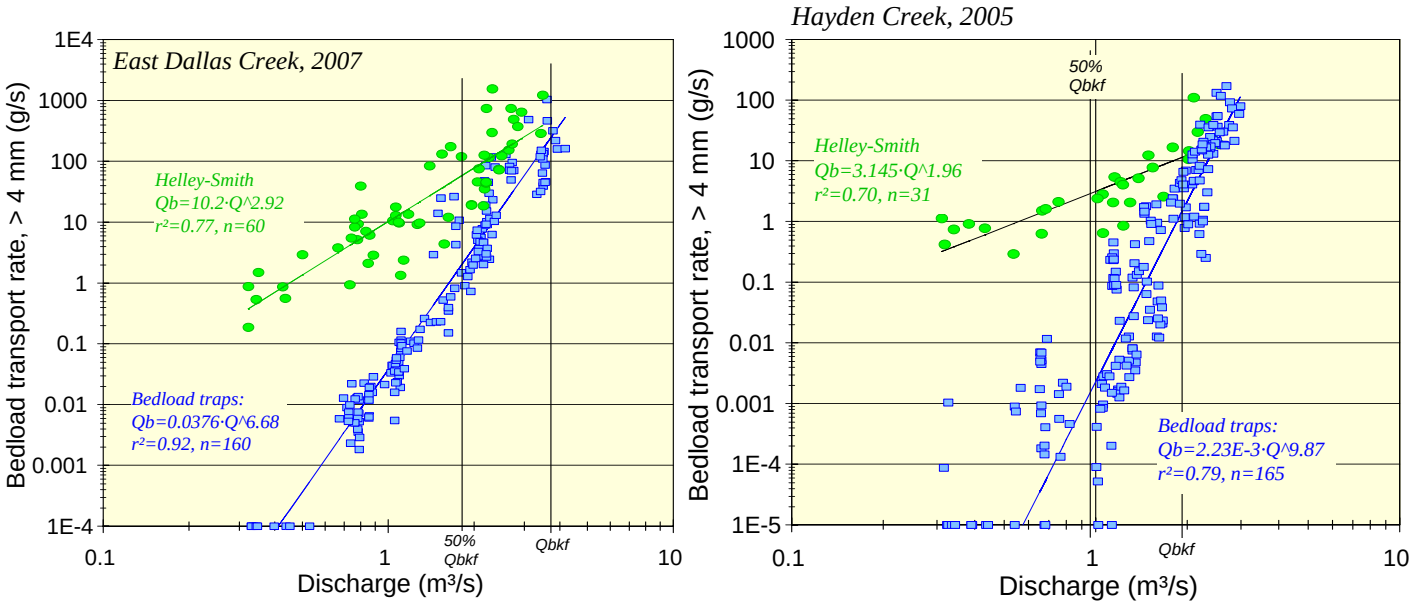

Figure A1: Sampling results from bedload traps and the HS sampler deployed directly on the bed. Examples from East Dallas Creek (left) and Hayden Creek (right).

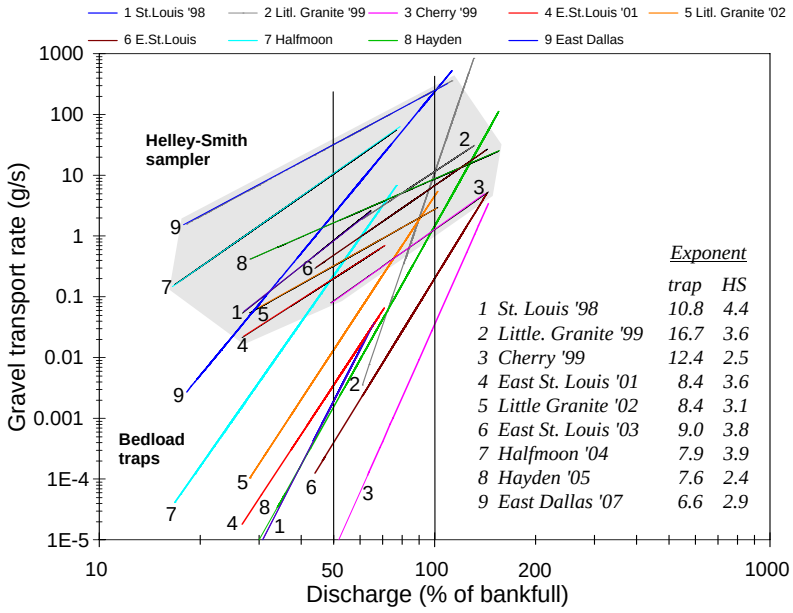

Figure A2: Gravel transport rates plotted versus percent of bankfull flow for bedload traps and the HS sampler at all study streams. Transport relationships measured with the HS sampler are within the gray-shaded area.

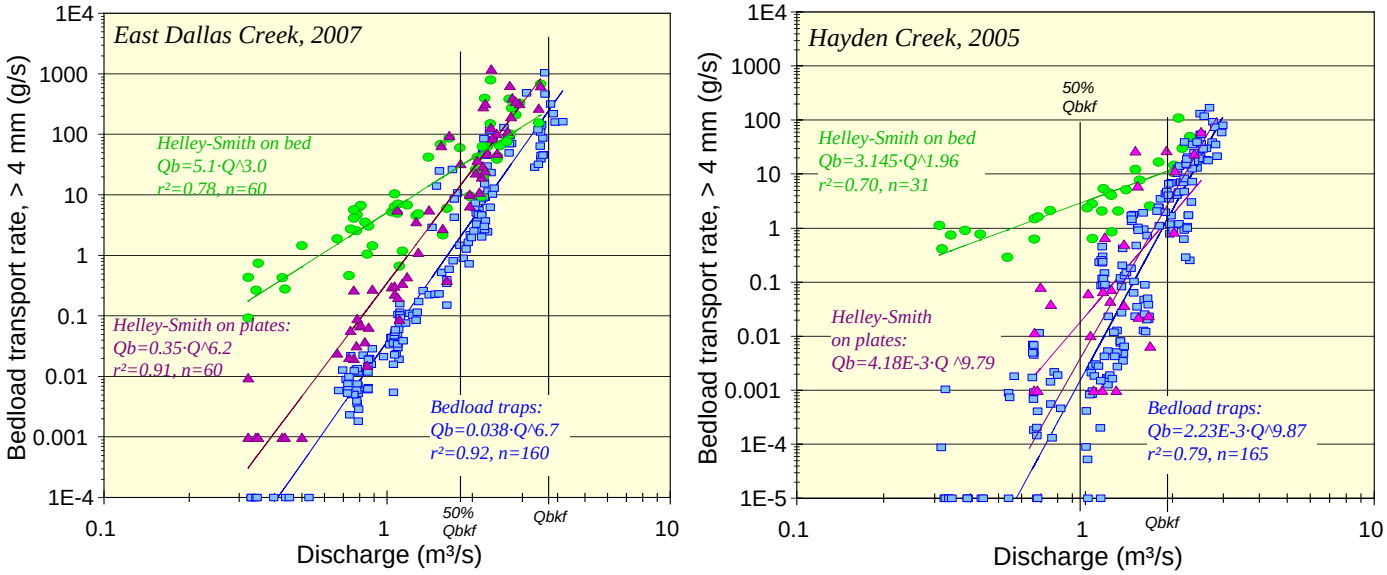

Figure A3: Sampling results from bedload traps (blue symbols) and the HS sampler deployed directly on the bed (green symbols) and on ground plates (magenta symbols). Examples from East Dallas Creek (left) and Hayden Creek (right) (from Bunte and Swingle 2008; Bunte et al. 2007b).

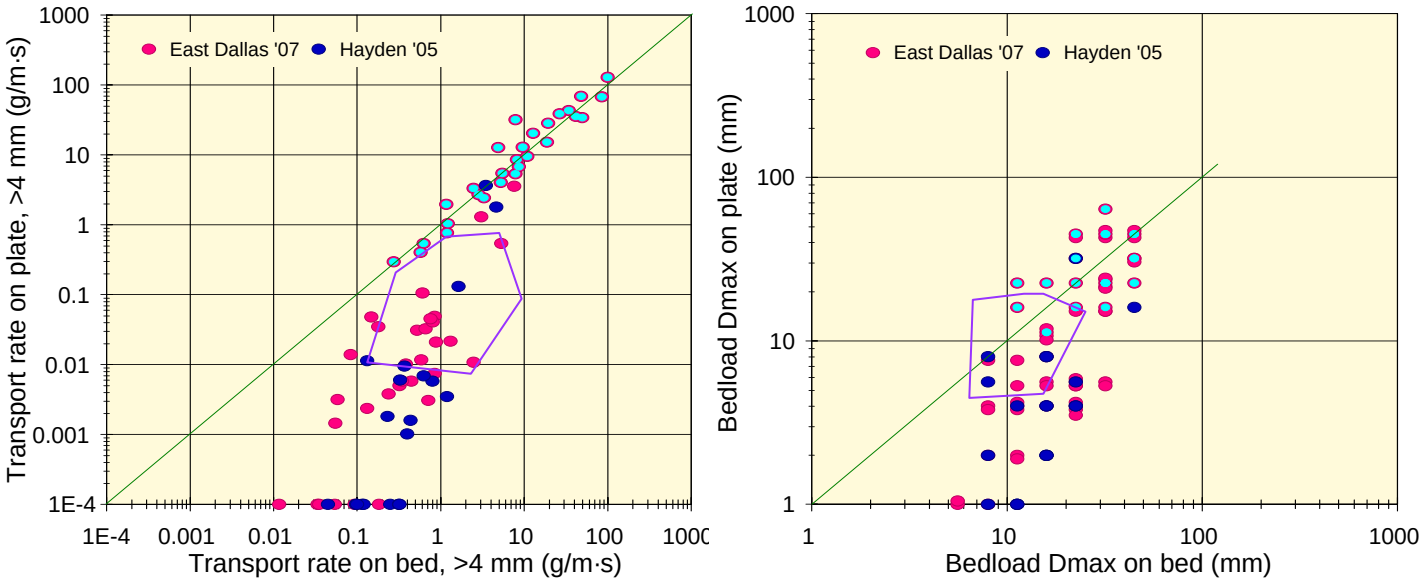

Figure A4: Relationship of sampling results obtained for HS samples collected on ground plates and on the bed: bedload transport rates (left) and bedload D_{max} particle sizes (right). For data that would otherwise plot on top of each other, data points are slightly shifted to visualize all samples. The light-blue overlay symbols are applied to the same group of samples in both plots. When transport is high, samples with similar transport rates for both HS deployments tend to have similar D_{max} particle sizes. When transport is low, on-bed samples with larger transport rates also tend to have larger D_{max} particles.

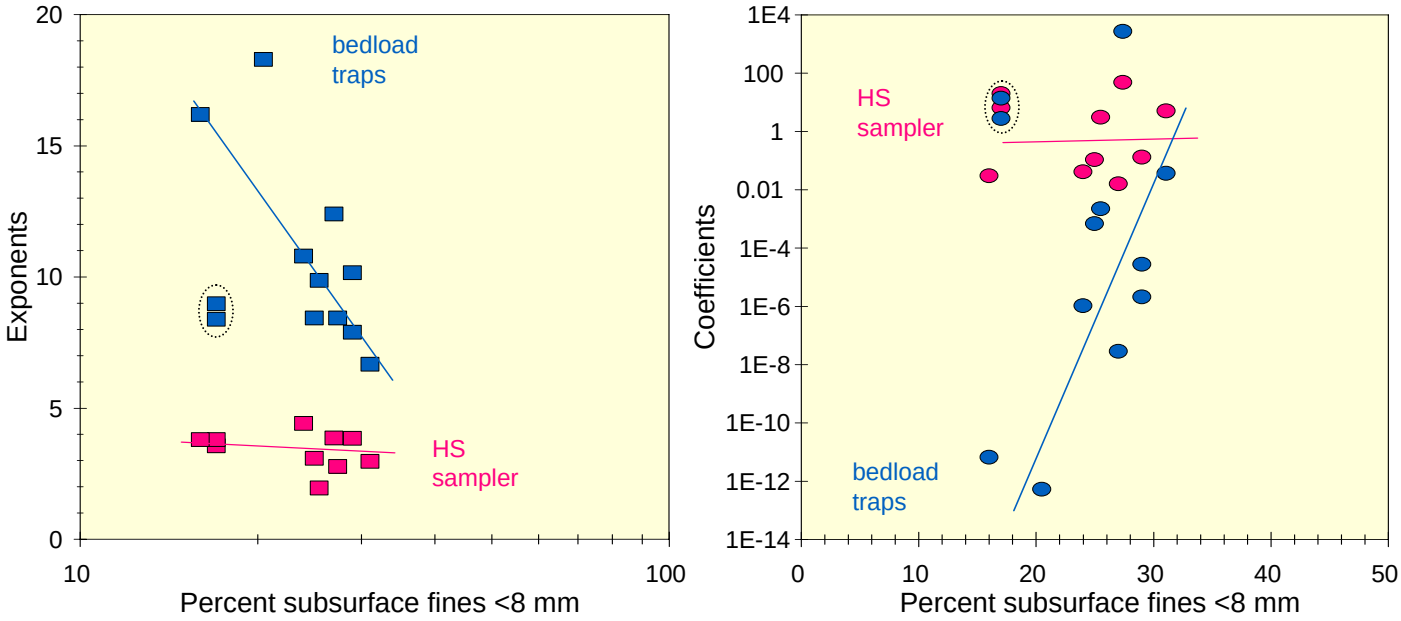

Figure A5: Relationships of exponents (left) and coefficients (right) of gravel bedload rating curves fitted to gravel transport rates collected with bedload traps and the HS sampler with the percent subsurface fines < 8 mm. While there is hardly any trend for HS gravel rating curves, the trend is moderately well developed for gravel bedload rating curves measured using bedload traps. One step-pool stream (circled data points), however, appears to deviate from the general trends observed for bedload traps.

B. Tables 11 to 17

Table 10: Parameters of power function regressions fitted to data of transport rates (g/m·s) versus discharge (m^3/s) for individual size classes (mm) (= fractional transport relationships) and for all gravel size classes combined (=total gravel transport relationships), as well as for data of bedload D_{max} particle sizes (mm) versus discharge (m^3/s) (=flow competence curves). Table 11 is presented in two parts for each study site, once for measurements made with bedload traps and once for the HS sampler.

Cherry Creek	Bedload particle-size classes								
Bedload traps	4 - 5.6 mm	5.6 - 8 mm	8 - 11.2 mm	11.2 - 16 mm	16 - 22.4 mm	22.4 - 32 mm	32 - 45 mm	all gravel sizes	D_{max} (mm)
constant	-6.70	-6.62	-6.58	-7.78	-8.46	-6.64	-5.26	-7.21	-0.09
a-coefficient	2.00E-07	2.41E-07	2.60E-07	1.66E-08	3.46E-09	2.29E-07	5.50E-06	6.10E-08	8.15E-01
Std. err of y	0.54	0.44	0.38	0.42	0.51	0.22	0.28	0.59	0.13
$CF_{(Ferg)}$	2.15	1.69	1.48	1.60	1.98	1.14	1.23	2.55	1.04
$CF_{(Duan)}$	1.59	1.39	1.25	1.34	1.33	1.10	1.16	1.72	1.04
r^2	0.87	0.88	0.87	0.64	0.59	0.45	0.15	0.89	0.92
n	17	14	12	9	9	8	7	18	18
b-exponent	8.55	8.51	8.55	10.48	11.36	8.23	5.82	10.71	2.60
p-values	<<0.05	<<0.05	<<0.05	<<0.05	0.0157	0.0698	0.383	<<0.05	<<0.05

Cherry Creek	Bedload particle-size classes								
Helley-Smith	4 - 5.6 mm	5.6 - 8 mm	8 - 11.2 mm	11.2 - 16 mm	16 - 22.4 mm	22.4 - 32 mm	32 - 45 mm	all gravel sizes	D_{max} (mm)
constant	-3.14	-2.96	-2.34	-1.64	-1.22	-1.30		-2.72	0.68
a-coefficient	7.28E-04	1.10E-03	4.52E-03	2.31E-02	5.98E-02	5.06E-02		1.91E-03	4.73
Std. err of y	0.59	0.52	0.40	0.16	0.38	0.17		0.68	0.20
$CF_{(Ferg)}$	2.55	2.07	1.54	1.07	1.47	1.08		3.44	1.12
$CF_{(Duan)}$	2.43	2.07	1.62	1.06	1.21	1.03		2.77	1.10
r^2	0.46	0.46	0.38	0.31	0.070	0.57		0.43	0.28
n	20	18	17	12	4	3		21	21
b-exponent	3.53	2.99	1.88	0.666	0.583	1.55		3.79	0.81
p-values	<<0.05	0.00191	0.00793	0.0606	0.735	0.457		0.00134	0.385

East Dallas Creek	Bedload particle-size classes								
Bedload traps	4 - 5.6 mm	5.6 - 8 mm	8 - 11.2 mm	11.2 - 16 mm	16 - 22.4 mm	22.4 - 32 mm	32 - 45 mm	all gravel sizes	D_{max} (mm)
constant	-2.72	-2.91	-3.07	-3.21	-3.21	-3.28	-3.63	-2.33	1.02
a-coefficient	1.90E-03	1.24E-03	8.61E-04	6.20E-04	6.10E-04	5.27E-04	2.34E-04	4.71E-03	10.47
Std. err of y	0.38	0.43	0.49	0.56	0.59	0.52	0.53	0.43	0.11
$CF_{(Ferg)}$	1.46	1.62	1.89	2.30	2.49	2.04	2.09	1.64	1.03
$CF_{(Duan)}$	1.53	1.93	2.60	3.13	2.65	2.05	3.37	1.97	1.03
r^2	0.91	0.91	0.90	0.84	0.70	0.67	0.66	0.92	0.87
n	157	157	148	121	90	76	56	160	160
b-exponent	5.57	6.20	6.68	6.94	6.63	6.53	6.71	6.71	1.32
p-values	<<0.05	<<0.05	<<0.05	<<0.05	<<0.05	<<0.05	<<0.05	<<0.05	<<0.05

East Dallas Creek			Bedload particle-size classes
Bedload traps	45 - 64 mm	64 - 90 mm	
constant	-3.61	-2.29	
a-coefficient	2.48E-04	5.07E-03	
Std. err of y	0.44	0.45	
$CF_{(Ferg)}$	1.67	1.71	
$CF_{(Duan)}$	1.73	1.50	
r^2	0.66	0.31	
n	36	9	
b-exponent	6.22	3.93	
p-values	<<0.05	0.118	

East Dallas Creek				Bedload particle-size classes				
Helley-Smith	4 - 5.6 mm	5.6 - 8 mm	8 - 11.2 mm	11.2 - 16 mm	16 - 22.4 mm	22.4 - 32 mm	32 - 45 mm	all gravel sizes	D_{max} (mm)
constant	-0.82	-0.92	-1.06	-1.03	-1.04	-0.59	-0.58	-0.19	1.22
a-coefficient	0.152	0.121	0.087	0.094	0.090	0.259	0.265	0.64	16.73
Std. err of y	0.38	0.45	0.55	0.53	0.46	0.43	0.32	0.44	0.16
$CF_{(Ferg)}$	1.47	1.70	2.25	2.08	1.76	1.61	1.31	1.68	1.07
$CF_{(Duan)}$	1.51	1.66	1.99	1.96	1.75	1.63	1.28	1.62	1.06
r^2	0.76	0.75	0.66	0.65	0.63	0.49	0.39	0.78	0.59
n	60	60	57	50	40	34	20	60	60
b-exponent	2.39	2.73	2.99	3.03	3.12	1.87	1.81	2.97	0.670
p-values	<<0.05	<<0.05	<<0.05	<<0.05	<<0.05	<<0.05	0.00302	<<0.05	<<0.05

East Dallas Creek		Bedload particle-size classes
Helley-Smith	45 - 64 mm	
constant	-0.18	
a-coefficient	0.658	
Std. err of y	0.34	
$CF_{(Ferg)}$	1.36	
$CF_{(Duan)}$	1.22	
r^2	0.10	
n	7	
b-exponent	1.22	
p-values	0.479	

East St. Louis Cr.'01				Bedload particle-size classes					
Bedload traps	4 - 5.6 mm	5.6 - 8 mm	8 - 11.2 mm	11.2 - 16 mm	16 - 22.4 mm	22.4 - 32 mm	32 - 45 mm	all gravel sizes	D_{max} (mm)
constant	-0.22	0.21	0.03	-1.72				0.59	1.50
a-coefficient	0.601	1.60	1.08	1.92E-02				3.86	31.97
Std. err of y	0.37	0.31	0.26	0.28				0.35	0.10
$CF_{(Ferg)}$	1.45	1.29	1.19	1.24				1.38	1.03
$CF_{(Duan)}$									
r^2	0.69	0.76	0.69	0.21				0.78	0.60
n	77	73	50	27				79	79
b-exponent	7.24	8.62	8.64	3.79				8.39	1.52
p-values	<<0.05	<<0.05	<<0.05	0.0158				<<0.05	<<0.05

East St. Louis Cr. '01	Bedload particle-size classes								
Helley-Smith	4 - 5.6 mm	5.6 - 8 mm	8 - 11.2 mm	11.2 - 16 mm	16 - 22.4 mm	22.4 - 32 mm	32 - 45 mm	all gravel sizes	D_{max} (mm)
constant	-0.07	-0.59	-0.86	-0.40	-1.12			0.68	1.37
a-coefficient	0.860	0.258	0.137	0.394	0.077			4.80	23.27
Std. err of y	0.43	0.44	0.36	0.27	0.18			0.56	0.17
$CF_{(Ferg)}$	1.64	1.66	1.41	1.21	1.09			2.28	1.08
$CF_{(Duan)}$									
r^2	0.38	0.17	0.05	0.13	0.01			0.39	0.45
n	80	64	41	26	3			81	91
b-exponent	4.07	2.66	1.61	2.29	-0.15			4.88	1.29
p-values	<<0.05	<<0.05	0.167	0.0708	0.923			<<0.05	<<0.05

East St. Louis Cr.'03	Bedload particle-size classes								
Bedload traps	4 - 5.6 mm	5.6 - 8 mm	8 - 11.2 mm	11.2 - 16 mm	16 - 22.4 mm	22.4 - 32 mm	32 - 45 mm	all gravel sizes	D_{max} (mm)
constant	-1.18	-1.10	-1.17	-1.02	-0.96	-0.97	-1.01	-0.16	1.62
a-coefficient	6.63E-02	7.87E-02	6.78E-02	9.54E-02	1.09E-01	1.07E-01	9.75E-02	6.99E-01	41.45
Std. err of y	0.39	0.46	0.44	0.48	0.39	0.37	0.36	0.42	0.14
$CF_{(Ferg)}$	1.49	1.76	1.66	1.84	1.50	1.43	1.42	1.58	1.06
$CF_{(Duan)}$									
r^2	0.80	0.74	0.69	0.63	0.70	0.64	0.41	0.81	0.68
n	131	131	122	103	86	57	24	131	133
b-exponent	7.70	7.90	7.09	7.39	7.36	6.36	4.47	8.47	1.97
p-values	<<0.05	<<0.05	<<0.05	<<0.05	<<0.05	<<0.05	<<0.05	<<0.05	<<0.05

East St. Louis Cr.'03	Bedload particle-size classes
Bedload traps	45 - 64 mm
constant	-0.99
a-coefficient	1.02E-01
Std. err of y	0.31
$CF_{(Ferg)}$	1.28
$CF_{(Duan)}$	
r^2	0.11
n	6
b-exponent	3.10
p-values	0.523

East St. Louis Cr. '03	Bedload particle-size classes								
Helley-Smith	4 - 5.6 mm	5.6 - 8 mm	8 - 11.2 mm	11.2 - 16 mm	16 - 22.4 mm	22.4 - 32 mm	32 - 45 mm	all gravel sizes	D_{max} (mm)
constant	-0.24	-0.20	-0.33	-0.42	-0.45	-0.28		0.54	1.40
a-coefficient	0.58	0.63	0.46	0.38	0.36	0.53		3.44	24.99
Std. err of y	0.18	0.16	0.27	0.34	0.28	0.07		0.19	0.12
$CF_{(Ferg)}$	1.09	1.07	1.21	1.36	1.24	1.01		1.10	1.04
$CF_{(Duan)}$									
r^2	0.83	0.86	0.65	0.39	0.44	0.89		0.85	0.50
n	40	40	39	34	23	7		40	40
b-exponent	3.39	3.36	3.31	2.75	2.43	1.82		3.81	1.07
p-values	<<0.05	<<0.05	<<0.05	<<0.05	0.00247	0.00164		<<0.05	<<0.05

Halfmoon Cr.			Bedload particle-size classes						
Bedload traps	4 - 5.6 mm	5.6 - 8 mm	8 - 11.2 mm	11.2 - 16 mm	16 - 22.4 mm	22.4 - 32 mm	32 - 45 mm	all gravel sizes	D_{max} (mm)
constant	-2.33	-2.19	-2.08	-1.69	-1.47	-0.97	0.08	-1.65	0.84
a-coefficient	4.72E-03	6.52E-03	8.32E-03	2.03E-02	0.034	0.11	1.20	2.23E-02	6.86
Std. err of y	0.43	0.35	0.38	0.32	0.27	0.30	0.14	0.46	0.17
$CF_{(Ferg)}$	1.65	1.38	1.48	1.31	1.22	1.27	1.05	1.73	1.08
$CF_{(Duan)}$									
r^2	0.61	0.66	0.51	0.42	0.40	0.19	0.47	0.66	0.59
n	49	46	37	29	13	7	4	49	49
b-exponent	2.78	2.51	2.31	1.72	1.65	0.96	-0.49	3.28	1.03
p-values	<<0.05	<<0.05	<<0.05	<<0.05	0.0185	0.323	0.310	<<0.05	<<0.05

Halfmoon Cr.			Bedload particle-size classes						
Helley-Smith	4 - 5.6 mm	5.6 - 8 mm	8 - 11.2 mm	11.2 - 16 mm	16 - 22.4 mm	22.4 - 32 mm	32 - 45 mm	all gravel sizes	D_{max} (mm)
constant	-2.33	-2.19	-2.08	-1.69	-1.47	-0.97	0.08	-1.65	0.84
a-coefficient	4.72E-03	6.52E-03	8.32E-03	2.03E-02	0.034	0.11	1.20	2.23E-02	6.86
Std. err of y	0.43	0.35	0.38	0.32	0.27	0.30	0.14	0.46	0.17
$CF_{(Ferg)}$	1.65	1.38	1.48	1.31	1.22	1.27	1.05	1.73	1.08
$CF_{(Duan)}$									
r^2	0.61	0.66	0.51	0.42	0.40	0.19	0.47	0.66	0.59
n	49	46	37	29	13	7	4	49	49
b-exponent	2.78	2.51	2.31	1.72	1.65	0.96	-0.49	3.28	1.03
p-values	<<0.05	<<0.05	<<0.05	<<0.05	0.0185	0.323	0.310	<<0.05	<<0.05

Hayden Cr.			Bedload particle-size classes						
Bedload traps	4 - 5.6 mm	5.6 - 8 mm	8 - 11.2 mm	11.2 - 16 mm	16 - 22.4 mm	22.4 - 32 mm	32 - 45 mm	all gravel sizes	D_{max} (mm)
constant	-3.52	-3.39	-3.24	-3.15	-3.08	-3.08	-3.60	-2.85	1.01
a-coefficient	3.03E-04	4.11E-04	5.71E-04	7.02E-04	8.31E-04	8.39E-04	2.52E-04	1.41E-03	10.27
Std. err of y	0.78	0.76	0.73	0.59	0.51	0.66	0.47	0.86	0.20
$CF_{(Ferg)}$	4.99	4.57	4.14	2.55	2.01	3.13	1.79	7.16	1.11
$CF_{(Duan)}$	3.48	2.74	4.07	1.91	1.75	1.62	1.55	5.91	1.11
r^2	0.73	0.69	0.68	0.70	0.73	0.67	0.66	0.75	0.71
n	172	159	151	125	113	94	75	177	177
b-exponent	6.83	6.51	6.20	6.42	6.41	6.58	7.93	7.50	1.62
p-values	<<0.05	<<0.05	<<0.05	<<0.05	<<0.05	<<0.05	<<0.05	<<0.05	<<0.05

Hayden Cr.			Bedload particle-size classes
Bedload traps	45 - 64 mm	64 – 90 mm	
constant	-3.34	-3.48	
a-coefficient	4.52E-04	3.33E-04	
Std. err of y	0.37	0.36	
$CF_{(Ferg)}$	1.43	1.41	
$CF_{(Duan)}$	1.46	1.65	
r^2	0.53	0.36	
n	50	22	
b-exponent	7.18	7.13	
p-values	<<0.05	0.00316	

Hayden Cr.			Bedload particle-size classes						
Helley-	4 - 5.6	5.6 - 8	8 - 11.2	11.2 - 16	16 - 22.4	22.4 - 32	32 - 45	all gravel	D_{max}
Smith	mm	mm	mm	mm	mm	mm	mm	sizes	(mm)
constant	-0.97	-1.13	-1.24	-1.10	-1.18	-0.83	0.45	-0.35	1.20
a-coefficient	0.107	0.073	0.058	0.080	0.066	0.147	2.815	0.45	16.03
Std. err of y	0.28	0.37	0.45	0.40	0.27	0.36	0.49	0.36	0.16
$CF_{(Ferg)}$	1.23	1.44	1.73	1.52	1.21	1.40	1.90	1.42	1.07
$CF_{(Duan)}$	1.20	1.31	1.50	1.36	1.17	1.32	4.54	1.40	1.07
r^2	0.74	0.66	0.40	0.26	0.59	0.10	0.09	0.70	0.60
n	31	31	30	25	18	11	4	31	31
b-exponent	1.66	1.87	1.39	0.91	1.94	0.93	-1.28	1.97	0.72
p-values	<<0.05	<<0.05	<<0.05	<<0.05	<<0.05	0.337	0.690	<<0.05	<<0.05

Little Granite Cr. '02			Bedload particle-size classes						
Bedload	4 - 5.6	5.6 - 8	8 - 11.2	11.2 - 16	16 - 22.4	22.4 - 32	32 - 45	all gravel	D_{max}
traps	mm	mm	mm	mm	mm	mm	mm	sizes	(mm)
constant	-3.76	-3.84	-3.86	-3.78	-3.32	-3.36	-3.32	-3.55	0.73
a-coefficient	1.73E-04	1.43E-04	1.39E-04	1.68E-04	4.78E-04	4.36E-04	4.79E-04	2.81E-04	5.31
Std. err of y	0.38	0.45	0.47	0.42	0.37	0.34	0.29	0.44	0.16
$CF_{(Ferg)}$	1.48	1.72	1.81	1.60	1.43	1.37	1.26	1.69	1.07
$CF_{(Duan)}$									
r^2	0.81	0.71	0.55	0.59	0.48	0.57	0.68	0.84	0.71
n	52	48	38	37	21	16	6	52	52
b-exponent	5.79	5.96	5.80	5.57	4.60	4.86	5.02	7.35	1.78
p-values	<<0.05	<<0.05	<<0.05	<<0.05	<<0.05	<<0.05	0.0409	<<0.05	<<0.05

Little Granite Cr. '02			Bedload particle-size classes						
Helley-	4 - 5.6	5.6 - 8	8 - 11.2	11.2 - 16	16 - 22.4	22.4 - 32	32 - 45	all gravel	D_{max}
Smith	mm	mm	mm	mm	mm	mm	mm	sizes	(mm)
constant	-1.81	-2.03	-1.98	-1.68	-1.24			-1.50	0.87
a-coefficient	0.016	0.009	0.010	0.021	0.058			0.032	7.46
Std. err of y	0.49	0.39	0.47	0.50	0.56			0.50	0.23
$CF_{(Ferg)}$	1.90	1.51	1.79	1.92	2.27			1.92	1.15
$CF_{(Duan)}$									
r^2	0.40	0.57	0.43	0.66	0.21			0.53	0.08
n	20	19	11	4	3			21	21
b-exponent	2.04	2.43	2.21	1.99	0.89			2.60	0.35
p-values	<<0.05	<<0.05	0.0271	0.190	0.696			<<0.05	0.202

Little Granite Cr. '99			Bedload particle-size classes						
Bedload	4 - 5.6	5.6 - 8	8 - 11.2	11.2 - 16	16 - 22.4	22.4 - 32	32 - 45	all gravel	D_{max}
traps	mm	mm	mm	mm	mm	mm	mm	sizes	(mm)
constant	-10.83	-10.78	-10.16	-9.96	-8.86	-8.83	-8.20	-11.13	-0.57
a-coefficient	1.49E-11	1.66E-11	6.98E-11	1.10E-10	1.37E-09	1.47E-09	6.26E-09	7.35E-12	0.27
Std. err of y	0.62	0.62	0.58	0.52	0.42	0.42	0.44	0.64	0.18
$CF_{(Ferg)}$	2.75	2.75	2.43	2.03	1.61	1.59	1.68	2.94	1.09
$CF_{(Duan)}$									
r^2	0.70	0.72	0.69	0.74	0.73	0.76	0.69	0.76	0.62
n	53	54	51	52	47	46	40	54	54
b-exponent	12.7	12.7	12.0	11.9	10.6	10.8	9.87	14.7	2.98
p-values	<<0.05	<<0.05	<<0.05	<<0.05	<<0.05	<<0.05	<<0.05	<<0.05	<<0.05

Little Granite Cr. '99		Bedload particle-size classes	
Bedload traps	45 - 64 mm	64 - 90 mm	90 – 128 mm
constant	-7.16	-5.26	-6.53
a-coefficient	6.97E-08	5.44E-06	2.93E-07
Std. err of y	0.59	0.61	0.61
$CF_{(Ferg)}$	2.56	2.70	2.70
$CF_{(Duan)}$			
r^2	0.48	0.20	0.28
n	31	19	5
b-exponent	8.52	6.02	7.83
p-values	<<0.05	0.0594	0.358

Little Granite Cr. '99				Bedload particle-size classes				
Helley-Smith	4 - 5.6 mm	5.6 - 8 mm	8 - 11.2 mm	11.2 - 16 mm	16 - 22.4 mm	22.4 - 32 mm	32 - 45 mm	all gravel sizes	D_{max} (mm)
constant	-5.39	-5.83	-5.56	-4.80	-5.25	-3.18	-0.590	-3.02	0.33
a-coefficient	4.10E-06	1.46E-06	2.74E-06	1.57E-05	5.64E-06	6.54E-04	0.257	0.001	2.12
Std. err of y	0.31	0.36	0.39	0.36	0.31	0.31	0.24	0.42	0.17
$CF_{(Ferg)}$	1.29	1.42	1.51	1.40	1.28	1.30	1.17	1.61	1.08
$CF_{(Duan)}$									
r^2	0.63	0.59	0.51	0.49	0.65	0.43	0.04	0.59	0.51
n	42	42	41	38	27	20	9	43	43
b-exponent	6.21	6.74	6.32	5.33	6.18	3.77	0.71	4.14	1.37
p-values	<<0.05	<<0.05	<<0.05	<<0.05	<<0.05	0.00192	0.624	<<0.05	<<0.05

Little Granite Cr. '99		Bedload particle-size classes
Helley-Smith	45 - 64 mm	
constant	0.373	
a-coefficient	2.360	
Std. err of y	0.35	
$CF_{(Ferg)}$	1.37	
$CF_{(Duan)}$		
r^2	0.00	
n	7	
b-exponent	-0.24	
p-values	0.898	

Table 11: Parameters of best-fit power functions relating the *b*-exponent, *a*-coefficient, and intersection with 1:1 line of inter-sampler transport relationships to exponents and coefficients of rating and flow competence curves measured with bedload traps.

	coefficient	exponent	r^2	*n*	*p-value*[#]	s_y
Correlations of inter-sampler transport relationships' *b*-exponent with:						
rating curve exponent	0.12	0.430	0.18	8	-*	0.108
rating curve coefficient	2.17	-0.019	0.39	8	0.0971	0.099
flow comp. exponent	1.83	0.559	0.35	8	-	0.102
flow comp. coefficient	3.02	-0.094	0.36	8	-	0.101
Correlation of inter-sampler transport relationships' *a*-coefficient with:						
rating curve exponent	2.2E-04	2.77	0.20	8	-	0.691
rating curve coefficient	0.049	-0.058	0.10	8	-	0.733
flow comp. exponent	0.010	3.47	0.37	8	0.110	0.613
flow comp. coefficient	0.151	-0.354	0.14	8	-	0.716
Correlations of inter-sampler transport relationships' intersection with 1:1 line with:						
rating curve exponent	3653	-2.920	0.24	8	-	0.645
rating curve coefficient	15.9	0.091	0.26	8	-	0.636
flow comp. exponent	**79.3**	**-3.986**	**0.53**	**8**	**0.041**	**0.507**
flow comp. coefficient	3.06	0.489	0.29	8	-	0.625

[#] two-tailed; * No values indicate $p >> 0.05$

Table 12: Parameters of best-fit power functions relating the *b*-exponent, *a*-coefficient, and intersection with 1:1 line of inter-sampler **bedload D_{max}** relationships to exponents and coefficients of rating and flow competence curves measured with bedload traps.

	coefficient	exponent	r^2	*n*	*p-value*[#]	s_y
Correlations of inter-sampler transport relationships' *b*-exponent with:						
rating curve exponent	1.51	0.168	0.01	8	-	0.218
rating curve coefficient	1.86	-0.017	0.10	8	-	0.208
flow comp. exponent	1.47	0.635	0.15	8	-	0.202
flow comp. coefficient	2.55	-0.099	0.13	8	-	0.204
Correlation of inter-sampler transport relationships' *a*-coefficient with:						
rating curve exponent	0.011	0.418	0.00	8	-	1.32
rating curve coefficient	0.052	0.073	0.05	8	-	1.28
flow comp. exponent	0.120	-2.45	0.06	8	-	1.28
flow comp. coefficient	0.012	0.469	0.08	8	-	1.26
Correlations of inter-sampler transport relationships' intersection with 1:1 line with:						
rating curve exponent	94.3	-0.855	0.14	8	-	0.262
rating curve coefficient	13.7	-0.011	0.02	8	-	0.279
flow comp. exponent	23.0	-0.695	0.11	8	-	0.267
flow comp. coefficient	15.8	-0.027	0.01	8	-	0.282

Table 13: Parameters of best-fit power functions relating the *b*-exponent, *a*-coefficient, and intersection with 1:1 line of inter-sampler transport relationships to exponents and coefficients of rating and flow competence curves measured with a HS sampler.

	coefficient	exponent	r^2	*n*	*p-value*[#]	s_y
Correlations of inter-sampler transport relationships' *b*-exponent with:						
rating curve exponent	4.83	-0.523	0.31	8	-*	0.105
rating curve coefficient	2.32	-0.046	0.31	8	-	0.105
flow comp. exponent	2.52	-0.150	0.06	8	-	0.123
flow comp. coefficient	3.79	-0.168	0.29	8	-	0.107
Correlations of inter-sampler transport relationships' *a*-coefficient with:						
rating curve exponent	0.052	0.396	0.00	8	-	0.769
rating curve coefficient	0.049	-0.226	0.20	8	-	0.690
flow comp. exponent	0.068	-1.25	0.12	8	-	0.725
flow comp. coefficient	0.478	-0.765	0.16	8	-	0.706
Correlations of inter-sampler transport relationships' intersection with 1:1 line with:						
rating curve exponent	1.13	1.506	0.08	8	-	0.710
rating curve coefficient	13.4	0.280	0.33	8	0.1334	0.603
flow comp. exponent	8.74	1.407	0.16	8	-	0.678
flow comp. coefficient	0.70	1.005	0.30	8	-	0.616

[#] two-tailed; * No values indicate $p >> 0.05$

Table 14: Parameters of best-fit power functions relating the *b*-exponent, *a*-coefficient, and intersection with 1:1 line of inter-sampler bedload D_{max} relationships to exponents and coefficients of rating and flow competence curves measured with the HS sampler.

	coefficient	exponent	r^2	*n*	*p-value*[#]	s_y
Correlations of inter-sampler bedload D_{max} relationships' *b*-exponent with:						
rating curve exponent	5.19	-0.730	0.20	8	-	0.196
rating curve coefficient	1.85	-0.066	0.21	8	-	0.194
flow comp. exponent	**1.88**	**-0.836**	**0.64**	**8**	**0.0176**	**0.132**
flow comp. coefficient	3.44	-0.204	0.14	8	-	0.203
Correlations of inter-sampler bedload D_{max} relationships' *a*-coefficient with:						
rating curve exponent	6.73E-05	4.99	0.26	8	-	1.13
rating curve coefficient	0.060	0.342	0.16	8	-	1.21
flow comp. exponent	**0.067**	**5.53**	**0.77**	**8**	**0.0044**	**0.64**
flow comp. coefficient	2.68E-03	1.01	0.10	8	-	1.25
Correlations of inter-sampler bedload D_{max} relationships' intersection with 1:1 line with:						
rating curve exponent	59.5	-1.147	0.30	8	-	0.237
rating curve coefficient	14.5	-0.016	0.01	8	-	0.282
flow comp. exponent	14.7	-0.125	0.01	8	-	0.281
flow comp. coefficient	15.8	-0.020	0.00	8	-	0.283

[#] two-tailed; * No values indicate $p >> 0.05$

Table 15: Correlations of HS transport rates predicted for x = 0.1 and x = 1.0 g/m•s from the inter-sampler transport relationships for total gravel transport at all study streams to exponents and coefficients of rating and flow competence curves measured with bedload traps.

	coefficient	exponent	r^2	*n*	*p-value*[#]	s_y
HS transport rates for x = 0.1 g/m·s with:						
rating curve exponent	6.88E-06	2.05	0.02	10	-	1.54
rating curve coefficient	1.83E-04	-0.138	0.10	10	-	1.48
flow comp. exponent	1.36E-05	6.37	0.24	10	-	1.36
flow comp. coefficient	1.93E-03	-0.689	0.10	10	-	1.48
HS transport rates for x = 1.0 g/m·s with:						
rating curve exponent	2.82E-04	2.52	0.10	10	-	0.84
rating curve coefficient	2.30E-02	-0.128	0.27	10	-	0.76
flow comp. exponent	**3.05E-03**	**5.25**	**0.50**	**10**	**0.0222**	**0.63**
flow comp. coefficient	2.06E-01	-0.642	0.26	10	-	0.76

[#] two-tailed; * No values indicate $p >> 0.05$

Table 16: Correlations of HS transport rates predicted for x = 0.1 and x = 1.0 g/m·s from the inter-sampler transport relationships for total gravel transport at all study streams to exponents and coefficients of rating and flow competence curves measured with the HS sampler.

	coefficient	exponent	r^2	*n*	*p-value*[#]	s_y
HS transport rates for x = 0.1 g/m·s with:						
rating curve exponent	9.66E-06	3.42	0.07	10	-	1.51
rating curve coefficient	1.84E-04	-0.634	0.33	10	0.0830	1.28
flow comp. exponent	4.76E-04	-2.32	0.08	10	-	1.49
flow comp. coefficient	2.92E-02	-1.70	0.15	10	-	1.44
HS transport rates for x = 1.0 g/m·s with:						
rating curve exponent	0.0345	0.575	0.01	10	-	0.88
rating curve coefficient	**0.0306**	**-0.438**	**0.49**	**10**	**0.0249**	**0.63**
flow comp. exponent	0.0577	-1.82	0.16	10	-	0.81
flow comp. coefficient	1.26	-1.27	0.26	10	-	0.76

[#] two-tailed; * No values indicate $p >> 0.05$

C. Example computations of HS adjustment functions

Depending on three cases of data availability, example computations provide step-by-step guidance for the computations of HS adjustment functions:

1) Data of gravel transport rates and discharge exist at a site for a HS sampler and a non-HS sampler such as bedload traps, but the data were not necessarily collected side-by-side or immediately following each other. However, it is assumed that the relationship between bedload transport and discharge remained unchanged between measurements made with both samplers.

2) Data pairs of gravel transport rates are available that were measured almost concurrently with both samplers.

3) Gravel transport rates were measured only with a HS sampler.

Each of the three cases requires a different approach for the computation of HS adjustment functions.

1. Rating curve method

The rating curve method is employed when the two samplers were deployed at a site but not necessarily concurrently.

1. Data compilation and plotting

A) Compile data of gravel transport rates and discharges for the HS sampler (Table 17) and the non-HS sampler, such as bedload traps (Table 18). Gravel transport rates (>4 mm) collected at Little Granite Creek, 2002, were used for the example computations. The tables provided below can be copied and pasted into a spreadsheet program.

Table 17: Gravel transport rates (> 4 mm) collected with 3-inch HS sampler at Little Granite Creek, 2002.

Date	Time	Q (m^3/s)	$Q_{B\,HS}$ (g/m·s)	Date	Time	Q (m^3/s)	$Q_{B\,HS}$ (g/m·s)
May 9	17:54	0.272	1E-6	May 25	16:13	0.828	0.00398
May 15	15:43	0.627	0.00790	May 28	20:17	1.304	0.176
May 16	13:58	0.596	0.00547	May 29	20:14	1.882	0.463
May 17	12:52	0.693	0.0705	May 30	17:59	2.422	1.26
May 18	12:01	0.828	1E-6	May 31	18:29	2.840	1.41
May 18	17:36	1.192	0.146	June 1	18:24	2.171	0.252
May 19	12:20	1.060	0.0536	June 3	15:34	1.669	0.129
May 19	16:21	1.576	0.652	June 4	15:37	1.481	0.0268
May 20	16:58	2.282	0.0825	June 5	14:27	1.384	0.0567
May 20	20:53	2.364	0.167	June 5	17:50	1.579	0.0179
May 21	15:50	1.862	0.0457	June 6	16:26	1.741	0.0467
				June 6	18:44	1.900	0.127

Table 18: Gravel transport rates (> 4 mm) collected with bedload traps at Little Granite Creek, 2002.

Date	Time	Q (m^3/s)	$Q_{B,\ traps}$ (g/m·s)
May 9	15:22	0.272	1E-6
May 15	13:27	0.596	1E-6
May 15	13:54	0.596	1E-6
May 15	14:44	0.596	1E-6
May 16	11:21	0.627	1E-6
May 18	11:05	0.836	1E-6
May 18	16:34	1.112	1E-6
May 19	11:19	1.043	1E-6
May 19	13:45	1.147	0.000287
May 19	15:17	1.372	0.000324
May 19	17:05	1.740	0.00578
May 19	17:38	1.854	0.00656
May 19	18:11	1.877	0.0140
May 20	12:55	1.778	0.00235
May 20	13:47	1.945	0.0134
May 20	14:54	2.131	0.0308
May 20	16:00	2.286	0.0967
May 21	13:27	1.924	0.0150
May 21	16:49	1.797	0.0143
May 21	17:26	1.769	0.00774
May 23	14:21	1.078	0.000560
May 23	15:29	1.070	0.000461
May 23	16:33	1.074	0.000731
May 23	17:46	1.095	0.000999
May 24	13:45	0.900	0.000133
May 24	15:16	0.899	8.26E-05
May 25	13:56	0.799	1E-6
May 25	15:25	0.811	5.74E-05
May 26	14:29	0.793	1E-6
May 26	15:35	0.816	0.000103
May 28	11:42	0.960	8.289E-05
May 28	16:30	1.123	0.000228
May 28	18:04	1.245	0.00387
May 29	14:24	1.511	0.00289
May 29	16:01	1.823	0.0684
May 29	17:50	1.954	0.130
May 29	20:17	1.879	0.103
May 30	13:37	1.892	0.00548
May 30	15:23	2.065	0.0428
May 30	17:10	2.342	0.253
May 30	20:58	2.562	0.774
May 31	14:06	2.324	0.0405
May 31	16:36	2.670	0.564
May 31	20:57	2.881	0.435
June 1	14:35	2.233	0.0803
June 1	16:26	2.231	0.138
June 1	19:36	2.235	0.152
June 3	11:50	1.596	0.00369
June 3	14:04	1.610	0.0138
June 3	17:28	1.699	0.0660
June 3	19:44	1.680	0.171
June 4	12:31	1.458	0.00713
June 4	14:45	1.487	0.0145
June 4	17:58	1.517	0.0340
June 5	12:44	1.354	0.00514
June 5	16:17	1.473	0.00814
June 5	18:41	1.598	0.0525
June 6	14:58	1.586	0.00810
June 6	17:50	1.845	0.0313
June 6	20:18	1.931	0.119
June 7	20:52	1.703	0.00958
June 9	12:51	1.140	0.000688

B) Plot both data sets in log-log space.

2) Regression analysis

A) Fit power function regressions in the form of $Q_B = c\ Q^d$ to the transport relationship of each sampler (i.e., a linear regression function to log-transformed data of transport rates *vs*. discharge. Zero-values were assigned a value of 1E-6 for plotting and were excluded from the analysis, but might be included at the user's discretion.

B) Print a regression table (Table 19).

Table 19: Parameters of power function rating curves fitted to gravel transport rates collected with a HS sampler and bedload traps at Little Granite Creek, 2002.

	Little Granite Creek, 2002	
Parameter	HS sampler	Bedload traps
constant	-1.50	-3.55
c-coefficient	0.0316	2.81E-04
d-exponent	2.60	7.35
s_y	0.50	0.44
r^2	0.53	0.84
n	21	52
$CF_{(Ferg)}$	1.92	1.69
$CF_{(Duan)}$		
p-value	<<0.05	<<0.05

C) Compute the *c*-coefficient as 10^{constant} (or e^{constant} when using natural logarithms).

D) Compute the bias correction factor after Ferguson (1986, 1987) (CF_{Ferg}) from the standard error of the *y*-estimate (s_y) using Eq. 6. If s_y exceeds 0.5, compute the Duan (1983) smearing estimate (CF_{Duan}) instead using the residuals (Eq. 7).

E) Compute the *p*-value to evaluate the statistical significance of the regression.

3) Plotting fitted functions

Add the fitted regression functions to the plotted data (Figure 23). Check that the regression fits the data.

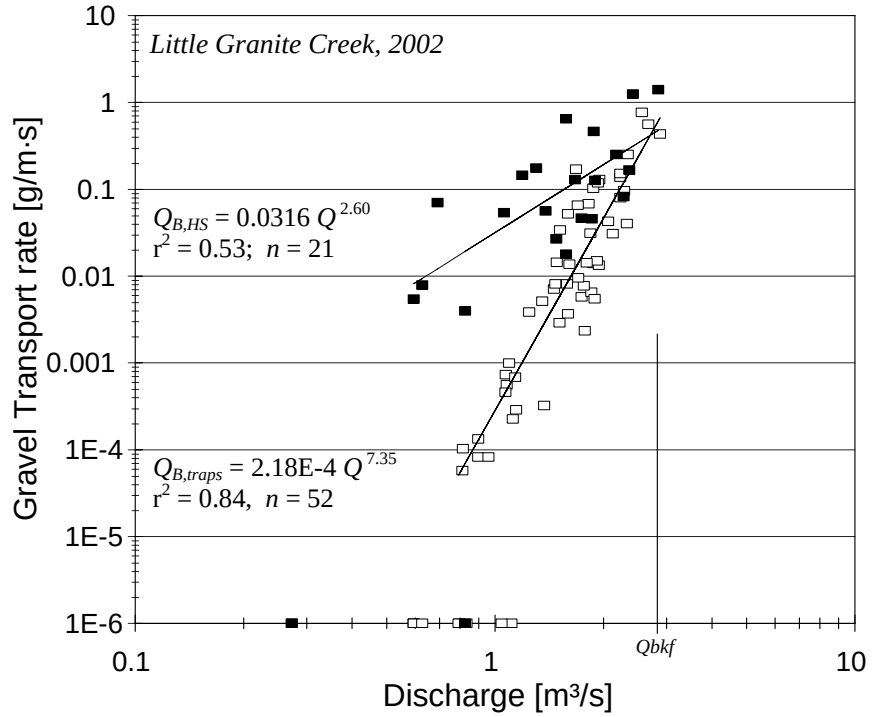

Figure 23: Relationships of gravel bedload transport and discharge for HS sampler and bedload traps and fitted rating curves. Measured zero-values are plotted along the x-axis.

4) Prediction of transport rates from fitted rating curves

A) Predict transport rates for each of the samplers for specified discharges from the fitted rating curves (Table 20).

B) Multiply transport predictions by CF_{Ferg} to account for the inherent underprediction of *y* from fitted power functions.

$$Q_{B,HS\ pred} = c\ Q^{d} \cdot CF$$

$$Q_{B,trap\ pred} = c\ Q^{d} \cdot CF.$$

For example, for the HS sampler, the rating curve predicted gravel transport rate at a discharge of $Q = 2.1$ m^3/s is

$$Q_{B,HS\ pred.} = 2.1^{2.60} \cdot 0.0316 \cdot 1.92 = 0.42$$

Table 20: Gravel transport rates predicted from the HS and bedload trap rating curves for specified discharges and log-transformations.

Discharge m^3/s	$Q_{B,HS\ pred}$ (g/m·s) CF_{Ferg} = 1.92	$Q_{B,traps\ pred}$ (g/m·s) CF_{Ferg} = 1.60	log($Q_{B,HS\ pred}$)	log($Q_{B,traps\ pred}$)
0.6	0.0161	1.11E-05	-1.79	-4.95
0.9	0.0461	0.000219	-1.34	-3.66
1.2	0.0974	0.00181	-1.01	-2.74
1.5	0.174	0.00934	-0.759	-2.03
1.8	0.280	0.0356	-0.553	-1.45
2.1	0.418	0.111	-0.379	-0.956
2.4	0.591	0.295	-0.228	-0.530
2.65	0.765	0.611	-0.116	-0.214
2.9	0.967	1.185	-0.0146	0.074

5. Computation of inter-sampler transport relationship

A) Regress data pairs of predicted $Q_{B\ traps}$ *vs*. predicted $Q_{B,HS}$ using a power function for specified discharges (i.e., linear regression of log-transformed predicted transport rates $Q_{B,trap\ pred}$ *vs*. $Q_{B,HS\ pred}$).

B) Compute the *a*-coefficient as 10 ^{constant} (or e ^{constant} when using natural logarithms).

For the Example computation, the regression parameters *a* and *b* of the inter-sampler transport relationship $Q_{B,HS,\ adj.} = a\ Q_{B,HS}{}^{b}$ are:

a = 10^0.115 = 1.30;
b = 2.82

6. Plotting the inter-sampler transport relationship

Plot the predicted transport rates for bedload traps and the HS sampler (Table 20) against each other in log-log space in a 1:1 plot (Figure 24). The line connecting the data points (i.e., the fitted power function) is the inter-sampler transport relationship $Q_{B,HS,\,adj.} = a\,Q_{B,HS}^{\,b}$.

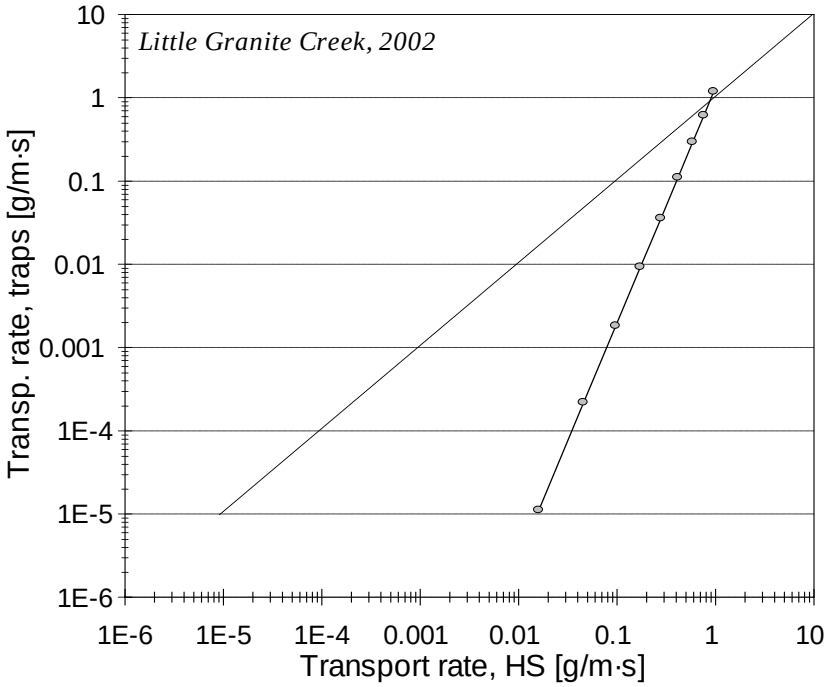

Figure 24: Inter-sampler transport relationship computed from rating curve approach.

7. Computation of intersection with 1:1 line

The transport rate at which $Q_{B,HS\,adj.}$ (x) equals $Q_{B,traps}$ (y) can be computed from the intersection of $Q_{B,HS\,adj.}$ with the 1:1 line as

$$x = a^{1/(1-b)} = 1.30^{(1/1-2.82)} = 0.87 \text{ g/m·s}$$

8. Use inter-sampler transport relationship to adjust HS transport rates

The computed inter-sampler transport relationship $Q_{B,HS,\,adj.} = a\,Q_{B,HS}^{\,b}$ serves as the HS adjustment function that may be applied to either individually measured HS gravel transport rates $Q_{B,HS}$ or to the HS transport relationship predicted from discharge $Q_{B,HS} = CF \cdot c\,Q^{d}$ to yield the HS adjustment function

$$Q_{B,HS,\,adj.} = a\,Q_{B,HS}^{\,b} = a\,(CF \cdot c\,Q^{d})^{b}$$

For example, at a discharge of $Q = 2.1$ m^3/s at Little Granite Creek, 2002, the adjusted HS gravel transport rate is

$$Q_{B,HS\,adj.} = 1.30\,(1.92 \cdot 0.0316 \cdot 2.1^{2.60})^{2.82} = 1.30\,(0.418 \text{ g/m·s})^{2.82} = 0.111 \text{ g/m·s}.$$

Note that the regressed data stem from predicted functions (i.e., the gravel bedload rating curves for the two samplers). The data points making up the inter-sampler transport relationship therefore have no scatter ($r^2 = 1$; s_y and p approach 0). Consequently, when predicting an adjusted HS transport rates ($Q_{B,HS\ adj.}$) from the inter-sampler transport relationship $a\ Q_{B,HS}{}^{b}$ multiplication by a bias correction factor *CF* is not necessary.

2. Paired data approach

The paired data approach is used when gravel transport rates collected concurrently or immediately after one another with a HS and a non-HS sampler (such as bedload traps) are available. A large sample size (>20 or 30) and a wide range of transport rates are typically necessary for the computation of a satisfactory inter-sampler transport relationship.

1) Data compilation

Compile data pairs (Table 21). Set a limit of an allowable difference in time or discharge between data collected with both samplers.

Table 21: Data pairs of gravel transport rates collected almost concurrently with bedload traps and the HS sampler at Little Granite Creek, 2002.

Bedload traps				Helley-Smith sampler		
$Q_{B,\ traps}$ (g/m·s)	Time	Q (m^3/s)	Date	Time	Q (m^3/s)	$Q_{B,HS}$ (g/m·s)
1E-06	15:22	0.27	May 9	17:54	0.27	1E-6
1E-06	14:44	0.60	May 15	15:43	0.63	0.00790
1E-06	11:21	0.63	May 16	13:58	0.60	0.00547
1E-06	11:05	0.84	May 18	12:01	0.83	1E-6
1E-06	16:34	1.11	May 18	17:36	1.19	0.146
1E-06	11:19	1.04	May 19	12:20	1.06	0.0536
0.00578	17:05	1.74	May 19	16:21	1.58	0.652
0.0967	16:00	2.29	May 20	16:58	2.28	0.0825
0.0307*	15:56	1.86	May 21	15:50	1.86	0.0457
0.0000575	15:25	0.81	May 25	16:13	0.83	0.00398
0.00273*	19:40	1.29	May 28	20:17	1.30	0.176
0.103	20:17	1.88	May 29	20:14	1.88	0.463
0.253	17:10	2.34	May 30	17:59	2.42	1.257
1.66*	19:05	2.95	May 31	18:29	2.84	1.41
0.152	19:36	2.23	June 1	18:24	2.17	0.252
0.0207*	14:51	1.63	June 3	15:34	1.67	0.129
0.0145	14:45	1.49	June 4	15:37	1.48	0.0268
0.00433*	13:31	1.38	June 5	14:27	1.38	0.0567
0.0525	18:41	1.60	June 5	17:50	1.58	0.0179
0.0217*	16:55	1.78	June 6	16:26	1.74	0.0467
0.113*	19:20	1.92	June 6	18:44	1.90	0.127

* 10-minute samples; gray shading indicates samples included in the paired data approach.

2. Plotting data pairs

Plot data pairs of transport rates measured with bedload traps *vs*. those measured with the HS sampler in a 1:1 plot in log-log space (Figure 25).

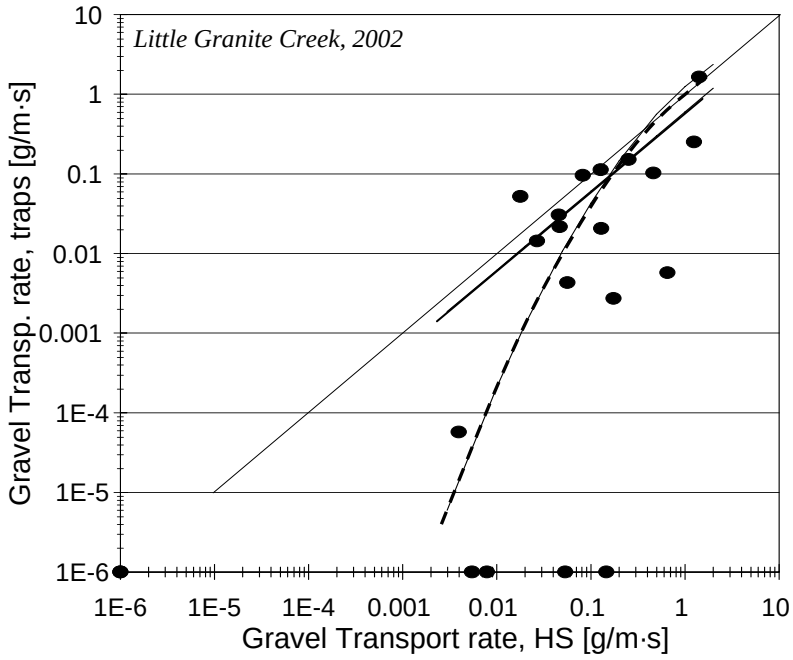

Figure 25: Bedload trap and HS gravel transport rates plotted *vs*. each other in a 1:1 plot. Also included are the two inter-sampler transport relationships: a fitted power function (solid line) and a guided 2nd order polynomial function (dashed line).

3. Regression analysis

A) Fit a power function regression to transport rates measured with bedload traps and the HS sampler (i.e., a linear regression of log-transformed measured data) to obtain the inter-sampler transport relationship. Zero-values are assigned a value one order of magnitude lower that the lowest transport rate collected by a sampler (the assigned value was 1E-6 for the example stream) Zero values (i.e., the assigned small transport rate) should be plotted, and they may be included in the analysis at the user's discretion.

B) Print a regression table (Table 22).

C) Compute the *a*-coefficient as 10^{constant} (or e^{constant} when using natural logarithms).

D) Because the standard error of the *y*-estimate s_y likely exceeds 0.5 which overpredicts the Ferguson (1986, 1987) bias correction factor CF_{Ferg}, compute instead the Duan (1983) smearing estimate (CF_{Duan}) from the residuals of the fitted power function (Eq. 7).

E) Compute the *p*-value to evaluate the statistical significance of the regression.

Table 22: Parameters of a power function regression and a 2nd order polynomial function fitted to the inter-sampler transport relationship of gravel transport rates collected with bedload traps and the HS sampler at Little Granite Cr. 2002 using the paired data approach.

Power function		2nd order polynomial function	
Parameters	Values	Parameters	Values
constant	-0.633	*A*	-0.4242
a-coefficient	0.233	*B*	1.0398
s_y	0.80*	*c*	-0.1
$CF_{(Ferg)}$	5.39*		
$CF_{(Duan)}$	2.58		
r^2	0.45		
n	15		
b-exponent	0.993		
p-values	0.00588		

* values too high; do not use.

4. Computation of inter-sampler transport relationship

A) Compute the inter-sampler transport relationship that serves as the HS adjustment function using the regression parameters *a* and *b*.

B) Multiply result by CF_{Duan} to account for the inherent underprediction of *y*-values from *x* in power functions fitted to scattered data sets.

$$Q_{B,HS,\,adj.} = Q_{B,trap} = a\, Q_{B,HS}^{\,b} \cdot CF_{Duan}$$

with

$a = 10^{-0.633} = 0.233$;
$b = 0.993$
$CF_{Duan} = 2.58$

5. Plotting the inter-sampler transport relationship

Add the graphed fitted inter-sampler transport relationship to the plotted data pairs (Figure 25).

6. Determining intersection point with 1:1 line

The point at which the inter-sampler transport relationships intersects the 1:1 line indicates the transport rate at which HS and bedload traps measurements are identical. The intersection point can be computed from

$$x = CF \cdot a^{1/(1-b)} = 2.58 \cdot 0.233^{(1/1-0.993)} = 1.1\text{ E-}90$$

There is no intersection for the inter-sampler transport relationship computed for Little Granit Creek within the range of commonly observed transport rates; the inter-sampler transport relationship runs nearly parallel to the 1:1 line.

7. Fitting a curvilinear function if necessary

A) Visually evaluate whether the inter-sampler transport relationship obtained from the fitted power function represents the plotted data. If not, consider fitting a curvilinear function such as a 2nd order polynomial function with the general form

$$y = a \cdot x^2 + b \cdot x + c$$

to log-transformed HS transport rates[7], thus $x = \log(Q_{B,HS})$.

B) Consider that a 2nd order polynomial function may need guiding to fit the data trend, particularly when the data set is relatively small and does not include a sufficient number of data points within the range of low to moderate transport rates. Several options are available for guiding the fit. The user may:

1) add a data point to the lower end of the data range and enter that data point multiple times if needed;
2) add a data point at the upper end of the data range and enter it several times if needed;
3) set the *y*-intercept.

To improve the fit for low data points from Little Granite Creek, 2002, two of the data pairs where $Q_{B,traps}$ = 1E-6 (see gray-shaded data in Table 21) that were not included in fitting the power function were included in the polynomial curve fitting. At the upper end of the data range a data pair ($\log(Q_{B,traps}) = \log 1$; $\log(Q_{B,HS}) = \log 1.0$) was added, and the *y*-intercept *c* was set to a value of log(-0.1). The parameters of the polynomial function for Little Granite Creek 2002 are a = -0.4242, b = 1.0398, and c = -0.1 (Table 22). Note that the parameters *a* and *b* obtained from the 2nd order polynomial fit are not the same as the power function *a*-coefficient and *b*-exponents.

8. Computation of inter-sampler transport relationship from 2nd order polynomial function

A) To compute an inter-sampler transport relationship from a 2nd order polynomial function, the parameters *a*, *b*, and *c* need to be applied to specified log-transformed values of *x* ($\log(Q_{B,HS})$) to compute

$$\log(Q_{B,HS\ adj.}) = a \cdot \log(Q_{B.HS})^2 + b \log(Q_{B.HS}) + c$$

The antilog of the result provides the adjusted HS transport rate

$$10\text{^}\log(Q_{B,HS\ adj.}) = Q_{B,HS\ adj.}$$

Computations need to be repeated for all HS transport rates for which adjustment is desired.

B) Intersection points with the 1:1 line are less important for polynomial inter-sampler transport relationships because the fitted polynomial functions tend to approach the 1:1 line asymptotically.

[7] The Excel function "fit trendline" may be used for this purpose. When guiding the fit, it may be useful to plot log-transformed data.

C) An estimated bias correction factor *CF* may be applied when using a polynomial function for the inter-sampler transport relationship. Values of 0.5 - 0.8 CF_{Duan} that should be within the range of >1 to <3 are suggested.

For the example of Little Granite Creek, 2002, the adjusted HS transport rate for a measured gravel transport rate of e.g., 0.02 g/m·s is computed as

$$Q_{B,HS,\,adj.} = 0.8\ CF_{Duan} \cdot 10\text{^}[\log(Q_{B,HS\,adj.}) = -0.4242 \cdot \log(Q_{B.HS})^2 + 1.0398 \log(Q_{B.HS}) + -0.1]$$

$$= 0.8\ CF_{Duan} \cdot 10\text{^}[-1.224 -1.767 - 0.1]$$

$$= 2.06 \cdot 10\text{^}[-3.091]$$

$$= 0.00167\ \text{g/m·s}$$

3. Prediction from bedmaterial and measured HS gravel transport rating curve

If measurements with a sampler other than the HS are not available, an adjustment function can be selected based on the parameters of the measured HS gravel transport relationship. It is assumed that data from the HS sampler extend over the range of flows commonly observed for the study stream.

1) Categorizing the study stream

Determine whether the study stream falls into the category of "red" or "blue" streams depending on the conditions listed in Table 23. Parameters printed in bold should be given highest consideration and values in gray the lowest for the categorization.

Table 23: Bedmaterial characteristics and parameters of the HS gravel transport relationship that determine the stream group and the respective inter-sampler relationships for the paired data approach.

Bedload conditions measured with HS sampler:	Streams in "red" group	Stream in "blue" group
Exponent of bedload rating curve	< 3.4*	> 3.4*
Coefficient of bedload rating curve	< 0.094	> 0.094
Exponent of flow competence curve	> 0.91*	< 0.91*
Coefficient of flow competence curve	< 9.7	> 9.7
Bedload D_{max} at 50% Q_{bkf}	**< 13 mm**	**> 13 mm**
Gravel transport rate at 50% Q_{bkf}	**< 0.15 g/m·s**	**> 0.15 g/m·s**
Bedload D_{max} at gravel transp. rate of 1 g/m·s	< 18 mm	> 18 mm

* Values from parameters printed in gray did not result from a statistically significant relationship.

The coefficients of the gravel bedload rating curve and the flow competence curve

$$Q_{B,HS} = 0.032\ Q^{2.60}$$

$$D_{max,HS} = 7.46\ Q^{0.35}$$

suggest a "red" stream group, while the exponent of the flow competence curve suggests a "blue" stream. The bedload D_{max} and transport rate measured at 50% Q_{bkf} are 8.4 mm and 0.078 g/m·s, while the bedload D_{max} measured at $Q_{B,HS}$ = 1 g/m·s is 11.8 mm. These two parameters should be given most weight, and they suggest that Little Granite Creek, 2002, falls in to the "red" stream group.

2) Applying the appropriate adjustment function for the HS sampler

Almost all of the criteria examined classified Little Granite Creek (2002) as a "red" stream. The adjustment function $Q_{B,HS\ adj} = a\ Q^{b}$ for "red" streams is

$$Q_{B,HS\ adj} = 0.532\ Q_{B\ HS}^{1.58}$$

and needs to be applied to the measured HS gravel transport relationship $Q_{B,HS} = c\ Q^{d}$ which for Little Granite Creek is

$$Q_{B,HS} = 0.0316\ Q^{2.60}$$

to yield the adjusted HS gravel transport rating relationship $Q_{B,HS\ adj} = a\ (c\ Q^{d})^{b}$ that for Little Granite Creek is

$$Q_{B,HS\ adj} = 0.532\ (0.0316\ Q^{2.60})^{1.58}$$

For streams categorized as "blue", the HS adjustment function is

$$Q_{B,HS\ adj} = 0.0235\ Q_{B\ HS}^{2.10}$$

For streams that appear to fall near the middle of red and blue streams, the user might take the geometric mean value obtained from applying the "red" and the "blue" adjustment functions to a measured HS transport rate.

C. Data tables

Time = Central time of sampling (mid point between start and stop of sampling time)
Q = Discharge (m^3/s)
$Q_{Bi\ traps}$ = Fractional Bedload Transport Rates, all traps (g/m·s)
$Q_{B,\ traps}$ = Total Gravel Transport Rates, all traps (g/m·s)
D_{max} = Sieve size class of largest collected bedload particle (mm)

Cherry Creek, OR, May and June 1999, bedload traps

Date	Time	Q	$Q_{B,\ traps}$ 4 – 64 mm	D_{max}
		(m^3/s)	(g/m·s)	(mm)
May 12	12:17	1.50	0	
May 12	13:52	1.51	1.40E-05	4
May 20	12:49	2.20	0.001813	8
May 24	12:04	3.85	0.024149	22.4
May 24	15:37	4.07	0.207165	45
May 25	12:46	4.47	0.695056	45
May 25	16:38	4.41	0.472336	32
May 26	11:56	4.12	0.598179	45
May 26	15:45	4.24	0.262162	32
May 27	11:28	4.18	0.393019	32
May 27	13:35	3.96	0.301449	32
June 7	13:19	2.32	0.000337	8
June 7	14:35	2.28	1.11E-05	4
June 9	12:22	1.97	0.000341	5.6
June 9	13:29	1.95	0.000185	4
June 11	10:34	2.16	0.000039	4
June 11	13:29	2.16	0	
June 11	13:29	2.12	6.60E-05	5.6
June 11	13:29	2.12	0	
June 18	11:42	3.03	0.014518	16
June 18	15:29	2.78	0.009506	8

Cherry Creek, May and June 1999, Helley-Smith samples

Date	Time	Q	$Q_{B\,HS}$ 4 – 64 mm	D_{max}
		(m^3/s)	(g/m·s)	(mm)
May 12	12:25	1.50	0.2135	11.2
May 12	14:02	1.51	0.0214	8
May 20	12:42	2.20	0.0138	4
May 20	13:37	2.20	0.0049	5.6
May 24	15:40	4.12	0.2549	11.2
May 25	12:25	4.50	0.9856	16
May 26	12:06	4.21	0.1558	11.2
May 26	15:56	4.24	0.2947	11.2
May 27	11:19	4.18	1.2636	22.4
May 27	13:40	3.96	1.6427	32
June 7	13:13	2.36	0.0057	5.6
June 7	14:02	2.32	0.1014	11.2
June 9	12:24	1.97	0.0787	11.2
June 9	13:29	1.95	0.0085	8
June 11	10:43	2.16	0.0131	8
June 11	11:51	2.16	0.1472	16
June 11	13:14	2.12	0.0015	4
June11	14:19	2.12	0.0127	8
June 18	11:47	3.08	0.5130	11.2
June 18	12:57	2.99	0.1055	11.2
June 18	15:28	2.85	0.4868	22.4

East Dallas Creek, May and June 2007, bedload traps

Date	Time	Q	$Q_{B,\ traps}$ 4 – 64 mm	D_{max}
		(m^3/s)	(g/m·s)	(mm)
May 3	15:06	0.53	0	
May 9	14:39	0.33	0	
May 9	18:00	0.34	0	
May 10	13:36	0.33	0	
May 10	15:56	0.34	0	
May 10	18:00	0.35	0	
May 11	17:27	0.40	0	
May 12	12:38	0.44	0	
May 12	15:31	0.45	0	
May 14	14:04	0.68	0.0007322	8.0
May 14	15:10	0.70	0.0016146	8.0
May 14	16:17	0.72	0.0011238	8.0
May 14	17:56	0.75	0.0027698	8.0
May 15	12:08	0.78	0.001637	8.0
May 15	13:24	0.79	0.0015238	8.0
May 15	14:41	0.79	0.0014907	8.0
May 15	15:51	0.82	0.0028389	8.0
May 15	16:58	0.87	0.0024873	11.3
May 15	18:09	0.89	0.0036156	11.3
May 17	11:50	0.79	0.0002284	5.6
May 17	13:05	0.79	0.0009091	5.6
May 17	14:20	0.79	0.0009441	11.3
May 17	15:20	0.79	0.0004449	5.6
May 17	16:18	0.79	0.0003639	5.6
May 17	17:17	0.79	0.0006564	8.0
May 19	11:56	0.86	0.0008212	8.0
May 19	12:57	0.86	0.0007562	5.6
May 19	13:56	0.86	0.0007829	5.6
May 19	14:56	0.88	0.0020036	8.0
May 19	15:56	0.97	0.0026986	8.0
May 19	16:56	1.02	0.0042112	8.0
May 19	17:58	1.03	0.00556	11.3
May 19	18:58	1.04	0.0055154	11.3
May 20	12:12	1.06	0.0057123	11.3
May 20	13:26	1.08	0.0047079	11.3
May 20	14:40	1.11	0.0145497	11.3
May 20	15:40	1.09	0.0133107	8.0
May 20	16:41	1.11	0.009325	8.0
May 20	17:41	1.11	0.0105365	11.3
May 20	18:40	1.11	0.0200509	8.0

Date	Time	Q	$Q_{B,\ traps}$ 4 – 64 mm	D_{max}
		(m^3/s)	(g/m·s)	(mm)
May 21	12:16	1.10	0.0023999	8.0
May 21	13:17	1.09	0.0037742	11.3
May 21	14:17	1.09	0.006335	16.0
May 21	15:17	1.10	0.0075309	11.3
May 21	16:18	1.11	0.0129758	11.3
May 21	17:19	1.11	0.0116095	16.0
May 21	18:19	1.16	0.0096276	11.3
May 24	14:53	0.86	0.0017242	8.0
May 24	15:58	0.86	0.0024042	11.3
May 24	16:59	0.86	0.0018385	8.0
May 24	18:01	0.86	0.0014956	8.0
May 25	11:53	0.78	0.0004969	5.6
May 25	12:56	0.79	0.0017054	8.0
May 25	14:00	0.78	0.0007428	5.6
May 25	15:03	0.77	0.0015535	11.3
May 25	16:06	0.76	0.000631	8.0
May 25	17:06	0.76	0.0006306	11.3
May 26	11:38	0.74	0.0002925	8.0
May 26	12:37	0.73	0.001237	8.0
May 26	13:38	0.73	0.0009453	8.0
May 26	14:41	0.73	0.000756	8.0
May 26	15:47	0.73	0.00067	11.3
May 29	12:02	1.05	0.0006926	8.0
May 29	13:02	1.05	0.0019999	16.0
May 29	14:04	1.05	0.0044618	8.0
May 29	15:03	1.06	0.0059677	11.3
May 29	16:04	1.07	0.0067372	11.3
May 29	17:05	1.09	0.0043194	11.3
May 30	12:09	1.08	0.003003	11.3
May 30	13:08	1.06	0.0028578	11.3
May 30	14:09	1.07	0.0073563	11.3
May 30	15:09	1.09	0.0043233	11.3
May 30	16:08	1.14	0.0049058	11.3
May 30	17:08	1.20	0.0138925	16.0
May 30	18:08	1.23	0.0128013	11.3
May 31	12:18	1.27	0.0106981	11.3
May 31	13:19	1.28	0.0145043	16.0
May 31	14:19	1.29	0.0216543	11.3
May 31	15:19	1.34	0.0327271	16.0
May 31	16:19	1.41	0.0282924	11.3
May 31	17:19	1.48	0.0288767	22.6

Date	Time	Q	$Q_{B,\ traps}$ 4 – 64 mm	D_{max}
		(m^3/s)	(g/m·s)	(mm)
May 31	18:21	1.53	0.0292188	11.3
May 31	19:21	1.56	0.0660094	16.0
June 1	11:59	1.63	0.0191316	11.3
June 1	13:00	1.63	0.0437138	16.0
June 1	14:01	1.63	0.0495472	16.0
June 1	15:02	1.66	0.0737532	16.0
June 1	16:03	1.71	0.1028313	16.0
June 1	17:04	1.81	0.1849609	16.0
June 1	18:06	1.86	0.1130675	32.0
June 1	19:05	1.90	0.1602192	22.6
June 2	12:15	1.95	0.0914691	16.0
June 2	13:15	1.94	0.2086881	16.0
June 2	14:18	1.97	0.2762846	22.6
June 2	15:17	1.98	0.2489274	22.6
June 2	16:18	2.11	0.511799	32.0
June 2	17:20	2.22	1.1459382	45.0
June 2	18:58	2.32	1.4082488	32.0
June 2	19:22	2.33	2.9455234	45.0
June 3	12:20	2.14	0.9808347	45.0
June 3	13:17	2.12	0.7084541	22.6
June 3	15:31	2.16	0.5854594	32.0
June 3	16:32	2.18	1.1287996	45.0
June 3	17:33	2.26	3.7659156	45.0
June 4	12:38	2.12	0.3310781	22.6
June 4	13:39	2.10	0.438143	22.6
June 4	14:39	2.08	0.345996	32.0
June 4	15:39	2.08	0.4605854	22.6
June 4	16:43	2.06	0.6294873	45.0
June 4	17:48	2.07	0.4153059	32.0
June 5	12:02	2.03	0.3172452	22.6
June 5	13:02	2.04	0.7781837	22.6
June 5	14:02	2.05	0.9234684	32.0
June 5	15:03	2.10	0.6013334	22.6
June 5	16:02	2.16	0.5847846	22.6
June 5	17:01	2.22	1.2893027	32.0
June 5	18:01	2.28	1.4447717	32.0
June 5	19:02	2.35	1.2973961	32.0
June 5	20:02	2.40	1.6275827	32.0
June 6	12:14	2.31	0.7850425	45.0
June 6	14:44	2.26	0.3089275	45.0
June 6	15:45	2.23	0.465448	32.0

Date	Time	Q	$Q_{B,\ traps}$ 4 – 64 mm	D_{max}
		(m^3/s)	(g/m·s)	(mm)
June 6	16:47	2.21	0.3382736	32.0
June 6	17:49	2.16	0.2521886	32.0
June 7	13:43	1.77	1.3577909	22.6
June 7	14:50	1.73	1.0792451	22.6
June 7	15:56	1.73	0.5377632	22.6
June 7	16:56	1.70	3.2997147	32.0
June 8	16:45	1.44	0.3674659	22.6
June 8	17:47	1.49	1.7493586	32.0
June 8	18:47	1.53	3.1465703	32.0
June 10	12:45	2.17	6.0390568	22.6
June 10	14:32	2.20	2.392673	45.0
June 10	15:19	2.22	1.9117372	32.0
June 10	15:48	2.24	5.6802385	64.0
June 11	11:26	2.76	8.9035243	45.0
June 11	13:18	2.73	12.105054	45.0
June 11	14:14	2.70	6.2235313	45.0
June 11	15:39	2.66	10.368195	45.0
June 11	16:13	2.67	8.9902864	45.0
June 13	11:30	2.21	0.3786963	22.6
June 13	12:32	2.21	1.1604304	45.0
June 13	15:52	2.19	5.8982614	45.0
June 13	16:15	2.20	10.717403	45.0
June 14	12:34	2.30	14.880883	32.0
June 14	15:57	2.37	10.142837	32.0
June 14	18:35	2.59	16.37302	45.0
June 15	12:16	2.71	8.844647	45.0
June 15	17:11	3.11	61.0389	45.0
June 16	12:58	3.44	16.3528	45.0
June 16	14:56	3.49	4.95697	32.0
June 16	15:10	3.49	5.65275	45.0
June 16	16:26	3.52	18.1688	45.0
June 16	17:12	3.55	10.9979	45.0
June 16	17:26	3.57	5.82899	64.0
June 17	13:36	3.32	3.60872	45.0
June 17	15:12	3.42	4.02045	45.0
June 17	15:45	3.49	16.9790	45.0
June 17	16:15	3.55	5.66976	64.0
June 17	17:35	3.92	20.1593	64.0
June 17	18:35	4.17	20.3260	45.0
June 18	14:11	3.48	13.8126	45.0
June 18	15:23	3.47	8.07285	64.0

Date	Time	Q	$Q_{B,\ traps}$ 4 – 64 mm	D_{max}
		(m^3/s)	(g/m·s)	(mm)
June 18	16:43	3.61	58.1703	64.0
June 18	17:08	3.61	130.854	64.0
June 20	13:56	3.42	15.0726	64.0
June 20	15:16	3.44	18.9801	45.0
June 20	18:34	3.78	39.7645	45.0
June 20	19:27	3.86	27.7277	64.0

East Dallas Creek, Helley-Smith samples, May and June 2007

Date	Time	Q	$Q_{B\,HS}$ 4 – 64 mm	D_{max}
		(m^3/s)	(g/m·s)	(mm)
May 3	17:25	0.50	0.1837	11.3
May 9	11:17	0.32	0.0117	5.6
May 10	11:11	0.32	0.0547	8
May 10	19:20	0.34	0.0335	11.3
May 11	13:23	0.35	0.0933	8
May 11	19:25	0.43	0.0542	8
May 12	11:16	0.44	0.0350	5.6
May 14	13:01	0.67	0.2377	11.3
May 14	19:49	0.79	0.5891	22.6
May 15	10:49	0.76	0.5220	22.6
May 15	19:25	0.89	0.1801	11.3
May 17	10:16	0.80	0.8122	22.6
May 17	18:37	0.81	0.8472	22.6
May 19	10:50	0.86	0.3842	11.3
May 19	20:17	1.04	0.6591	11.3
May 20	11:06	1.06	1.3138	32
May 20	19:55	1.13	0.1487	8
May 21	11:11	1.11	0.0838	11.3
May 21	19:48	1.18	0.8552	16
May 24	13:47	0.85	0.1320	16
May 24	19:15	0.84	0.4447	22.6
May 25	10:44	0.78	0.3230	22.6
May 25	18:20	0.76	0.7101	22.6
May 26	10:34	0.74	0.3456	22.6
May 26	17:29	0.73	0.0583	8
May 29	10:18	1.06	0.8034	16
May 29	18:38	1.09	0.8815	32
May 30	10:59	1.09	0.6255	16
May 30	19:26	1.27	0.5752	11.3
May 31	11:12	1.29	0.6088	16
May 31	20:27	1.57	0.2741	16
June 1	10:50	1.63	0.7553	16
June 1	21:02	1.96	1.2212	11.3
June 2	10:58	1.96	1.1913	22.6
June 2	20:57	2.44	4.8702	32
June 3	11:02	2.18	2.4708	32
June 3	18:45	2.26	7.8631	32
June 4	11:09	2.16	1.1702	16
June 4	19:03	2.09	5.2574	45
June 5	10:57	2.06	3.3180	32
June 5	21:08	2.45	5.5045	45

Date	Time	Q	$Q_{B\,HS}$ 4 – 64 mm	D_{max}
		(m^3/s)	(g/m·s)	(mm)
June 6	11:02	2.50	8.1678	32
June 6	19:05	2.20	3.0650	32
June 7	12:30	1.81	7.5970	32
June 7	18:54	1.65	10.924	22.6
June 8	15:33	1.40	5.3004	16
June 8	19:46	1.54	8.6483	32
June 10	11:47	2.17	7.9024	22.6
June 10	16:37	2.32	18.788	22.6
June 11	10:32	2.76	34.361	45
June 11	17:05	2.65	9.606	22.6
June 13	10:08	2.21	2.8434	22.6
June 13	17:30	2.21	49.590	45
June 14	11:11	2.32	99.516	32
June 14	19:35	2.72	12.746	32
June 15	12:07	2.70	48.272	32
June 16	12:12	2.93	41.449	32

East St. Louis Creek, bedload traps, May to July 2003

Date	Time	Q	$Q_{B,\ traps}$ 4 – 64 mm	D_{max}
		(m^3/s)	(g/m·s)	(mm)
May 30	13:27	0.801	0.175057	32
May 30	14:26	0.848	0.686412	32
May 30	15:30	0.889	0.837128	32
May 30	16:30	0.901	1.177065	45
May 30	18:36	0.901	0.763306	22.4
May 31	11:55	0.782	0.045635	32
May 31	12:56	0.823	0.036326	16
May 31	14:06	0.910	0.577494	32
May 31	15:02	0.989	1.023730	32
May 31	16:51	1.063	0.869915	32
May 31	17:30	1.071	0.984289	32
May 31	19:02	1.043	1.171875	45
May 31	19:21	1.041	1.869204	45
June 1	10:03	0.943	0.128637	45
June 1	10:50	0.941	0.220191	45
June 2	10:56	0.780	0.106006	32
June 2	11:58	0.779	0.035550	16
June 2	13:01	0.796	0.101559	22.4
June 2	14:00	0.826	0.337246	32
June 2	15:00	0.872	1.011652	32
June 2	15:54	0.904	2.842542	32
June 2	16:57	0.919	2.604593	45
June 2	18:47	0.931	0.785344	64
June 3	11:34	0.742	0.035369	32
June 3	12:38	0.743	0.012784	16
June 3	13:41	0.758	0.032828	22.4
June 3	14:46	0.783	0.060938	22.4
June 3	15:52	0.808	0.154280	32
June 3	17:01	0.824	0.279287	32
June 3	18:06	0.830	0.182011	22.4
June 4	10:36	0.681	0.026380	22.4
June 4	12:24	0.679	0.025432	22.4
June 4	13:37	0.689	0.009935	16
June 4	14:48	0.706	0.024265	32
June 4	15:55	0.716	0.013877	22.4
June 4	17:00	0.723	0.008430	16
June 5	09:39	0.622	0.011363	22.4
June 5	10:46	0.616	0.010727	22.4
June 7	19:25	0.508	0.002955	11.2
June 8	10:33	0.456	0.000290	5.6

Date	Time	Q	$Q_{B,\ traps}$ 4 – 64 mm	D_{max}
		(m^3/s)	(g/m·s)	(mm)
June 8	11:38	0.454	0.000598	8
June 8	12:56	0.459	0.000599	8
June 8	14:12	0.480	0.001996	16
June 8	15:18	0.502	0.007231	16
June 8	16:27	0.523	0.016832	16
June 8	17:34	0.542	0.007608	11.2
June 8	18:39	0.546	0.010301	11.2
June 9	13:02	0.478	0.009700	11.2
June 9	14:09	0.513	0.009117	16
June 9	15:16	0.544	0.013689	16
June 9	16:22	0.569	0.064545	22.4
June 9	17:28	0.592	0.015949	11.2
June 9	18:33	0.595	0.025036	22.4
June 10	11:56	0.534	0.009265	16
June 10	13:02	0.562	0.010079	16
June 10	14:07	0.611	0.030491	16
June 10	15:11	0.659	0.064788	22.4
June 10	16:18	0.676	0.044055	16
June 10	17:23	0.670	0.054766	22.4
June 10	18:28	0.661	0.033322	22.4
June 11	11:53	0.573	0.001945	8
June 11	12:58	0.596	0.002808	11.2
June 11	14:02	0.629	0.009041	22.4
June 11	15:07	0.678	0.029987	22.4
June 11	16:11	0.723	0.050899	22.4
June 11	17:17	0.744	0.131845	32
June 11	18:22	0.742	0.069745	32
June 11	19:27	0.731	0.060146	22.4
June 12	12:08	0.595	0.002047	11.2
June 12	13:14	0.604	0.003725	11.2
June 12	14:23	0.621	0.015875	22.4
June 12	15:28	0.633	0.002960	11.2
June 12	16:32	0.645	0.013774	22.4
June 12	17:37	0.655	0.005216	11.2
June 13	11:47	0.586	0.010188	22.4
June 13	12:56	0.591	0.002225	8
June 13	14:03	0.593	0.003032	16
June 13	15:06	0.596	0.000821	8
June 13	16:09	0.601	0.004046	16
June 13	18:50	0.611	0.003250	16
June 14	09:53	0.559	0.001392	8

Date	Time	Q	$Q_{B,\ traps}$ 4 – 64 mm	D_{max}
		(m^3/s)	(g/m·s)	(mm)
June 15	14:07	0.633	0.014016	16
June 15	15:12	0.663	0.013066	22.4
June 15	16:17	0.681	0.020163	22.4
June 15	17:23	0.681	0.024221	22.4
June 15	18:27	0.691	0.027614	22.4
June 15	19:31	0.701	0.026388	22.4
June 16	12:35	0.613	0.002876	8
June 16	13:42	0.616	0.012686	22.4
June 16	14:47	0.614	0.008954	22.4
June 16	15:49	0.616	0.009377	16
June 16	16:54	0.623	0.025533	32
June 16	18:00	0.636	0.015514	22.4
June 16	19:04	0.640	0.004898	8
June 17	11:43	0.572	0.005071	8
June 17	12:47	0.588	0.003289	11.2
June 17	13:49	0.608	0.008827	16
June 17	14:56	0.637	0.019407	22.4
June 17	16:02	0.657	0.026581	22.4
June 17	17:07	0.659	0.043424	22.4
June 17	18:13	0.654	0.027223	16
June 17	19:18	0.648	0.019410	16
June 18	12:13	0.575	0.005370	11.2
June 18	13:22	0.582	0.003009	8
June 18	14:29	0.595	0.006748	16
June 18	15:33	0.611	0.007327	11.2
June 18	16:39	0.628	0.022359	22.4
June 18	17:46	0.640	0.009613	16
June 18	18:51	0.643	0.034105	22.4
June 19	11:10	0.575	0.005198	16
June 19	13:26	0.582	0.006387	16
June 19	14:46	0.590	0.002714	11.2
June 19	17:30	0.606	0.007734	16
June 20	13:17	0.572	0.003970	11.2
June 20	14:24	0.579	0.002032	8
June 20	15:28	0.590	0.009519	22.4
June 20	17:47	0.595	0.004042	11.2
June 21	12:28	0.543	0.001024	8
June 21	14:04	0.562	0.002154	8
June 21	15:09	0.585	0.016354	32
June 21	16:14	0.601	0.006976	16
June 21	17:21	0.608	0.013178	16

Date	Time	Q	$Q_{B,\ traps}$ 4 – 64 mm	D_{max}
		(m^3/s)	(g/m·s)	(mm)
June 21	18:28	0.608	0.011778	16
June 22	10:52	0.538	0.001249	8
June 22	13:27	0.543	0.000799	8
July 3	13:25	0.346	0.000031	4
July 3	15:06	0.346	0.000059	4
July 3	16:12	0.346	0.001305	11.2
July 3	17:18	0.347	0.000690	8
July 3	18:27	0.352	0.000334	5.6
July 4	15:02	0.328	0.000114	2.8
July 4	10:43	0.337	0	2.8
July 4	11:54	0.333	0	2.8

East St. Louis Creek, May to July 2003, Helley-Smith samplers

Date	Time	Q	$Q_{B\,HS}$ 4 – 64 mm	D_{max}
		(m^3/s)	(g/m·s)	(mm)
May 30	17:39	0.908	3.0512	22.6
May 31	15:45	1.037	6.2286	22.6
May 31	18:11	1.059	7.7975	45
June 2	17:50	0.929	0.9952	16
June 3	10:18	0.748	0.8093	11.3
June 3	18:53	0.832	2.0113	32
June 4	11:29	0.679	0.6383	16
June 4	17:46	0.721	1.0230	22.6
June 5	11:37	0.614	0.5001	16
June 8	09:31	0.456	0.1750	16
June 8	19:26	0.543	0.5200	16
June 9	09:59	0.456	0.2903	16
June 9	19:25	0.593	0.3599	16
June 10	09:36	0.499	0.2157	11.3
June 10	19:16	0.653	0.4593	11.3
June 11	11:05	0.566	0.3162	8
June 11	20:20	0.715	1.7627	22.6
June 12	10:00	0.591	0.3500	11.3
June 13	09:39	0.587	0.5369	16
June 13	16:56	0.606	0.6393	16
June 14	08:57	0.561	0.3589	11.3
June 15	13:21	0.612	0.9335	22.6
June 15	20:18	0.698	1.1920	16
June 16	10:51	0.599	0.5776	11.3
June 16	19:53	0.640	0.5796	11.3
June 17	09:46	0.566	0.3997	11.3
June 17	20:06	0.643	1.1006	22.6
June 18	11:07	0.572	0.3191	16
June 18	19:43	0.640	0.4573	16
June 19	12:33	0.577	0.3271	11.3
June 19	19:46	0.619	0.3838	16
June 20	09:31	0.553	0.3867	11.3
June 20	19:49	0.598	0.2098	8
June 21	13:13	0.543	0.3629	16
June 21	19:20	0.603	0.6422	16
June 22	12:30	0.531	0.0974	11.3
July 3	14:13	0.346	0.0557	8
July 3	19:18	0.355	0.0875	8
July 4	09:44	0.337	0.1362	11.3
July 4	17:48	0.328	0.0318	5.6

East St. Louis Creek, May and June 2001, bedload traps

Date	Time	Q	$Q_{B,\ traps}$ 4 – 64 mm	D_{max}
		(m^3/s)	(g/m·s)	(mm)
May 16	16:00	0.194	0	
May 16	17:32	0.242	0	
May 22	14:30	0.189	0	
May 22	16:12	0.197	0	
May 23	11:29	0.179	0	
May 23	13:10	0.184	0	
May 23	14:45	0.199	2.746E-05	4
May 23	16:15	0.232	0	
May 24	13:15	0.200	0	
May 24	14:48	0.212	0	
May 24	16:25	0.227	8.777E-05	4
May 24	18:05	0.243	0	
May 24	19:36	0.254	0	
May 31	14:03	0.331	0.0002408	4
May 31	15:35	0.355	0.0005147	5.6
May 31	17:07	0.382	0.0010796	5.6
May 31	18:40	0.401	0.0016103	8
June 1	12:09	0.324	0.0003286	5.6
June 1	13:41	0.358	0.0010721	8
June 1	15:13	0.419	0.0058902	8
June 1	16:46	0.479	0.0150107	8
June 1	18:21	0.505	0.055562	11.2
June 1	19:54	0.505	0.0572851	11.2
June 2	10:36	0.379	0.0007056	5.6
June 2	12:16	0.385	0.0004006	5.6
June 2	13:53	0.425	0.0017579	8
June 2	15:28	0.473	0.0056868	11.2
June 2	17:03	0.496	0.0085603	11.2
June 2	18:39	0.519	0.0088685	16
June 2	20:14	0.528	0.0414671	11.2
June 3	10:37	0.411	0.0014916	8
June 3	12:10	0.414	0.0011613	8
June 3	13:53	0.425	0.0033717	11.2
June 4	12:06	0.391	0.0003333	5.6
June 4	13:45	0.386	0.0018198	11.2
June 4	15:17	0.389	0.0012045	5.6
June 4	16:49	0.398	0.0027106	11.2
June 4	18:29	0.405	0.0014336	5.6
June 5	10:10	0.350	0.0010388	5.6
June 5	05:31	0.348	0.0013276	8

Date	Time	Q	$Q_{B,\ traps}$ 4 – 64 mm	D_{max}
		(m^3/s)	(g/m·s)	(mm)
June 6	14:55	0.414	0.0033908	8
June 6	16:28	0.461	0.0148712	11.2
June 6	18:00	0.481	0.0184284	11.2
June 6	19:29	0.488	0.0198118	11.2
June 7	10:23	0.379	0.0012114	8
June 7	12:09	0.384	0.0035036	8
June 7	13:38	0.413	0.0025846	8
June 7	15:10	0.443	0.0075493	11.2
June 7	16:50	0.477	0.0115176	8
June 7	18:23	0.505	0.023105	11.2
June 7	19:57	0.508	0.0240305	11.2
June 8	10:32	0.400	0.0028831	11.2
June 8	12:06	0.405	0.0011409	5.6
June 8	13:38	0.420	0.0025819	8
June 8	15:11	0.456	0.0044074	11.2
June 8	16:45	0.485	0.0068805	11.2
June 8	18:19	0.496	0.0136237	11.2
June 8	19:51	0.498	0.0127155	11.2
June 9	11:42	0.409	0.0011262	8
June 9	13:14	0.419	0.0011373	5.6
June 9	14:45	0.430	0.00179	8
June 9	16:45	0.435	0.0015505	11.2
June 9	18:58	0.450	0.0034931	8
June 10	10:41	0.395	0.001348	8
June 10	12:21	0.399	5.104E-05	4
June 10	13:56	0.415	0.00063	8
June 10	15:29	0.447	0.0046886	11.2
June 10	17:02	0.462	0.0092575	11.2
June 11	12:57	0.401	0.0023012	11.2
June 11	14:54	0.429	0.0044031	8
June 11	16:31	0.451	0.0093011	11.2
June 11	18:17	0.454	0.0079941	11.2
June 11	19:55	0.456	0.0082938	11.2
June 12	09:10	0.393	0.002073	8
June 12	11:19	0.395	0.0016667	8
June 12	12:54	0.395	0.001295	8
June 12	15:26	0.407	0.0016561	8
June 12	16:57	0.409	0.0011483	5.6
June 12	18:28	0.409	0.003362	11.2
June 13	10:01	0.379	0.0003171	5.6
June 15	12:28	0.311	0.0003089	5.6

Date	Time	Q	$Q_{B,\ traps}$ 4 – 64 mm	D_{max}
		(m^3/s)	(g/m·s)	(mm)
June 15	14:05	0.331	0.0001553	5.6
June 15	15:44	0.339	0.000209	5.6
June 15	17:18	0.333	0.0002387	5.6
June 15	18:49	0.324	4.951E-05	4
June 15	20:22	0.317	0.0001686	5.6
June 16	10:13	0.282	0	
June 16	11:47	0.281	9.68E-05	4
June 16	13:23	0.279	7.969E-05	5.6
June 16	14:58	0.284	0	
June 16	16:34	0.292	0.0002002	5.6
June 16	18:08	0.294	0.0001755	5.6
June 17	10:15	0.272	0	
June 17	11:53	0.270	0	

East St. Louis Creek, May and June 2001, Helley-Smith sampler

Date	Time	Q	$Q_{B\,HS}$ 4 – 64 mm	D_{max}
		(m^3/s)	(g/m·s)	(mm)
May 22	15:20	0.193	0	2.8
May 22	17:00	0.198	0	2.8
May 23	10:45	0.179	0	2.8
May 23	12:15	0.179	0.0101	5.6
May 23	14:00	0.190	0	2.8
May 23	15:32	0.214	0	2
May 23	16:57	0.249	0	2.8
May 24	14:05	0.211	0.0091	4
May 24	15:32	0.223	0	2
May 24	17:10	0.235	0	2
May 24	18:48	0.249	0.0013	4
May 31	14:45	0.340	0.0328	8
May 31	16:18	0.367	0.0513	8
May 31	17:50	0.391	0.1430	11.2
May 31	19:20	0.409	0.2412	16
June 1	12:53	0.336	0.1520	16
June 1	14:25	0.382	0.1818	11.2
June 1	15:55	0.448	0.0377	5.6
June 1	17:30	0.499	0.2873	8
June 1	19:05	0.505	0.0995	5.6
June 1	20:40	0.505	0.1405	8
June 2	11:20	0.377	0.0403	8
June 2	13:00	0.395	0.0012	4
June 2	14:36	0.450	0.0203	8
June 2	16:13	0.486	0.2418	11.2
June 2	17:48	0.508	0	2.8
June 2	19:21	0.525	0.0100	4
June 2	21:00	0.531	0.1789	16
June 3	11:20	0.409	0.3243	11.2
June 3	12:55	0.409	0.1869	11.2
June 3	14:36	0.442	0.7036	22.4
June 4	12:50	0.389	0.0100	5.6
June 4	14:28	0.386	0.0013	4
June 4	16:00	0.394	0.0382	8
June 4	17:36	0.400	0.0601	5.6
June 4	19:14	0.409	0.2960	11.2
June 5	10:54	0.350	0.0498	8
June 5	12:00	0.346	0.0036	4
June 6	15:38	0.442	0.3372	11.2
June 6	17:12	0.474	0.7347	11.2
June 6	18:41	0.486	0.2333	11.2

Date	Time	Q	$Q_{B\,HS}$ 4 – 64 mm	D_{max}
		(m^3/s)	(g/m·s)	(mm)
June 6	20:13	0.491	0.3722	11.2
June 7	11:07	0.377	0.2402	8
June 7	12:53	0.393	0.0174	5.6
June 7	14:21	0.433	0.1160	5.6
June 7	16:01	0.458	0.0896	8
June 7	17:33	0.490	0.3846	11.2
June 7	19:07	0.508	0.4230	11.2
June 7	20:40	0.505	0.0527	5.6
June 8	11:17	0.400	0.1349	8
June 8	12:48	0.409	0.3814	11.2
June 8	14:17	0.435	0.0835	8
June 8	15:56	0.473	0.3150	11.2
June 8	17:27	0.491	0.1696	11.2
June 8	19:03	0.500	0.3673	11.2
June 8	20:36	0.495	0.1542	11.2
June 9	12:26	0.409	0.0796	8
June 9	13:58	0.428	0.0276	5.6
June 9	15:30	0.432	0.1536	8
June 9	18:01	0.447	0.0828	8
June 9	19:42	0.452	0.1645	11.2
June 10	11:27	0.395	0.0383	5.6
June 10	13:06	0.404	0.0578	5.6
June 10	14:39	0.429	0.0423	5.6
June 10	16:12	0.456	0.0943	11.2
June 10	17:46	0.469	0.0226	5.6
June 11	13:58	0.411	0.1592	8
June 11	15:39	0.440	0.1423	11.2
June 11	17:16	0.453	0.0228	5.6
June 11	19:02	0.456	0.2171	11.2
June 11	20:41	0.456	0.2130	8
June 12	09:55	0.392	0.1199	8
June 12	12:04	0.395	0.0987	11.2
June 12	13:38	0.395	0.0260	5.6
June 12	16:10	0.409	0.1000	11.2
June 12	17:40	0.409	0.0151	5.6
June 12	19:12	0.409	0.0077	5.6
June 13	10:45	0.381	0.0259	5.6
June 15	13:15	0.319	0	2.8
June 15	14:39	0.338	0.0129	4
June 15	16:29	0.337	0.0610	4
June 15	18:01	0.329	0.0168	4
June 15	19:33	0.320	0.0203	5.6

Date	Time	Q	$Q_{B\,HS}$ 4 – 64 mm	D_{max}
		(m^3/s)	(g/m·s)	(mm)
June 16	10:57	0.282	0.0073	5.6
June 16	12:33	0.279	0.0066	4
June 16	14:08	0.280	0.0156	4
June 16	15:43	0.288	0.0017	4
June 16	17:18	0.294	0.0004	4
June 16	18:50	0.294	0.0152	5.6
June 17	11:00	0.271	0.0081	4
June 17	12:39	0.270	0.0044	4

Halfmoon Creek, May and June 2004, bedload traps

Date	Time	Q	$Q_{B,\ traps}$ 4 – 64 mm	D_{max}
		(m^3/s)	(g/m·s)	(mm)
May 4	11:21	0.584	0	1.0
May 4	12:30	0.578	0	1.0
May 4	16:13	0.587	0	1.0
May 4	18:01	0.648	0	1.0
May 5	10:57	0.758	0	1.0
May 5	14:19	0.732	0	1.0
May 5	17:37	0.871	0	1.0
May 6	11:03	0.994	0	1.0
May 6	16:50	1.073	0.0002037	11.3
May 7	10:52	1.238	2.543E-05	4.0
May 7	13:36	1.181	1.312E-05	4.0
May 7	14:49	1.180	0	1.0
May 7	15:59	1.224	0.000024	4.0
May 7	17:08	1.340	0.000182	8.0
May 7	19:01	1.617	0.001219	11.3
May 8	10:52	1.468	0.000662	11.3
May 8	12:47	1.441	0.000725	11.3
May 8	14:39	1.405	0.000157	8.0
May 8	15:50	1.446	0.000254	8.0
May 8	16:59	1.547	0.000102	5.6
May 8	18:07	1.753	0.000024	4.0
May 9	10:46	1.608	0.000113	5.6
May 9	11:47	1.568	0.000283	8.0
May 9	14:22	1.497	0.000114	5.6
May 9	15:25	1.528	0.000066	5.6
May 9	16:35	1.610	0.000148	5.6
May 9	17:43	1.769	0.000554	5.6
May 9	19:30	2.039	0.000502	8.0
May 10	11:02	1.600	0.000219	5.6
May 10	12:54	1.545	0.000143	5.6
May 10	14:26	1.522	0.000108	5.6
May 10	15:57	1.584	0.000096	4.0
May 10	16:58	1.744	0.000190	8.0
May 10	17:53	1.950	0.001900	11.3
May 10	19:39	2.306	0.001590	11.3
May 11	15:54	1.741	0.000513	8.0
May 11	16:54	1.852	0.000261	5.6
May 11	17:55	1.965	0.001025	11.3
May 11	19:58	2.106	0.000880	8.0
May 14	12:39	1.034	0.000016	4.0

Date	Time	Q	$Q_{B,\ traps}$ 4 – 64 mm	D_{max}
		(m^3/s)	(g/m·s)	(mm)
May 14	13:50	1.047	0	1.0
May 14	15:11	1.015	0	1.0
May 14	16:28	0.954	0	1.0
May 15	11:53	0.845	0	1.0
May 15	13:22	0.844	0	1.0
May 15	15:48	0.821	0	1.0
May 17	15:26	0.937	0	1.0
May 17	16:25	0.945	0	1.0
May 18	11:19	1.024	0	1.0
May 18	13:33	1.029	0	1.0
May 18	15:45	1.046	0	1.0
May 18	16:46	1.120	0	1.0
May 18	17:45	1.282	0.000042	5.6
May 18	18:44	1.496	0.000108	8.0
May 18	19:44	1.710	0.003426	16.0
May 19	11:45	1.427	0.008885	32.0
May 19	13:35	1.414	0.000022	4.0
May 19	15:23	1.440	0	1.0
May 19	16:22	1.595	0.000562	11.3
May 19	17:22	1.933	0.0021015	16.0
May 19	18:21	2.348	0.0033236	11.3
May 19	20:12	2.890	0.0099668	22.6
May 20	12:23	1.820	0.0001333	5.6
May 20	14:21	1.844	5.502E-05	5.6
May 20	16:15	1.957	0.0001067	5.6
May 20	17:18	2.261	0.0011904	11.3
May 20	18:12	2.574	0.0003169	8.0
May 20	20:00	2.997	0.0034585	16.0
May 21	12:35	1.834	0.0005128	5.6
May 21	14:04	1.834	0.0006406	11.3
May 21	15:33	1.898	0.0005952	11.3
May 21	16:33	2.067	0.0025236	16.0
May 21	17:32	2.274	0.0020727	8.0
May 21	19:34	2.752	0.0040336	16.0
May 22	12:40	1.894	0.0017099	16.0
May 22	14:13	1.880	0.0007281	11.3
May 22	15:47	1.890	0.0008323	8.0
May 22	16:48	1.950	0.0063056	22.6
May 22	17:47	2.013	0.0004149	8.0
May 22	19:41	2.107	0.0044536	16.0
May 23	12:29	1.616	5.918E-05	4.0

Date	Time	Q	$Q_{B,\ traps}$ 4 – 64 mm	D_{max}
		(m^3/s)	(g/m·s)	(mm)
May 23	14:18	1.600	0.0001288	8.0
May 23	16:07	1.625	1.783E-05	4.0
May 23	17:09	1.632	5.92E-05	5.6
May 24	13:25	1.488	0.000267	16.0
May 26	16:24	1.460	7.37E-05	5.6
May 26	17:24	1.529	6.557E-05	5.6
May 27	11:44	1.503	8.866E-05	4.0
May 27	13:45	1.488	5.952E-05	8.0
May 27	15:47	1.512	4.74E-05	5.6
May 27	16:47	1.604	2.168E-05	4.0
May 27	17:48	1.711	0.0001736	5.6
May 28	11:42	1.629	9.942E-05	5.6
May 28	13:43	1.615	6.876E-05	5.6
May 28	15:44	1.648	2.19E-05	4.0
May 28	16:44	1.803	0.0001863	8.0
May 28	17:44	2.057	0.0002095	5.6
May 28	18:44	2.339	0.0006286	5.6
May 29	08:40	2.260	0.0006555	8.0
May 29	09:40	2.186	0.0035371	16.0
May 29	13:54	1.981	0.0007973	11.3
May 29	16:19	1.904	0.0002324	5.6
May 31	12:51	1.291	0.0001003	5.6
May 31	14:25	1.339	0.0020539	22.6
May 31	15:59	1.364	3.808E-05	4.0
May 31	16:59	1.391	0.0003313	11.3
May 31	17:58	1.429	0	1.0
June 1	11:49	1.185	5.437E-05	5.6
June 1	13:53	1.187	0	1.0
June 1	15:57	1.174	0	1.0
June 1	16:58	1.185	0	1.0
June 1	18:02	1.210	0	1.0
June 3	11:01	1.434	3.81E-05	4.0
June 3	13:43	1.434	0.0007745	16.0
June 3	16:23	1.445	1.749E-05	4.0
June 3	17:23	1.473	0.0006633	11.3
June 3	18:23	1.500	2.233E-05	4.0
June 3	19:23	1.540	0.0004148	8.0
June 4	10:02	1.572	0.0001171	5.6
June 4	11:02	1.566	0.0018899	16.0
June 4	13:36	1.565	0.000131	11.3
June 4	16:10	1.643	0.0026835	16.0

Date	Time	Q	$Q_{B,\ traps}$ 4 – 64 mm	D_{max}
		(m^3/s)	(g/m·s)	(mm)
June 4	17:10	1.846	0.0012798	11.3
June 4	18:10	2.087	0.0011138	11.3
June 4	19:10	2.283	0.0040692	16.0
June 4	20:10	2.421	0.0020244	16.0
June 5	11:20	1.911	0.0021806	11.3
June 5	12:20	1.882	0.0009949	11.3
June 5	14:12	1.950	0.0007506	11.3
June 5	16:03	2.198	0.0054293	11.3
June 5	17:02	2.585	0.0035467	16.0
June 5	18:00	3.024	0.0085007	16.0
June 5	18:59	3.500	0.0088401	22.6
June 5	19:54	3.893	0.0166029	16.0
June 6	11:26	2.580	0.0149858	16.0
June 6	12:26	2.528	0.0240367	22.6
June 6	14:04	2.608	0.0175738	22.6
June 6	15:41	2.913	0.0256349	22.6
June 6	16:42	3.318	0.0270914	16.0
June 6	17:38	3.744	0.0542754	16.0
June 6	18:30	4.152	0.1075489	32.0
June 6	19:16	4.496	0.1331787	22.6
June 7	12:10	3.028	0.0157291	16.0
June 7	13:12	2.968	0.0304039	22.6
June 7	14:14	2.995	0.0182162	16.0
June 7	15:15	3.163	0.0442489	22.6
June 7	16:15	3.427	0.1912015	32.0
June 7	17:13	3.787	0.1493928	32.0
June 7	18:02	4.194	0.2288555	22.6
June 7	18:49	4.497	0.5458968	32.0
June 7	19:41	4.727	1.0284763	32.0
June 8	11:11	3.191	0.1872565	22.6
June 8	12:24	3.093	0.2114495	32.0
June 8	14:08	3.081	0.0596092	22.6
June 8	15:51	3.251	0.1197847	32.0
June 8	16:52	3.537	0.1762885	32.0
June 8	17:52	3.830	0.2268859	22.6
June 8	18:55	4.070	0.462856	32.0
June 9	11:17	2.967	0.020469	32.0
June 9	12:18	2.945	0.0059765	16.0
June 9	14:02	2.982	0.0426261	22.6
June 9	15:49	3.095	0.0831272	22.6
June 9	16:56	3.258	0.0806028	32.0

Date	Time	Q	$Q_{B,\ traps}$ 4 – 64 mm	D_{max}
		(m^3/s)	(g/m·s)	(mm)
June 9	18:04	3.461	0.0911206	22.6
June 9	19:09	3.680	0.1084489	32.0
June 10	11:06	2.889	0.0049539	16.0
June 10	12:06	2.833	0.0055564	22.6
June 10	13:46	2.770	0.0048086	22.6
June 10	15:24	2.750	0.0056082	22.6
June 10	16:26	2.750	0.0059209	16.0
June 10	17:28	2.750	0.0039813	11.3
June 10	18:26	2.764	0.003576	11.3
June 11	14:14	2.210	0.0105146	22.6
June 15	16:39	2.184	0.0100509	16.0
June 15	17:39	2.270	0.0145539	16.0
June 15	18:39	2.334	0.0151749	22.6

Halfmoon Creek, May and June 2004, Helley-Smith samplers

Date	Time	Q	$Q_{B\,HS}$ 4 – 64 mm	D_{max}
		(m^3/s)	(g/m·s)	(mm)
May 4	13:38	0.578	0	2
May 4	19:33	0.689	0.0016	4
May 5	12:06	0.742	0.0146	5.6
May 5	19:25	1.023	0.0032	5.6
May 6	12:00	0.980	0.0217	8
May 6	18:25	1.249	0.0819	8
May 7	11:52	1.236	0.0651	11.3
May 7	18:05	1.532	0.0732	8
May 8	11:50	1.496	2.6479	45
May 8	19:25	1.943	0.5542	16
May 9	13:20	1.524	0.1045	11.3
May 9	18:39	1.975	0.4478	16
May 10	12:01	1.651	0.1118	8
May 10	18:48	2.216	0.3015	16
May 11	14:39	1.651	0.1656	11.3
May 11	18:55	2.133	0.0666	11.3
May 14	11:21	1.028	0.0744	11.3
May 14	17:29	0.922	0.0189	5.6
May 15	10:52	0.830	0.0389	5.6
May 15	17:36	0.819	0.0142	5.6
May 17	14:22	0.922	0.0263	8
May 18	10:09	1.038	0.0096	5.6
May 19	10:23	1.445	0.0550	11.3
May 19	19:20	2.756	0.1804	11.3
May 20	10:38	1.885	0.2375	16
May 20	19:03	2.882	1.8282	22.6
May 21	11:09	1.919	0.4768	16
May 21	18:32	2.631	0.0776	8
May 22	11:23	1.933	0.1294	11.3
May 22	18:47	2.165	0.2487	22.6
May 23	11:17	1.606	0.0584	11.3
May 23	18:09	1.666	0.0806	8
May 24	10:54	1.495	0.0863	11.3
May 26	15:08	1.452	0.0492	11.3
May 27	10:47	1.525	1.1089	32
May 27	18:50	1.816	0.0944	11.3
May 28	10:38	1.651	0.1480	11.3
May 28	20:15	2.719	0.6169	16
May 29	11:20	2.050	0.0530	8
May 31	11:43	1.265	0.0213	8
June 1	10:47	1.171	0.0104	5.6

Date	Time	Q	$Q_{B\,HS}$ 4 – 64 mm	D_{max}
		(m^3/s)	(g/m·s)	(mm)
June 3	09:58	1.445	0.0258	8
June 5	10:17	1.957	0.4461	22.6
June 6	10:08	2.621	0.1367	11.3
June 6	20:40	4.502	1.9790	32
June 7	10:37	3.086	2.5984	32
June 8	20:40	4.161	5.6471	45
June 9	20:55	3.769	2.9946	22.6
June 10	20:30	2.722	0.4404	16
June 15	20:10	2.480	0.4646	11.3

Hayden Creek, April to June, 2005, bedload traps

Date	Time	Q	$Q_{B,\ traps}$ 4 – 64 mm	D_{max}
		(m^3/s)	(g/m·s)	(mm)
April 27	13:02	0.390	0	
April 28	10:39	0.392	0	
April 28	12:13	0.390	0	
April 30	16:37	0.317	0.000013	4
May 4	16:36	0.324	0	
May 4	17:48	0.327	0.000149	8
May 5	11:15	0.337	0	
May 5	12:36	0.328	0	
May 5	14:00	0.336	0	
May 5	16:04	0.345	0	
May 6	11:55	0.436	0	
May 6	13:12	0.442	0	
May 6	17:22	0.542	0	
May 9	11:10	0.542	0.000128	5.6
May 9	12:14	0.546	0.000107	5.6
May 9	18:44	0.567	0.000261	8
May 10	10:32	0.663	0.000026	4
May 10	11:33	0.663	0.000644	5.6
May 10	12:33	0.662	0.000739	11.3
May 10	13:33	0.657	0.001006	8
May 10	14:34	0.659	0.000818	8
May 10	15:35	0.662	0.000986	11.3
May 10	17:31	0.691	0.001666	16
May 14	12:23	0.662	0.000134	5.6
May 14	13:24	0.654	0.000248	5.6
May 14	14:24	0.658	0.000705	11.3
May 14	15:24	0.661	0.000099	4
May 15	12:31	0.678	0	
May 15	13:33	0.679	0.000029	4
May 15	14:33	0.683	0.000059	4
May 15	15:32	0.683	0	
May 15	16:32	0.679	0.000021	4
May 16	13:12	0.757	0.000206	8
May 16	14:12	0.760	0.000080	5.6
May 16	15:12	0.765	0.000019	4
May 16	16:12	0.780	0.000316	8
May 16	17:12	0.802	0.000273	8
May 16	18:11	0.821	0.000066	4
May 17	10:05	1.164	0.021231	16
May 17	11:05	1.147	0.043062	16

Date	Time	Q	$Q_{B,\ traps}$ 4 – 64 mm	D_{max}
		(m^3/s)	(g/m·s)	(mm)
May 17	12:05	1.144	0.064955	22.6
May 17	13:05	1.133	0.033812	16
May 17	14:05	1.132	0.037043	22.6
May 17	15:05	1.117	0.033522	16
May 17	16:06	1.143	0.016864	16
May 17	17:05	1.145	0.033074	22.6
May 18	10:17	1.170	0.010911	16
May 18	11:17	1.155	0.016583	16
May 18	13:27	1.134	0.012523	22.6
May 18	15:37	1.147	0.034039	22.6
May 18	16:38	1.149	0.012836	16
May 18	17:40	1.169	0.012926	16
May 19	10:31	1.344	0.060558	32
May 19	11:32	1.334	0.011819	16
May 19	12:36	1.320	0.017179	22.6
May 19	13:39	1.342	0.029402	32
May 19	14:39	1.366	0.019022	16
May 19	15:40	1.388	0.021900	16
May 19	16:41	1.440	0.025821	16
May 19	17:40	1.498	0.068250	22.6
May 19	18:37	1.593	0.137056	32
May 19	19:16	1.635	0.104050	22.6
May 20	10:16	1.520	0.148813	22.6
May 20	11:23	1.463	0.257195	32
May 20	12:31	1.442	0.247326	22.6
May 20	13:36	1.446	0.191896	32
May 20	14:38	1.448	0.209685	32
May 20	17:38	1.524	0.130614	22.6
May 20	18:41	1.583	0.276041	32
May 21	10:37	1.798	0.343968	32
May 21	11:38	1.792	0.348951	45
May 21	12:38	1.802	0.160203	32
May 21	13:37	1.770	0.295668	32
May 21	14:41	1.818	0.499981	45
May 21	16:27	1.978	0.988975	45
May 21	17:07	2.085	1.501734	45
May 21	17:38	2.206	5.689891	45
May 21	18:52	2.499	19.05790	64
May 21	19:41	2.580	16.95861	64
May 22	11:34	2.075	0.588132	22.6
May 22	12:06	2.100	0.661036	32

Date	Time	Q	$Q_{B,\ traps}$ 4 – 64 mm	D_{max}
		(m^3/s)	(g/m·s)	(mm)
May 22	12:54	2.101	0.670980	32
May 22	15:02	2.140	1.012654	32
May 22	15:44	2.182	1.011514	45
May 22	17:25	2.351	5.075833	45
May 22	18:14	2.515	5.217394	64
May 22	19:12	2.745	5.606453	64
May 22	19:56	2.856	3.076023	64
May 23	11:35	2.439	1.883309	45
May 23	13:05	2.370	2.299692	64
May 23	14:23	2.500	3.040953	64
May 23	15:05	2.607	2.640360	45
May 23	16:12	2.633	2.626850	64
May 23	17:11	2.630	4.324902	64
May 23	18:29	2.765	13.31949	64
May 23	19:16	2.990	11.45183	64
May 24	11:00	2.437	3.116277	45
May 24	12:17	2.380	3.570883	64
May 24	13:46	2.322	2.124372	45
May 24	14:44	2.477	2.824924	64
May 24	15:17	2.440	5.630600	45
May 24	16:28	2.495	7.726509	64
May 24	17:22	2.520	7.880259	45
May 24	18:26	2.810	10.53074	64
May 24	19:29	2.695	24.45251	64
May 25	11:30	2.329	0.435245	45
May 25	12:39	2.340	1.814095	45
May 25	13:38	2.224	2.173333	64
May 25	14:37	2.259	2.955895	45
May 25	15:41	2.384	2.487853	45
May 25	16:28	2.560	4.229307	64
May 25	17:01	2.656	2.562026	45
May 25	18:11	2.823	5.080207	64
May 25	19:00	2.966	8.484988	64
May 26	11:35	2.309	2.402184	90
May 26	12:30	2.200	1.193629	45
May 26	13:30	2.085	1.839228	45
May 26	14:30	2.123	2.030916	45
May 26	15:30	2.240	2.136377	45
May 26	16:30	2.230	2.203414	64
May 26	17:29	2.249	2.705968	45
May 27	12:33	1.980	0.244120	45

Date	Time	Q	$Q_{B,\ traps}$ 4 – 64 mm	D_{max}
		(m^3/s)	(g/m·s)	(mm)
May 27	13:41	1.891	0.282036	32
May 27	14:41	1.894	0.625050	32
May 27	15:40	1.916	0.687925	45
May 27	16:41	1.949	0.503840	45
May 27	17:40	1.941	0.942796	32
May 27	18:38	1.935	0.583623	45
May 28	11:52	1.961	0.112312	22.6
May 28	14:12	1.960	0.169851	32
May 28	15:12	2.013	0.129177	32
May 28	16:09	2.109	0.172574	32
May 28	17:21	2.201	0.684145	45
May 28	18:33	2.340	1.049426	90
May 29	11:49	2.299	0.036205	22.6
May 29	12:49	2.229	0.041922	32
May 29	13:49	2.193	0.089684	32
May 29	14:56	2.200	0.132418	22.6
May 29	16:01	2.254	0.153272	22.6
May 29	17:07	2.253	0.144384	32
May 29	18:14	2.276	0.247603	32
May 29	19:18	2.276	0.250650	32
June 1	16:36	1.588	0.001834	8
June 1	17:38	1.615	0.001750	8
June 1	18:36	1.655	0.002988	11.3
June 2	11:32	1.661	0.003342	11.3
June 2	12:32	1.630	0.002903	11.3
June 2	13:38	1.604	0.003662	16
June 2	14:42	1.599	0.006894	16
June 2	15:42	1.606	0.012706	22.6
June 2	16:42	1.644	0.007172	11.3
June 2	17:43	1.654	0.005509	11.3
June 3	13:06	1.507	0.005047	16
June 3	14:36	1.470	0.009122	22.6
June 3	16:23	1.471	0.014783	32
June 3	17:50	1.486	0.003385	16
June 4	13:39	1.332	0.003935	11.3
June 4	15:09	1.321	0.001160	11.3
June 4	16:49	1.321	0.001078	11.3
June 4	18:20	1.322	0.001164	11.3
June 5	12:03	1.200	0.003328	16
June 5	13:09	1.196	0.000757	8
June 5	14:11	1.185	0.000245	5.6

Date	Time	Q	$Q_{B,\ traps}$ 4 – 64 mm	D_{max}
		(m^3/s)	(g/m·s)	(mm)
June 5	15:16	1.178	0.000209	8
June 5	16:17	1.185	0.000229	8
June 5	17:16	1.197	0.000182	5.6
June 5	18:15	1.214	0.000273	5.6
June 6	12:07	1.354	0.000681	8
June 6	13:38	1.286	0.001828	16
June 6	15:31	1.287	0.000733	8
June 6	16:56	1.349	0.000503	8
June 6	18:00	1.363	0.000922	11.3
June 8	13:06	1.254	0.001700	11.3
June 8	14:38	1.241	0.000237	8
June 8	16:15	1.265	0.000609	8
June 8	17:22	1.291	0.000391	5.6
June 11	12:47	1.060	0.000405	8
June 11	13:48	1.056	0.000139	4
June 11	14:47	1.048	0.000303	8
June 11	15:49	1.053	0.000123	5.6
June 11	16:52	1.073	0.000263	8
June 11	17:54	1.089	0.000438	8
June 11	18:56	1.109	0.000404	8
June 12	13:31	1.164	0.000603	11.3
June 12	14:34	1.130	0	
June 12	16:01	1.129	0.000216	8
June 12	17:36	1.127	0.000029	5.6
June 13	13:37	1.036	0.000118	4
June 13	15:07	1.021	0	
June 13	17:11	1.016	0.000007	4
June 14	13:11	1.008	0.000059	4
June 14	14:12	1.004	0.000013	4

Hayden Creek, April to June, 2005, Helley-Smith samples

Date	Time	Q	$Q_{B\,HS}$ 4 – 64 mm	D_{max}
		(m^3/s)	(g/m·s)	(mm)
April 28	13:45	0.383	0.1307	8
April 30	15:46	0.319	0.0598	5.6
May 4	15:33	0.312	0.1622	11.3
May 5	10:15	0.341	0.1067	11.3
May 6	11:08	0.432	0.1118	11.3
May 9	09:58	0.537	0.0418	8
May 10	09:43	0.664	0.0900	8
May 14	11:34	0.666	0.2160	11.3
May 15	11:45	0.685	0.2322	16
May 16	11:52	0.754	0.3033	8
May 17	18:08	1.155	0.7727	16
May 18	18:48	1.207	0.6422	22.6
May 19	20:30	1.794	2.4061	45
May 20	16:20	1.492	1.7656	32
May 22	10:23	2.105	15.739	64
May 24	09:56	2.302	7.1024	32
May 25	10:03	2.547	2.6741	32
May 26	10:05	2.423	3.2421	22.6
May 27	10:18	2.169	4.3016	45
May 28	10:41	2.027	2.0885	22.6
May 30	10:50	2.021	1.5280	16
June 2	09:05	1.671	0.3690	22.6
June 3	11:13	1.539	1.1069	22.6
June 4	11:53	1.382	0.7400	16
June 5	10:22	1.234	0.1224	8
June 6	10:00	1.228	0.5809	16
June 8	11:15	1.298	0.2965	16
June 11	10:44	1.056	0.0927	11.3
June 12	11:37	1.140	0.2969	16
June 13	11:51	1.054	0.4055	22.6
June 14	11:26	1.013	0.3426	16

Little Granite Creek, May and June 2002, Bedload traps

Date	Time	Q	$Q_{B,\ traps}$ 4 – 64 mm	D_{max}
		(m^3/s)	(g/m·s)	(mm)
May 9	15:22	0.272	0	
May 15	13:27	0.596	0	
May 15	13:54	0.596	0	
May 15	14:44	0.596	0	
May 16	11:21	0.627	0	
May 18	11:05	0.836	0	
May 18	16:34	1.112	0	
May 19	11:19	1.043	0	
May 19	13:45	1.147	0.0002873	5.6
May 19	15:17	1.372	0.0003242	5.6
May 19	17:05	1.740	0.0057808	11.2
May 19	17:38	1.854	0.0065569	11.2
May 19	18:11	1.877	0.0140027	22.4
May 20	12:55	1.778	0.0023507	5.6
May 20	13:47	1.945	0.013415	16
May 20	14:54	2.131	0.0307982	11.2
May 20	16:00	2.286	0.0966596	22.4
May 21	13:27	1.924	0.0150159	11.2
May 21	16:49	1.797	0.0142546	16
May 21	17:26	1.769	0.0077374	11.2
May 23	14:21	1.078	0.0005599	5.6
May 23	15:29	1.070	0.0004609	5.6
May 23	16:33	1.074	0.0007313	5.6
May 23	17:46	1.095	0.0009992	11.2
May 24	13:45	0.900	0.0001332	4
May 24	15:16	0.899	8.262E-05	4
May 25	13:56	0.799	0	
May 25	15:25	0.811	5.745E-05	4
May 26	14:29	0.793	0	
May 26	15:35	0.816	0.0001028	5.6
May 28	11:42	0.960	8.289E-05	4
May 28	16:30	1.123	0.0002281	4
May 28	18:04	1.245	0.003867	11.2
May 29	14:24	1.511	0.0028946	5.6
May 29	16:01	1.823	0.0683941	22.4
May 29	17:50	1.954	0.129557	22.4
May 29	20:17	1.879	0.1032226	32
May 30	13:37	1.892	0.0054771	11.2
May 30	15:23	2.065	0.042811	16
May 30	17:10	2.342	0.2531673	22.4

Date	Time	Q	$Q_{B,\ traps}$ 4 – 64 mm	D_{max}
		(m^3/s)	(g/m·s)	(mm)
May 30	20:58	2.562	0.7739191	32
May 31	14:06	2.324	0.0405511	22.4
May 31	16:36	2.670	0.5635877	45
May 31	20:57	2.881	0.4348708	32
June 1	14:35	2.233	0.0802994	22.4
June 1	16:26	2.231	0.1379474	22.4
June 1	19:36	2.235	0.151956	32
June 3	11:50	1.596	0.0036908	11.2
June 3	14:04	1.610	0.0137807	11.2
June 3	17:28	1.699	0.0659694	16
June 3	19:44	1.680	0.1710815	16
June 4	12:31	1.458	0.0071262	22.4
June 4	14:45	1.487	0.0144648	11.2
June 4	17:58	1.517	0.0339895	16
June 5	12:44	1.354	0.0051386	11.2
June 5	16:17	1.473	0.0081372	11.2
June 5	18:41	1.598	0.0525299	22.4
June 6	14:58	1.586	0.0080966	11.2
June 6	17:50	1.845	0.0312536	16
June 6	20:18	1.931	0.1190096	32
June 7	20:52	1.703	0.0095795	11.2
June 9	12:51	1.140	0.0006882	5.6

Little Granite Creek, May and June, 2002, Helley-Smith sampler

Date	Time	Q	$Q_{B\,HS}$ 4 – 64 mm	D_{max}
		(m^3/s)	(g/m·s)	(mm)
May 9	17:54	0.272	0	2
May 15	15:43	0.627	0.0079	5.6
May 16	13:58	0.596	0.0055	4
May 17	12:52	0.693	0.0705	11.2
May 18	12:01	0.828	0	
May 18	17:36	1.192	0.1458	8
May 19	12:20	1.060	0.0536	16
May 19	16:21	1.576	0.6520	45
May 20	16:58	2.282	0.0825	5.6
May 20	20:53	2.364	0.1670	11.2
May 21	15:50	1.862	0.0457	5.6
May 25	16:13	0.828	0.0040	5.6
May 28	20:17	1.304	0.1760	8
May 29	20:14	1.882	0.4633	8
May 30	17:59	2.422	1.2567	16
May 31	18:29	2.840	1.4127	16
June 1	18:24	2.171	0.2515	8
June 3	15:34	1.669	0.1292	8
June 4	15:37	1.481	0.0268	5.6
June 5	14:27	1.384	0.0567	8
June 5	17:50	1.579	0.0179	5.6
June 6	16:26	1.741	0.0467	5.6
June 6	18:44	1.900	0.1273	8

Little Granite Creek, May to June, 1999, bedload traps

Date	Time	Q	$Q_{B,\ traps}$ 4 – 64 mm	D_{max}
		(m^3/s)	(g/m·s)	(mm)
May 21	11:35	3.455	5.493E-05	5.6
May 21	12:58	3.540	0	
May 21	14:25	3.625	0.000628	11.2
May 21	15:59	4.106	0.0031291	22.4
May 21	17:20	4.248	0.0001953	5.6
May 21	19:04	4.191	0.0352135	11.2
May 22	13:01	4.106	0.001139	11.2
May 22	17:35	4.955	0.0075118	16
May 24	11:35	5.040	0.0015134	11.2
May 24	13:26	5.239	0.4615349	32
May 24	15:53	6.654	2.2178424	64
May 25	11:10	6.513	10.338474	64
May 25	12:48	6.485	0.9342657	64
May 26	09:37	6.145	9.8871292	64
May 26	11:43	6.116	12.665421	90
May 26	13:22	6.371	4.2479281	64
May 27	09:48	6.938	8.8942897	64
May 28	10:45	6.371	15.822528	64
May 28	13:11	6.371	20.237784	64
May 28	15:33	6.683	16.826401	90
May 30	13:05	6.513	1.447266	45
June 1	10:47	4.955	0.4452143	45
June 1	12:44	4.870	0.3390384	45
June 1	14:35	4.955	0.5482411	45
June 1	16:11	5.154	0.5538199	45
June 2	10:31	4.672	0.1041748	32
June 2	12:21	4.587	0.1004512	22.4
June 2	13:43	4.672	0.1460974	45
June 2	15:38	5.012	0.2696919	32
June 3	09:57	7.419	42.713128	64
June 3	11:40	6.853	9.5702562	90
June 3	13:32	7.023	2.5008397	64
June 3	14:56	7.164	7.2504865	90
June 4	13:30	6.173	2.1530287	64
June 4	15:49	6.173	2.7485767	64
June 9	10:12	4.870	0.1012226	32
June 9	12:01	4.814	0.6918159	64
June 9	13:53	4.814	0.1947762	45
June 9	15:49	4.955	0.0676705	32
June 10	10:24	4.644	0.0163219	16

Date	Time	Q	$Q_{B,\ traps}$ 4 – 64 mm	D_{max}
		(m^3/s)	(g/m·s)	(mm)
June 10	12:10	4.672	0.0593393	32
June 10	14:25	4.672	0.1114619	45
June 10	16:01	4.899	0.2180624	45
June 11	10:02	4.701	0.0888873	32
June 11	11:37	4.672	0.1003987	22.4
June 11	13:46	4.757	0.227734	45
June 11	15:19	4.927	0.3124368	45
June 12	10:54	4.814	0.0752589	32
June 12	12:33	4.814	0.1997555	32
June 12	14:07	4.842	0.6274927	64
June 12	15:43	4.899	0.5279673	32
June 14	14:08	5.210	0.1833138	32
June 14	15:45	5.663	0.4081287	32
June 14	17:23	5.607	2.5042145	90
June 14	18:44	5.947	2.0387847	64
July 24		1.065	0	0
July 24		1.039	0	0
July 24		1.017	0	0

Little Granite Creek, May and June 1999, Helley-Smith sampler

Date	Time	Q	$Q_{B\,HS}$ 4 – 64 mm	D_{max}
		(m^3/s)	(g/m·s)	(mm)
May 21	15:42	3.964	0.0975	11.2
May 21	18:57	4.219	0.3208	11.2
May 22	13:16	4.134	0.0200	5.6
May 22	17:30	4.955	0.3126	8
May 24	11:40	4.870	0.4338	22.4
May 24	13:22	5.154	3.3282	45
May 24	15:49	6.711	7.9004	45
May 25	13:24	6.456	11.194	45
May 30	14:21	6.541	3.3638	32
June 1	10:35	4.955	3.7356	22.4
June 1	12:27	4.870	1.0845	22.4
June 1	14:29	4.955	1.1732	11.2
June 1	16:08	5.182	1.7759	32
June 2	10:25	4.672	0.4034	22.4
June 2	12:18	4.616	1.3026	16
June 2	14:07	4.672	1.7777	16
June 2	15:52	5.040	0.3415	16
June 3	10:53	7.136	7.1948	45
June 3	13:44	7.023	6.2816	32
June 3	15:18	7.249	5.4893	45
June 4	13:32	6.173	4.4048	22.4
June 4	15:53	6.201	8.1243	32
June 9	10:10	4.870	0.4897	16
June 9	11:58	4.814	0.2904	16
June 9	13:46	4.814	0.2521	16
June 9	15:43	4.955	0.3032	16
June 10	10:19	4.644	0.4071	22.4
June 10	12:05	4.672	0.5395	22.4
June 10	14:19	4.757	0.7224	32
June 10	15:56	4.870	0.7212	22.4
June 11	09:57	4.729	0.3463	11.2
June 11	11:35	4.672	0.1756	11.2
June 11	13:40	4.757	0.2412	16
June 11	15:18	4.899	0.5249	22.4
June 12	10:49	4.814	0.1628	11.2
June 12	12:27	4.814	0.3092	16
June 12	14:00	4.870	0.5778	22.4
June 12	15:39	4.899	0.5547	16
June 14	14:00	5.210	0.6270	22.4
June 14	15:47	5.663	1.1264	16
June 14	17:17	5.607	1.1945	32

Date	Time	Q	$Q_{B\,HS}$ 4 – 64 mm	D_{max}
		(m^3/s)	(g/m·s)	(mm)
June 14	18:57	5.975	0.7692	16
July 24		1.065	0.0085	4

St. Louis Creek, June 1998, bedload traps

Date	Time	Q	$Q_{B,\ traps}$ 4 – 64 mm	D_{max}
		(m^3/s)	(g/m·s)	(mm)
June 19	13:40	1.073	0.0002474	8
June 19	20:00	1.628	0	
June 22	19:25	2.004	0.000188	5.6
June 22	20:29	2.146	0.004967	16
June 23	11:00	1.744	0.000459	5.6
June 23	12:06	1.744	0.000297	5.6
June 23	15:31	1.857	0.000028	4
June 23	16:48	2.198	0.000376	5.6
June 23	18:01	2.284	0.001616	16
June 23	19:17	2.318	0.001223	11.2
June 23	20:25	2.318	0.001256	11.2
June 23	20:56	2.318	0.011717	11.2
June 24	10:40	1.875	0.000166	5.6
June 24	11:56	1.857	0.000208	8
June 24	15:23	1.913	0.000035	4
June 24	16:27	2.075	0.000150	4
June 24	17:27	2.129	0.000762	5.6
June 24	20:03	2.129	0.000149	5.6
June 24	21:03	2.110	0.000165	8
June 24	21:32	2.075	0.001224	8
June 25	16:36	2.300	0.002796	8
June 25	17:36	2.351	0.001634	5.6
June 25	18:56	2.402	0.001235	11.2
June 25	20:35	2.385	0.003492	16
June 25	21:34	2.318	0.005339	11.2
June 26	10:01	2.040	0.000293	5.6
June 26	14:23	2.180	0.000051	8
June 26	15:25	2.385	0.000715	5.6
June 26	16:28	2.367	0.001472	11.2
June 26	17:36	2.565	0.005435	11.2
June 26	18:33	2.582	0.002955	11.2
June 26	19:42	2.565	0.004478	16
June 29	19:01	2.582	0.005044	11.2
June 29	20:20	2.582	0.006086	11.2
June 30	11:21	2.351	0.006843	16
June 30	13:41	2.418	0.002504	11.2
June 30	15:00	2.335	0.001645	11.2
June 30	16:00	2.500	0.002224	11.2
June 30	17:11	2.550	0.019500	16
June 30	18:02	2.582	0.003410	8

Date	Time	Q	$Q_{B,\ traps}$ 4 – 64 mm	D_{max}
		(m^3/s)	(g/m·s)	(mm)
June 30	19:03	2.565	0.002886	11.2
June 30	20:15	2.546	0.003760	11.2

St. Louis Creek, June 1998, Helley-Smith sampler

Date	Time	Q	$Q_{B\,HS}$ 4 – 64 mm	D_{max}
		(m^3/s)	(g/m·s)	(mm)
June 19	12:05	1.073	0.1261	8
June 19	19:35	1.628	0.6451	11.2
June 22	19:04	2.040	0.4578	16
June 22	20:55	2.110	0.6003	16
June 23	10:19	1.744	0.0236	5.6
June 23	16:02	2.146	0.1156	11.2
June 23	14:19	2.318	0.1827	16
June 24	09:53	1.894	0.0498	8
June 24	11:34	1.820	0.0704	8
June 24	20:41	2.110	0.0256	8
June 25	16:14	2.318	0.3905	16
June 26	09:28	2.040	0.0017	4
June 26	16:10	2.550	0.0245	8
June 26	19:23	2.582	0.1822	16
June 29	18:44	2.582	0.0810	11.2
June 30	14:43	2.451	0.0574	11.2
June 30	16:40	2.582	0.0481	8
June 30	19:54	2.517	0.0354	5.6